CHEMICAL REVIEWS

Review

pubs.acs.org/CR

MOF-Polymer Hybrid Materials: From Simple Composites to Tailored Architectures

Mark Kalaj,[†] Kyle C. Bentz,[†] Sergio Ayala, Jr.,[†] Joseph M. Palomba,[†] Kyle S. Barcus,[†] Yuji Katayama,[†,‡] and Seth M. Cohen*[,†]

[†]Department of Chemistry and Biochemistry, University of California, San Diego, La Jolla, California 92093-0358, United States

[‡]Asahi Kasei Corporation, 2-1 Samejima, Fuji-city, Shizuoka 416-8501, Japan

ABSTRACT: Metal−organic frameworks (MOFs) are inherently crystalline, brittle porous solids. Conversely, polymers are flexible, malleable, and processable solids that are used for a broad range of commonly used technologies. The stark differences between the nature of MOFs and polymers has motivated efforts to hybridize crystalline MOFs and flexible polymers to produce composites that retain the desired properties of these disparate materials. Importantly, studies have shown that MOFs can be used to influence polymer structure, and polymers can be used to modulate MOF growth and characteristics. In this Review, we highlight the development and recent advances in the synthesis of MOF-polymer mixed-matrix membranes (MMMs) and applications of these MMMs in gas and liquid separations and purifications, including aqueous applications such as dye removal, toxic heavy metal sequestration, and desalination. Other elegant ways of synthesizing MOF-polymer hybrid materials, such as grafting polymers to and from MOFs, polymerization of polymers within MOFs, using polymers to template MOFs, and the bottom-up synthesis of polyMOFs and polyMOPs are also discussed. This review highlights recent papers in the advancement of MOF-polymer hybrid materials, as well as seminal reports that significantly advanced the field.

CONTENTS

1. INTRODUCTION

Metal−organic frameworks (MOFs) are three-dimensional porous materials composed of inorganic metal nodes termed

Special Issue: Porous Framework Chemistry

Received: September 15, 2019

DOI: 10.1021/acs.chemrev.9b00575
Chem. Rev. XXXX, XXX, XXX−XXX

secondary building units (SBUs) linked together by rigid multitopic organic linkers.[1,2] Over the last two decades, research in metal−organic frameworks (MOFs) has considerably pushed the limits of these porous, crystalline materials toward a wide range of applications[3−6] because of their exceptional storage, separation, and catalytic properties. However, the progress of MOFs toward commercialization has been limited by their crystalline or microcrystalline (e.g., powders) for factor, which inherently limits their integration into many technologies. As such, processable form factors containing MOFs and polymers have been sought in an effort to combine the properties of MOFs and polymers to advance the utility of MOFs (Figure 1). These materials have been

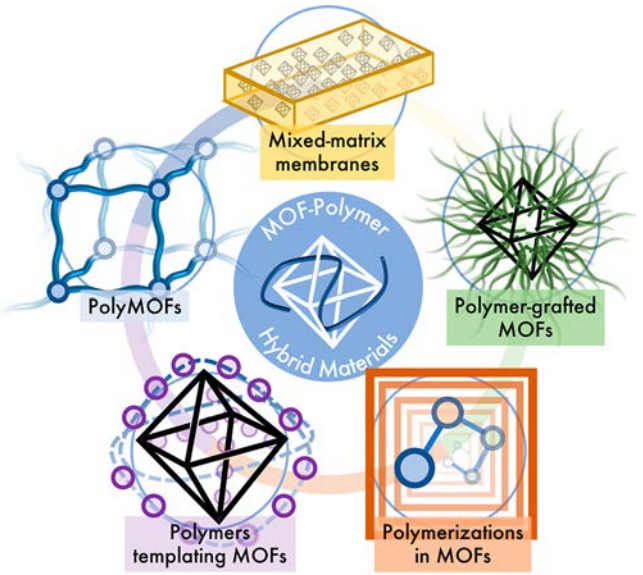

Figure 1. Overview of MOF-Polymer hybrid materials covered in this review. Sections 2 and 3 focus on mixed-matrix membranes (MMMs). Section 4 focuses on polymer-grafted MOFs. Section 5 focuses on Polymerization in MOFs. Section 6 focuses on polymers templating MOFs. Section 7 focuses on polyMOFs and related materials.

targeted through a top-down approach, in which MOFs are initially synthesized and subsequently incorporated into polymeric materials as well as through a bottom-up approach in which hybrid materials are synthesized as MOF formation is occurring. These approaches have yielded several elegant methods to synthesize MOF-polymer hybrid materials bringing MOFs closer to a useful material.

Beyond integrating MOFs and polymers to enable the utilization of MOFs, many other investigations have focused on other ways in which these two classes of materials can be comingled and interact. Studies examining the synthesis of polymers in and around MOF crystallites have been reported. Control over the outcome of polymerization reactions within MOF pores has yielded fascinating results, and many methods for decorating the surface of MOFs with polymer chains have been described.

Diverse approaches for MOF-polymer hybrid materials have been explored by research groups through the synthesis of mixed matrix membranes (MMMs), polymers grafted from MOF particles, polymers grafted through MOFs, polymers templating MOF growth, as well as the synthesis of MOFs using polymer ligands (polyMOFs, Figure 1). These approaches have utilized a wide range of polymers for the integration of MOF-polymer hybrid materials to achieve form factors of distinct polymer characteristics for several desired applications such as separations, sensing, catalysis, and storage (Figure 2).[7−9] Realization of MOF-polymer hybrid materials

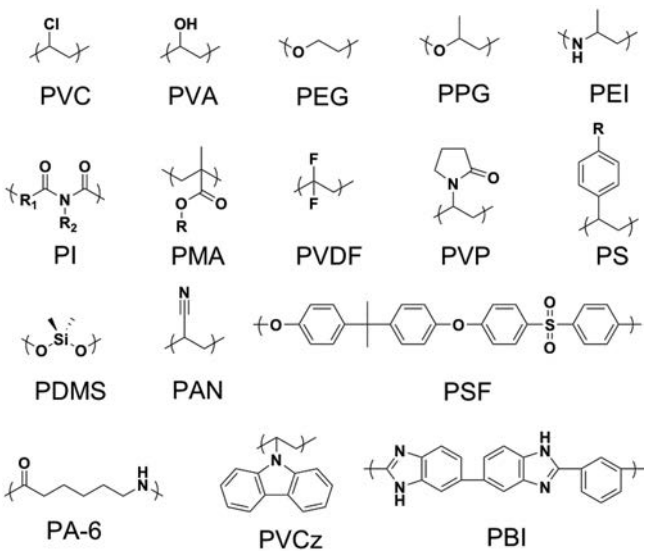

Figure 2. Common polymers used in the synthesis of MOF-polymer hybrid materials.

that maintains the properties of MOFs in a flexible form factor would provide a platform for these materials to be incorporated into the industrial realm. Several excellent reviews are available on the wide range of MOF-polymer studies that have been reported in the past decade.[7−14] This review aims to highlight some of the most influential papers in the advancement of MOF-polymer hybrid materials, including some of the most recent findings reported in this field to date.

2. MOF BASED MIXED-MATRIX MEMBRANES (MMMS)

One strategy to hybridize porous solids, such as zeolites, porous carbons, and MOFs, is via the synthesis of mixed-matrix membranes (MMMs). MMMs serve as a means to incorporating rigid materials into flexible, polymeric form factors.[15,16] MMMs consist of a polymer combined with a solid filler to make a hybrid material that contains the flexibility of the polymer while retaining the desired properties of the porous filler.[15,17] For example, incorporation of inorganic materials in polymer membranes have been sought after for a variety of gas separations due to the higher fluxes and better selectivity than polymer-only membranes.[15]

Zeolites are a mineral-like class of porous materials made up of metal oxide bonds that are used in applications such as separations, gas sorption, and catalysis.[16] Synthesis of MMMs with zeolites as inorganic fillers have been studied in an attempt to exploit the narrow pore sizes of zeolites to improve gas separations between gases with similar sizes and properties, such as O_2, N_2, and CO_2.[18,19] Combining zeolites and polymers, in the form of MMMs, in many cases results in improved selectivity and permeability for various gas separation applications.[15,17] For example, synthesis of faujasite type zeolite MMMs have shown encouraging results for separating N_2 and CO_2, while smaller pore zeolites like SAPO-34 (SAPO = silicoaluminophosphate)-based MMMs have

DOI: 10.1021/acs.chemrev.9b00575
Chem. Rev. XXXX, XXX, XXX−XXX

shown the ability to separate CO_2 and CH_4.[18,20,21] Despite the extensive work with zeolite MMMs, there are limitations with these systems, such as defective interfaces between the zeolites and polymers that lead to poorer than desired separation properties.[12,22]

Activated carbons have also been used as a filler in the synthesis of MMMs for applications such as gas separations.[23] These carbons have been combined with polymers to form MMMs with improved gas separation properties.[24] For example, polyvinyl chloride (PVC, Figure 2)-based MMMs were loaded with activated carbon (~20−60 wt %) and displayed higher selectivity for H_2 over CH_4.[25] Carbon molecular sieve (CMS) membranes have also shown promising gas separation abilities.[24] These MMMs are synthesized by pyrolyzing a polymer membrane resulting in porous hollow fiber membranes.[24] Miller et al. studied the pyrolyzing of polyimide (PI, Figure 2) polymers into CMS hollow fiber MMMs and found dramatic increases in selectivity for CO_2 over CH_4 and O_2 over N_2.[26,27] While interesting, the noncovalent interactions holding these MMMs together are not particularly robust, and as such, literature on these MMMs is rather limited.[28]

To some degree, MOFs are at the intersection of zeolites and porous carbons as fillers because MOFs are comprised of both organic and inorganic building units.[2] MOFs have been studied for just over a decade as fillers for MMMs. Efforts to synthesize MOF -based MMMs have been tailored toward applications such as gas or liquid separations. With this in mind, selection of a polymer that allows for permeance and selectivity of various gases or liquids has driven the selection of polymers for MOF-based MMMs.[29]

Frequently, for pure polymer membranes, permeance and selectivity are inversely correlated with highly permeable membranes lacking selectivity and vice versa. This trade-off between permeability and selectivity is defined as the Robeson Upper Bound.[30] For example, more rubbery polymers, such as polydimethylsiloxane (PDMS), tend to display higher permeability, whereas glassy polymers, such as polysulfone (PSF), polyimide (PI), and poly(methyl methacrylate) (PMMA, Figure 2, R = CH_3), tend to display better selectivity (Figure 2).[30] Incorporation of porous inorganic materials, such as MOFs, into polymer membranes in the form of MMMs is designed to produce materials that exceed the Robeson Upper Bound limits and has been much of the driving force in this area of research.[12] However, incorporation of a crystalline MOF material into a polymer matrix to improve selectivity and permeation performance presents several challenges, perhaps most notably the formation of gaps at the MOF−polymer interface, which result in poor selectivity due to the flow of gas through the resulting macrovoids (Figure 3). There have been two main approaches for the synthesis of MOF-based MMMs. One approach is through the physical mixture of unmodified MOFs and polymers to induce noncovalent bonding (i.e., hydrogen bonding, pi-pi stacking, etc.) between the MOF and the polymer. The second approach modifies the organic ligands of the MOF to append polymers to the MOF particles to improve the noncovalent interactions at the particle−polymer interface.

2.1. Conventional MOF-Polymer MMMs

The most widely used approach for the synthesis of MOF-based MMMs involves simple solution dispersion and casting methods. In this approach, insoluble MOF particles are suspended in a solvent and mixed with a solution of dissolved polymer until the two are homogeneously dispersed. This mixture, sometimes referred to as a MOF "ink", is then cast into a film after which the solvent evaporates (with or without heating) resulting in a freestanding MOF-based MMM film (Figure 4). The casting method has been widely utilized to synthesize a variety of MMMs containing various MOFs and polymers tailored toward specific applications.[13,32−34] As a result, several combinations of polymers and MOFs have been explored to synthesize MMMs and these materials have been extensively studied and reviewed elsewhere.[7−9,11−14,35−40] This section will only discuss more recent findings that are significant advancements in MOF-based MMMs.

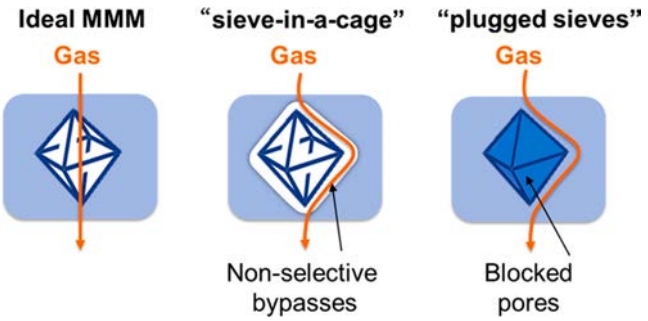

Figure 3. Examples of ideal MOF-based MMMs and nonideal MOF-based MMMs as a function of macrovoids or blocked pores. Reprinted from ref 31. Copyright 2019 American Chemical Society.

Figure 4. Schematic depiction of the synthesis of a standalone MOF-based MMMs using a casting method. Reprinted with permission from ref 34. Copyright 2015 Wiley Publishing Group.

An important property to consider in the synthesis of MOF-based MMMs is the compatibility of the MOF and polymer components. A more compatible MOF-polymer mixture results in tighter MOF−polymer interfaces, leading to improved membrane selectivity (and possibly permeability),[7,10] as well as conceivably better mechanical properties. Synthesis of MMMs using polymers such as PMMA (Figure 2, R = CH_3), PSF, polyvinylidene fluoride (PVDF), and PI have been utilized for their potential to form tight junctions (i.e., via hydrogen bonding) between the MOF and polymer components (Figure 2).[41] These polymers have been combined with MOFs that contain functionalized ligands (e.g., amines) in order to enhance interactions.[1,42,43] For example, Chen and Kong et al. reported an MMM containing CAU-1-NH_2 (CAU = Christian Albrechts University) and PMMA that displayed 3 orders of magnitude higher permeability of H_2 compared to a pure PMMA membrane. The same MMM was also more selective for H_2 than CO_2.[44] Urban et al. used UiO-66-NH_2 and PSF to obtain MMMs with up to 50 wt % MOF loadings and significantly improved permeability and high selectivity for CO_2 when compared to CH_4 and N_2.[45] Tavasoli et al. studied the differences in MIL-53(Al) and MIL-53(Al)-NH_2 PVDF-based membranes by monitoring their selectivity toward several gas combinations (He/CH_4 and CO_2/CH_4).[46] They found better selectivity for

DOI: 10.1021/acs.chemrev.9b00575
Chem. Rev. XXXX, XXX, XXX−XXX

He over CH_4 and for CO_2 over CH_4 when using the amine functionalized MIL-53(Al)-NH_2 MOF, attributing these observations to improved surface interactions between the amine groups and the PVDF polymer.

Much of the earlier research of MOF-based MMMs focused on synthesizing MMMs with relatively low MOF loadings (<40 wt %). Synthesis of MMMs with higher MOF loadings generally resulted in less flexible membranes with aggregation of particles and macrovoids at the MOF−polymer interface.[12] Cohen and co-workers reported one of the first syntheses of high MOF-loaded MMMs (67 wt % MOF) using PVDF with a wide variety of MOFs (UiO-66, UiO-66-NH_2, MIL-53, MIL-101, HKUST-1, and ZIF-8 (ZIF = zeolitic imidazolate framework)).[34] The flexibility and mechanical stability of these highly loaded PVDF MMMs suggested new avenues for MOF-based MMMs, where the MOF does not act as a simple filler but rather the MMM is composed predominately of MOF particles with the polymer behaving as a binder, producing a new, flexible MOF form factor. It was shown that these membranes displayed near complete retention of surface area, and the MOF particles remained accessible for postsynthetic modification (PSM)[47−51] or postsynthetic exchange (PSE) reactions.[34,52,53] In a follow-up study, Cohen et al. used the same PVDF polymer binder to synthesize multicomponent MOF-based MMMs to combine the properties of various MOFs into a single MMM.[54] A range of mixed MOF MMMs were synthesized using three methods: (a) cocasted MMM where two different MOF inks are casted in discrete regions resulting in spatially separated MOFs in the same MMM, (b) fully mixed MOF systems where two different MOFs were combined in one ink and then casted out into a completely mixed monolithic membrane, and (c) layered MMMs, where one layer of MOF ink is initially casted and subsequently another unique MOF layer is casted resulting in discrete layered MMM (Figure 5). Discrete MOF units are clearly visible from scanning electron microscopy (SEM) images and energy-dispersive X-ray (EDX) mapping across all three forms of mixed MOF MMMs. Interestingly, these layered MOF MMMs were used to conduct a catalytic two step reaction. A MIL-101-NO_2 top layer was used to convert a benzaldehyde dimethyl acetal into a benzaldehyde via an acid catalysis mechanism followed by a second layer of ZIF-8 MMM used in a Knoevenagel condensation of the benzaldehyde with malonitrile in a base-catalyzed step. One pass of all the reactants through the layered MMM yielded a 95% conversion to the final product.

Using PVDF, Maspoch et al. designed a MOF-based MMM that self-folds upon exposure to various solvents or vapors based on polarity.[55] To achieve this, MIL-88A (MIL = Materials from Institut Lavoisier), a MOF made up of Fe^{3+} centers and fumaric acid organic linkers was utilized because this material is known to swell and shrink in a reversible manner depending upon the presence of water (Figure 6). To prepare MMMs with this MOF, a homogeneous suspension containing MIL-88A and dissolved PVDF in a DMF solution was casted dropwise onto a silicon wafer. The resulting MMMs, containing 50 wt % MOF loading or higher, displayed a self-folding feature upon exposure to polar solvents (e.g., water, methanol, ethanol, acetone, chloroform, etc.) that was reversible upon drying at elevated temperatures. As expected, the solvents that caused the pure MIL-88A samples to swell were the same solvents that initiated the reversible folding mechanism in the MMMs, indicating the importance of the

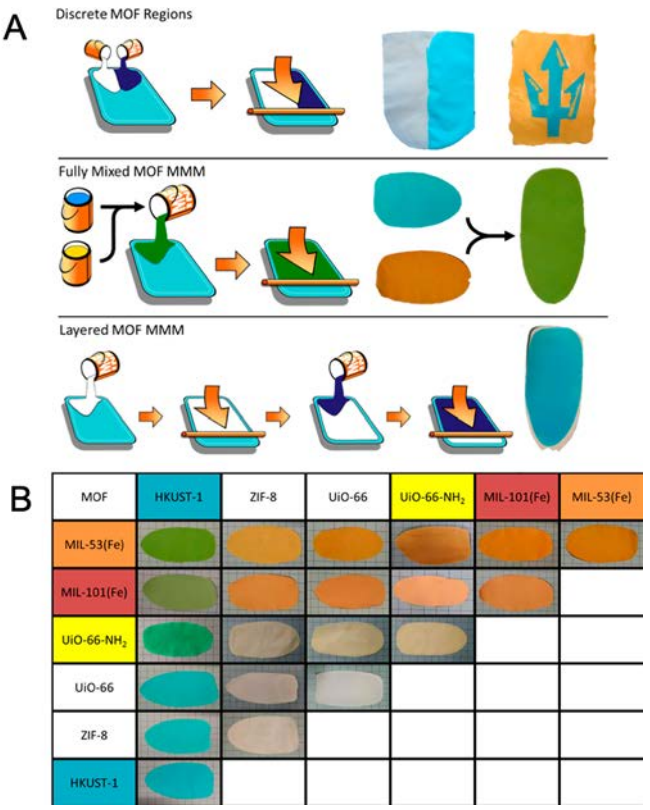

Figure 5. (A) Various methods used to prepare multicomponent MOF-based MMMs. (B) Examples of various mixed MOF MMMs. Reprinted with permission from ref 54. Copyright 2018 The Royal Society of Chemistry 2018.

MOF in the folding mechanism. Building off this work, the same group synthesized MOF-based MMMs where the MIL-88A MOF is patterned at specific sites of the silicon wafer to design materials that self-shape into preprogramed 3-dimensional architectures (Figure 6).[56] To achieve this, films were synthesized by selectively designing "passive" or nonfolding domains by mask protecting the substrate or active domains by exposing the substrate or the HCl where MOF etching can occur (Figure 6). These MOF-based MMMs displayed unique folding mechanisms based on the patterning of the active domains to form unique 2D and 3D shapes (Figure 6). Noncovalent mixtures of MOFs and polymers have also been used to synthesize composites beyond membranes and have taken monolithic forms such as extruded MOFs, MOF foams, or granulated MOF composites.

MMMs using PI polymers have also been popular due to the ubiquity, commercial availability, and hydrogen bonding ability of PI (Figure 2). Rodrigue et al. reported the synthesis of MIL-53(Al)-NH_2 and a cross-linked co-PI polymer and examined the permeability and selectivity of these membranes for CO_2.[57] When compared to the parent MIL-53(Al) MMMs, MIL-53(Al)-NH_2 MMMs displayed much higher MOF incorporation (35 wt %), better adhesion between the MOF and polymer (as evidenced by SEM images), and significantly better selectivity and permeability for CO_2 over CH_4. Li et al. recently covalently grafted PI brushes onto UiO-66-NH_2, and these materials displayed superior compatibility between the MOF and the polymer component.[58] To achieve this, UiO-66-NH_2 was modified via PSM with 4,4′-oxidiphthalicanhydride to create reactive handles on the MOF ligand. PI brushes were

DOI: 10.1021/acs.chemrev.9b00575
Chem. Rev. XXXX, XXX, XXX−XXX

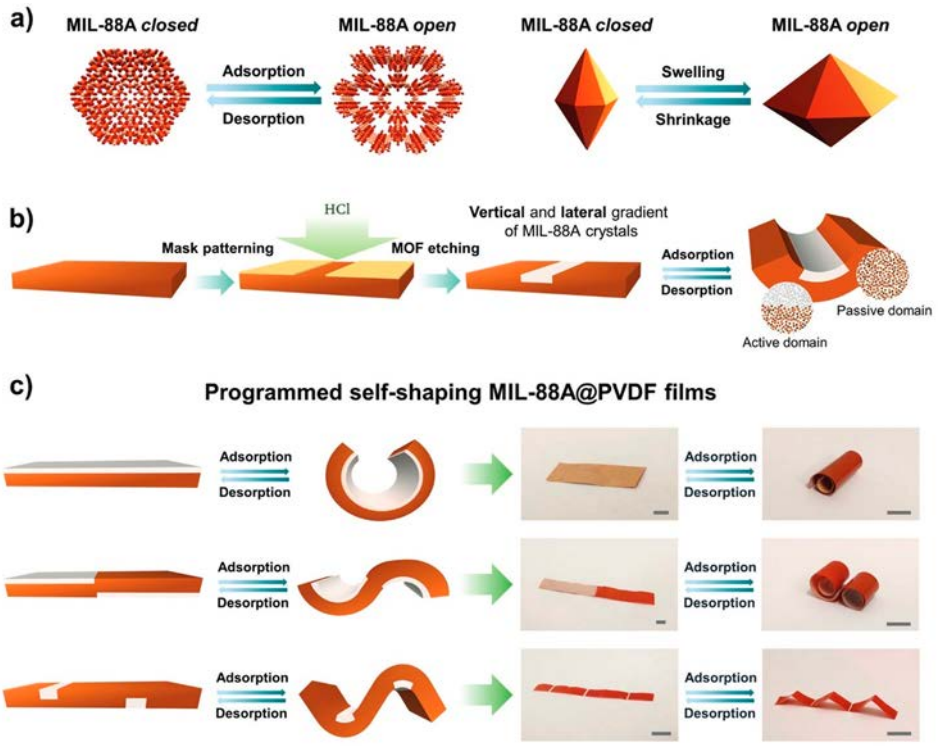

Figure 6. (a) Swelling and shrinking properties displayed in the MIL-88A MOF as a function of exposure to polar solvent. (b) Mechanism used to achieve programmable self-folding MOF-based MMMs. (c) Various shapes and forms achieved as a function of MOF etching at distinct regions of the MMM. Reprinted with permission from ref 56. Copyright 2019 Wiley Publishing Group.

then grown on this modified MOF through a step-growth polymerization method and subsequent in situ imidization. Up to 88 wt % MOF loading MMMs were prepared using these polyimide-functionalized MOFs (Figure 7). SEM images showed fewer defects at the MOF−polymer interface when using the brush-modified MOF as opposed to unmodified UiO-66-NH_2. These MMMs were tested for permeability of CO_2 as well as selectivity of CO_2/N_2 and CO_2/CH_4. MMMs with the polyimide brush grafted MOF displayed higher permeability than neat polymer membranes; however, selectivity in the MOF-containing MMMs was lower suggesting the occurrence of interfacial defects. While several combinations of MOF and polymer components have been synthesized in MOF-based MMMs, current work in the field has moved toward bridging the gap between the MOF and polymer components through covalent bonding.

2.2. Covalently Connected MOF-Polymer MMMs

One of the major goals of MOF-based MMMs is to utilize the narrow and tunable pores of the MOF component as a passage point for the separations of various gases or solutions in a more flexible form factor. As outlined above, despite efforts to combine various MOF and polymers in fabricating MMMs, the interface of these two distinct materials still harbors many defective sites that hinders the separation capability of these materials. Defects at the MOF−polymer interfaces have been shown to create large, nonselective macrovoids that cause reduced selectivity of various gases (Figure 3). As such, some studies have focused on covalent attachment of MOFs and polymers to bridge the gap at the interface of these two discrete materials.

One of the earliest, clever approaches to covalently combining MOFs and polymers was reported by Wang and

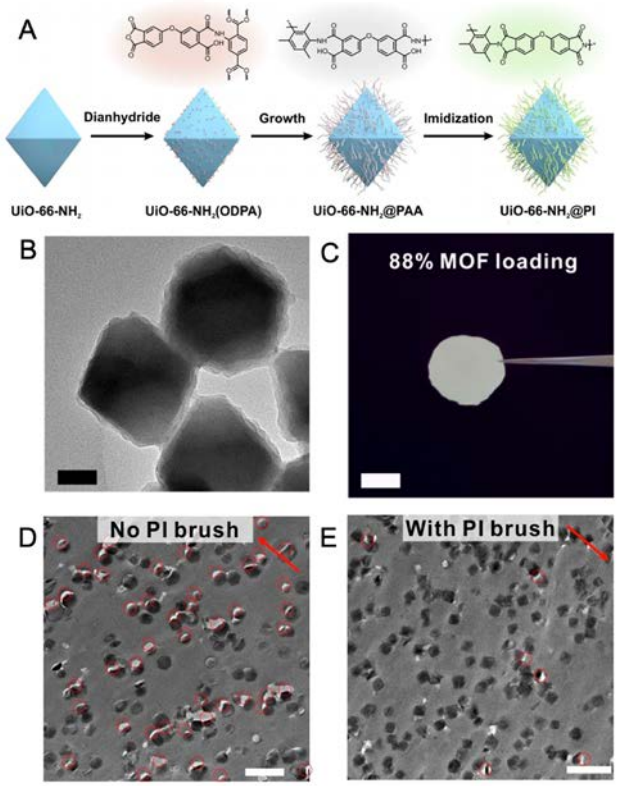

Figure 7. (A) Scheme for synthesizing UiO-66-NH_2 PI MMMs. (B) TEM images depicting the brush polymers around MOF particles. (C) Photograph of highly loading MOF-based MMM. (D and E) SEM images of MMMs using MOFs without and with PI brush. Reprinted from ref 58. Copyright 2018 American Chemical Society.

DOI: 10.1021/acs.chemrev.9b00575
Chem. Rev. XXXX, XXX, XXX−XXX

co-workers, who developed a covalent MOF-polymer linkage through postsynthetic polymerization (PSP) (Figure 8).[59] This approach used reactive amine handles in a UiO-66-NH_2 MOF as a site for PSM converting these amines to methacrylamides (UiO-66-NH-Met). This modified UiO-66-NH-Met was mixed with butyl methacrylate (BMA) and phenylbis(2,4,6-trimethylbenzoyl)phosphine oxide and subsequently cast out into a Teflon mold. This mixture was then cured with UV light, thereby polymerizing the MOF through the methacrylamide handles to give a stand-alone membrane. CO_2 isotherms of the membrane showed retained porosity in the MOF particles, suggesting that the MOF pores are not infiltrated by the polymer but rather decorated around the outside of the particles. The PSP membranes were characterized compared to physical mixtures of MOF and BMA which showed better adhesion of the MOF and polymer components in the covalently linked material (Figure 8). Using PSP, MMMs were obtained where the MOFs are directly, covalently integrated into the surrounding polymer matrix.

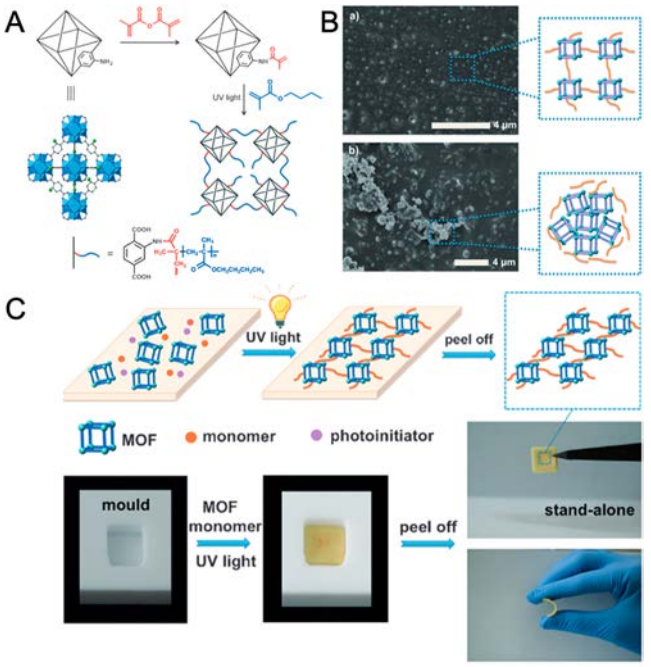

Figure 8. (A) Mechanistic used to synthesize PSP product. (B) Comparison of PSP product to a noncovalent control. (C) Pictorial depiction of method used to prepare PSP MOF-based MMMs. Reprinted with permission from ref 59. Copyright 2015 Wiley Publishing Company.

This seminal work by Wang et al. inspired several other researchers to utilize PSP in the synthesis of covalently grafted polymer MOF MMMs[60] as well as other hybrid materials.[61−63] Other groups have utilized photopolymerizations based on thiol−ene click chemistry to integrate MOFs into MMMs.[64] Using the same methacrylamide decorated UiO-66-NH-Met nanoparticles (NPs), Dong et al. utilized the thiol−ene click reaction to polymerize the methacrylamide groups with polysiloxane oligomers (PSI-SH) upon exposure to UV light to form a covalent PSP membrane.[65] These porous membranes displayed capacity to take up Au NPs that allow for the membranes to promote the Knoevenagel condensation of 4-nitrobenzaldehyde with malonitrile. The same group reported the PSP combination of a polyurethane oligomer with UiO-66-NH_2 nanoparticles making membranes with MOF loadings of up to 70 wt %.[66] Isocyanate-terminated polyurethane oligomers were synthesized by combining methylene diphenyl diisocyante (MDI) with polypropylene glycol (Figure 9).

Dong et al. built upon this work by designing ionic liquid (IL) decorated UiO-66 nanoparticles and cross-linking them to the same isocyanate terminate polyurethane oligomer (Figure 9). An imidazolium-based ionic liquid (charge balanced by a bromine ion) was synthesized starting from terephthalic acid. Then the ionic liquid was used to synthesize UiO-66-IL-Br via a standard acetic acid modulated synthesis.[67] The charge balancing anion was then exchanged with PF_6, SO_3CF_3, or ClO_4 and finally cross-linked with the isocyanate terminated

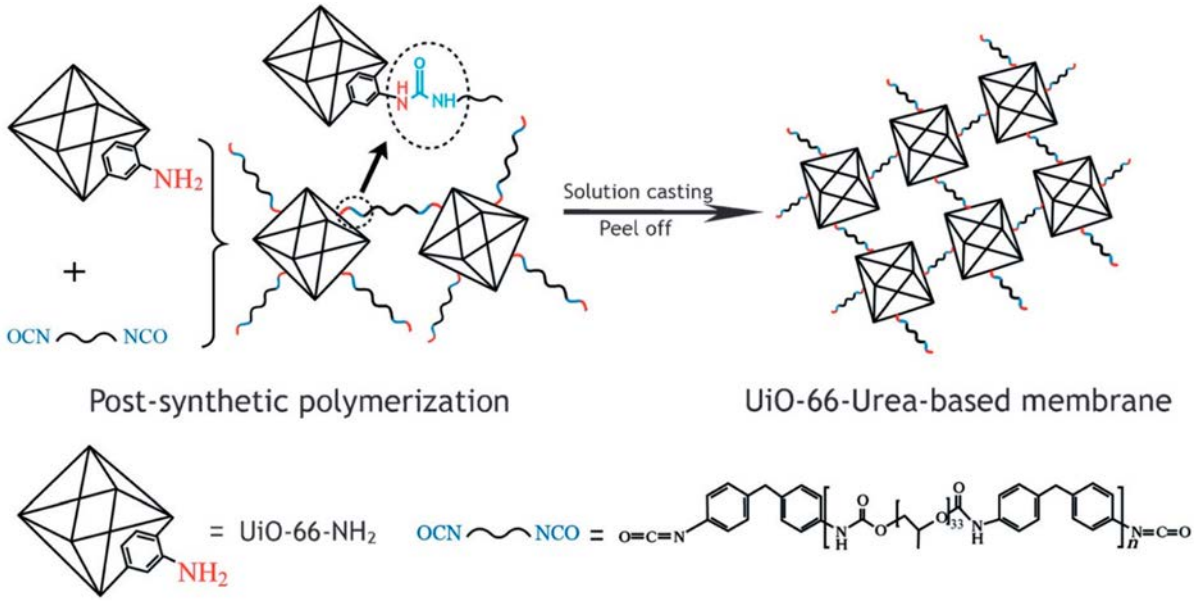

Figure 9. Schematic depiction of the synthesis of urea based UiO-66 membranes. Reprinted with permission from ref 66. Copyright 2016 Wiley Publishing Company.

DOI: 10.1021/acs.chemrev.9b00575
Chem. Rev. XXXX, XXX, XXX−XXX

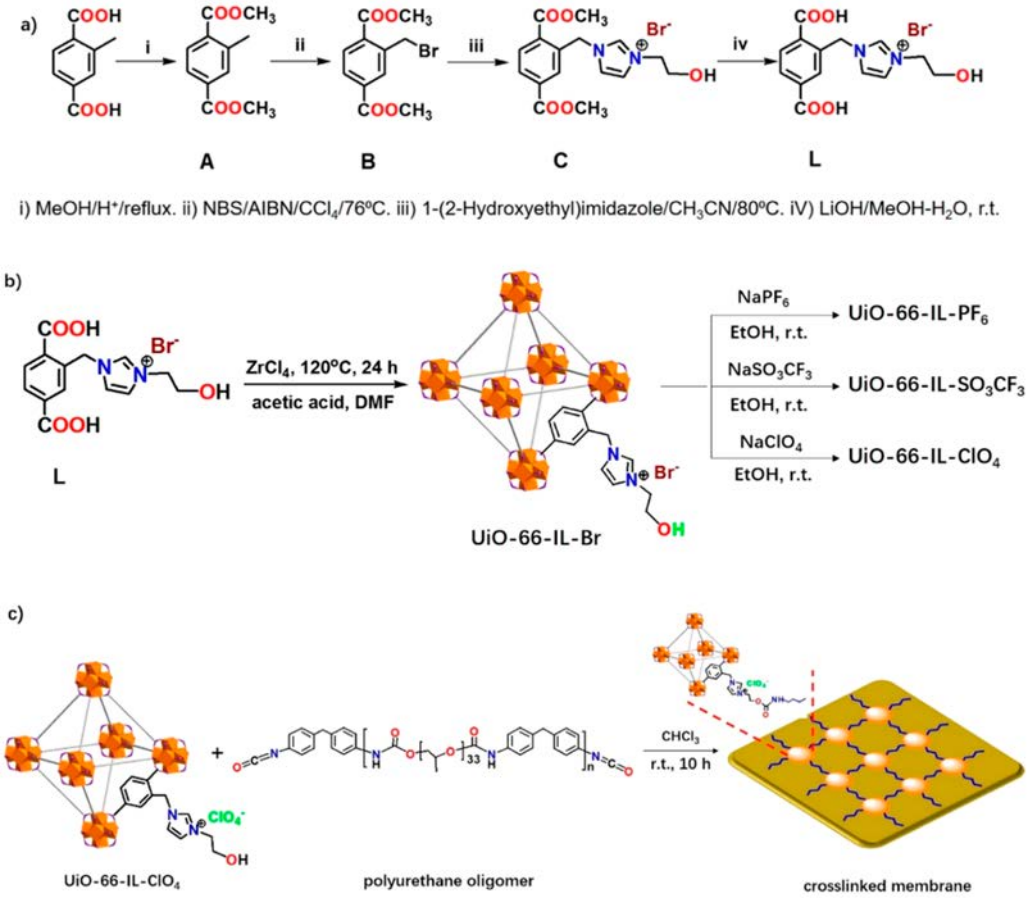

Figure 10. (a) Synthetic scheme of imidazolium ionic liquid functionalized terephthalic acid molecules. (b) Synthetic scheme of UiO-66-IL-Br synthesis and anion exchange. (c) Synthetic scheme for cross-linked MMM formation via the polyurethane oligomer. Reprinted from ref 67. Copyright 2017 American Chemical Society.

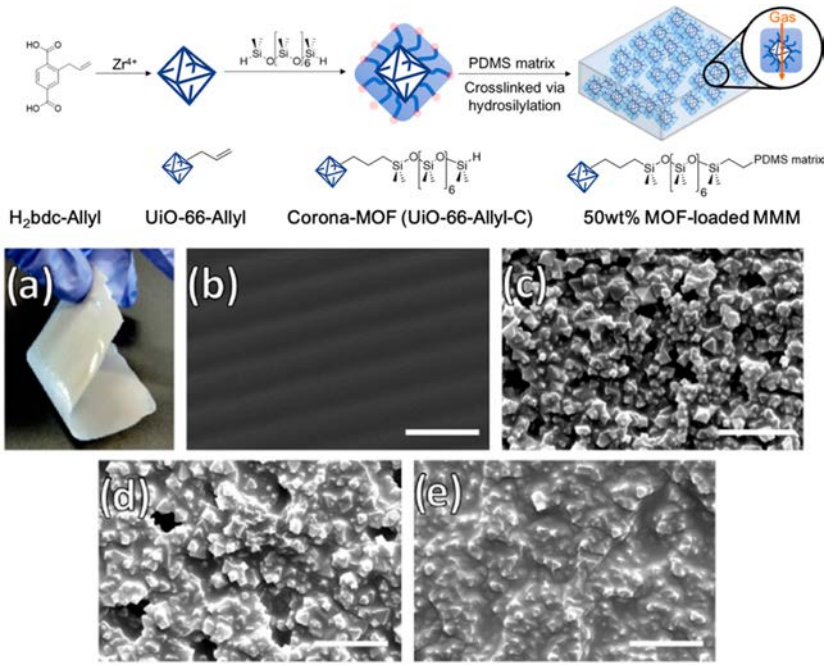

Figure 11. (Top) Scheme for the synthesis of UiO-66 Corona based MMMs. (Bottom) (a) Photographic image of the corona-MOF and (b–d) SEM images showing the control materials synthesized and (e) the experimental MMM. Reprinted from ref 31. Copyright 2019 American Chemical Society.

DOI: 10.1021/acs.chemrev.9b00575
Chem. Rev. XXXX, XXX, XXX−XXX

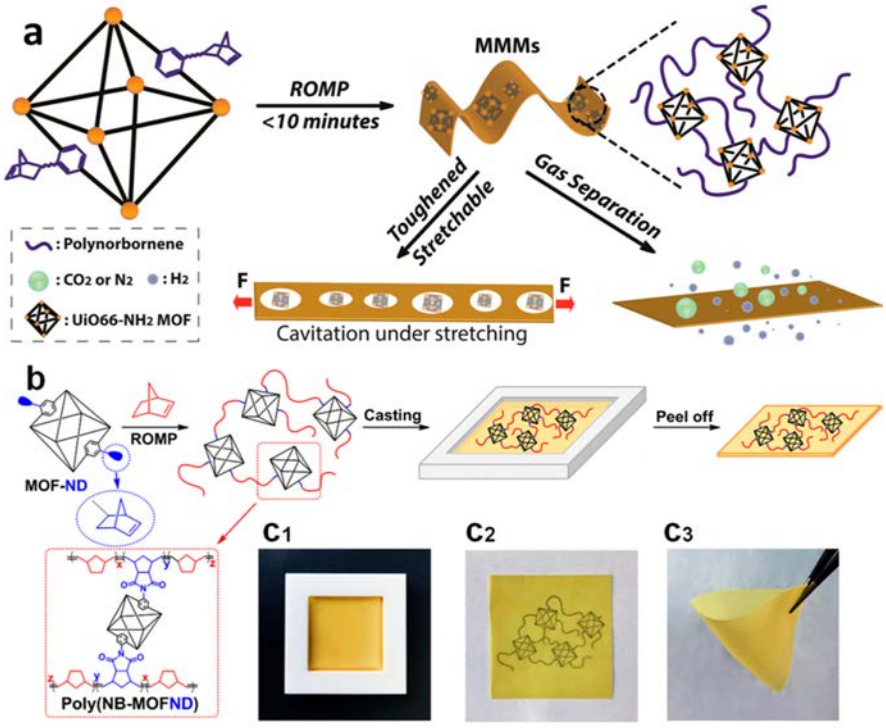

Figure 12. (a) Pictorial depiction of ROMP-based PSP MMMs. (b) Chemical depiction of ROMB based PSP MMMs utilizing the norbornene functional group. (c) Photographic images of MMMs. Reprinted from ref 70. Copyright 2018 American Chemical Society.

oligomer resulting in an MMM (Figure 10). The resulting MMMs displayed high selectivity for CO_2 over N_2 and CH_4 while also displaying catalytic activity for the cycloaddition of CO_2 with epoxide under ambient pressure.

Recently, a new approach using a "corona", or polymer brush, around the MOF particles has been developed to make the MOF and polymer components more compatible and limit macrovoids at the MOF−polymer interface. As mentioned above, Li et al. used PSM-functionalized MOF particles with brush polymers and these particles formed favorable noncovalent interactions with a PI polymer resulting in improved gas separation and permeation properties.[58] Using a similar approach, Cohen et al. combined allyl functionalized UiO-66 (UiO-66-allyl) with hydride-terminated poly(dimethylsiloxane) (PDMS)[31] to get a covalently linked PDMS "corona" around the MOF particles. These modified particles were then cross-linked with a PDMS matrix via hydrosilylation forming a defect free, 50 wt % MOF-based MMM (Figure 11). By installing a PDMS corona on the MOF, the resulting MMM displayed fewer macrovoids (when compared to MOFs lacking the corona) as evidenced by SEM images. When compared to MMMs using only noncovalent interactions, the corona MMMs displayed better CO_2 permeation and CO_2, N_2, and propane separation, suggesting that the gases are passing through the MOF pores as opposed to through macrovoids at the MOF−polymer interface (Figure 11).

Other polymerization techniques, such as atom transfer radical polymerization (ATRP) and ring opening metathesis polymerization (ROMP), have been used to develop covalently grafted, MOF-based MMMs. For example, Matzger et al. utilized ATRP to decorate the shell of IRMOF-3 with PMMA while maintaining the internal porosity of the MOF (as evidenced via N_2 sorption isotherms and single crystal Raman mapping).[68] Wu et al. covalently modified UiO-66-NH_2 with poly(sulfobetaine methacrylate) (PSBMA) using ATRP and incorporated the resulting MOF into PSF MMMs; the resulting hydrophilic MMM displayed two times higher water flux than the noncovalent UiO-66-NH_2 PSF membrane.[69]

ROMP was applied by Zhang et al. to polymerize UiO-66-NH_2 particles with polynorbornene to form MMMs with 20 wt % MOF loading.[70] To achieve this, UiO-66-NH_2 and *cis*-5-norbornene-exo-2,3-dicarboxylic anhydride (ND) were combined via PSM to form UiO-66-ND (Figure 12). ROMP was then performed using Grubbs generation III catalyst converting >95% of the norbornene monomers (in under 7 min) resulting in a standalone, flexible MMM. Cavitation experiments indicate that these MMMs displayed exceptional toughening effects compared to the free polymer membrane. These MMMs also displayed high permeability for H_2 and high selectivity for H_2/N_2 and H_2/CO_2 separations, both exceeding the 2008 Robeson Upper Bound. Several other groups have utilized these grafting from polymerization methods to develop MMMs[71,72] and related MOF-polymer hybrid materials that are discussed elsewhere in this review. Diverse and ingenious approaches for the synthesis of covalent MOF-polymer hybrid materials has been the focus of many recent research efforts in order to bridge the gap between MOF and polymer. As such, sophisticated characterization techniques have been applied to elucidate the interface between these materials and decipher the MOF-polymer interactions at the atomic level.

2.3. Investigations of the MOF−Polymer Interface

While several different MOFs and polymers have been combined to form MMMs with a range of properties, only a few reports have aimed at directly analyzing the MOF and polymer interface at the atomic level. From an imaging perspective, several reports use a low temperature fracturing of

DOI: 10.1021/acs.chemrev.9b00575
Chem. Rev. XXXX, XXX, XXX−XXX

MMMs, where the hybrid material is soaked in liquid N_2 and fractured. SEM images are taken of the MOF−polymer composite fractured cross-section allowing for imaging of the interface.[34,54,73] Gascon and co-workers used a focused ion beam (FIB) SEM technique to more closely image the interface of CuBDC MOF nanosheets or regular MOF crystals and PI MMMs.[74] The FIB SEM carves out portions of the composite material and images these sections to analyze the MOF−polymer interface. They found that MOF nanosheets occupied more of the cross-sectional space compared to regular MOF crystals resulting in more selective permeation pathways for gas separations. Taking a polymer characterization approach, Long and co-workers used dynamic mechanical analysis (DMA) to analyze the interface between MOF-74 and a range of copolymers.[75] In this study, copolymers containing larger blocks that are more rigid in nature appeared to form less favorable interactions with the MOF particles compared to polymers containing higher soft block content. Using a nondestructive approach, the same group also reported the use of Raman spectroscopy to probe the homogeneity of the MIL-53 particles in MMMs using two different polymers.[76] Transmission electron microscopy (TEM) imaging has also been used to study the MOF−polymer interface by being able to identify areas of MOF aggregates in a material as well as areas of polymer aggregates.[77] In another report by Li and co-workers, an ultramicrotoming technique was used wherein MOF-polymer materials are sliced into thin layers (∼100 nm section) and imaged using TEM giving further insight into MOF-polymer interactions inside the particles.[78]

Other work analyzing the MOF−polymer interface has been focused on computational modeling. Maurin and co-workers first reported a model to analyze this interface and found a unique compatibility between ZIF-8 and PIM-1 (PIM = polymers of intrinsic microporosity) is due to the −CN functional groups on the polymer interacting with the secondary amines on the ZIF-8 linkers.[79] This model has been used to analyze the MOF−polymer interface of several MMMs containing a range of MOFs and polymers.[29,77,80] In particular, this model was used to examine the interaction of MMMs consisting of UiO-66 and a flexible polymer such as poly(ethylene glycol) PEG or PVDF compared to more rigid polymer such as polystyrene (PS) or PIM-1. The results indicate that more flexible polymers such has PEG or PVDF have a more favorable interaction with the UiO-66 compared to rigid polymers.[29] Following this report, analysis of the MOF−polymer interface in MMMs was recently examined by in situ solid state NMR (SS-NMR) in combination with theoretical methods.[81] As described earlier, PVDF-based MMMs with MOFs maintain porosity and displayed surface areas proportional to their MOF loading, whereas poly(ethylene oxide) (PEO)-based MMMs displayed no surface area at loadings as high as 70 wt % MOF.[32,34] To untangle this difference, UiO-66 MMMs were prepared using PVDF and PEO to determine the amount (if any) of polymer infiltration into the MOF pores. ^{13}C and ^{1}H SS-NMR studies indicated almost complete pore infiltration in the case of the PEO-based MMMs while little to no pore infiltration in the case of the PVDF MMMs. These results highlight the significance in the selection of polymers for MMMs and the importance of understanding the MOF−polymer interface in these materials. Overall, several elegant approaches have been utilized in the synthesis of MOF-based MMMs. These approaches have made promising strides toward designing highly functional materials across a range of applications from gas and liquid separations to water purification and chemical warfare agent degradation.

3. APPLICATIONS OF MOF-POLYMER MATERIALS

The fabrication of MOF-based MMMs has expanded rapidly over the past decade through the methods described in the previous section. Functional materials with high MOF loadings have been achieved through the careful selection of MOF and polymer components, and synthetic methods have enabled covalent linkages between the MOF and polymer in some MMMs. The overarching goal of these fabrication techniques is to design membranes with little to no voids at the MOF−polymer interface, such that any gas or liquid passing through the MMM is transported through the MOF pore. In the ideal MOF-based MMMs, the interfacial morphology between particles and polymer is well controlled to prevent suboptimal structures such as "plugged sieves", "matrix rigidification", or "sieve-in-a-cage" from forming (Figure 3). The high loading of MOF particles in the polymer matrix is also important to maximally exploit the MOF particles. In many applications, composite thin film membranes in which a thin MMM layer is fabricated on a porous substrate is preferred in order to obtain high flux. Thinner membranes are more susceptible to void formation, generating critical pinhole defects that hinders the separation ability of the membrane. As such, the control of interface between MOF particles and the polymer matrix is increasingly more important in thin film composites. Such materials should allow for tuning of the MOF pores to produce MMMs suitable for size exclusion or affinity-based separations, catalysis, and other membrane-based applications.

3.1. Gas Separations

Gas mixtures such as CO_2/CH_4, CO_2/N_2, propane/propylene, etc. are largely separated via an energy intensive process such as cryogenic distillation, liquid-phase adsorption, pressure swing adsorption, and others. Therefore, energy-efficient separation processes, such as membrane separations, have received increased attention.[82] The inherent porosity and uniform nanopore composition of MOFs makes gas separations an attractive application. The highly tunable property of MOFs, such as the functionalization of MOF linkers, can be used to tune the affinity of the MOF toward specific gas molecules. Pure, solid, crystalline MOF membranes have already shown potential for good gas separation performances in terms of permeability and selectivity; however, shortcomings in flexibility/brittleness, durability, complicated fabrication, and limited scalability have made these pure MOF membranes suboptimal candidates for commercialization. With these practical considerations in mind, the integration of MOFs into engineered polymer hybrid structures, such as MMMs, is a particularly attractive route for utilizing MOFs. As described above, MMMs improve the processability of MOFs by embedding these microcrystalline particles in a polymer matrix. In order to use MMMs for gas separation, the proper selection of both polymer matrix and MOF particles is essential to obtain high performance gas separation membranes for the certain separation targets.

3.1.1. Acid Gas Removal from Natural Gas. In natural gas production, a crucial step in the process is the purification of methane gas from other impurities such as CO_2 and H_2S, which is also known as acid gas. Currently, the acid gas is removed from raw natural gas by amine scrubbing to meet

DOI: 10.1021/acs.chemrev.9b00575
Chem. Rev. XXXX, XXX, XXX−XXX

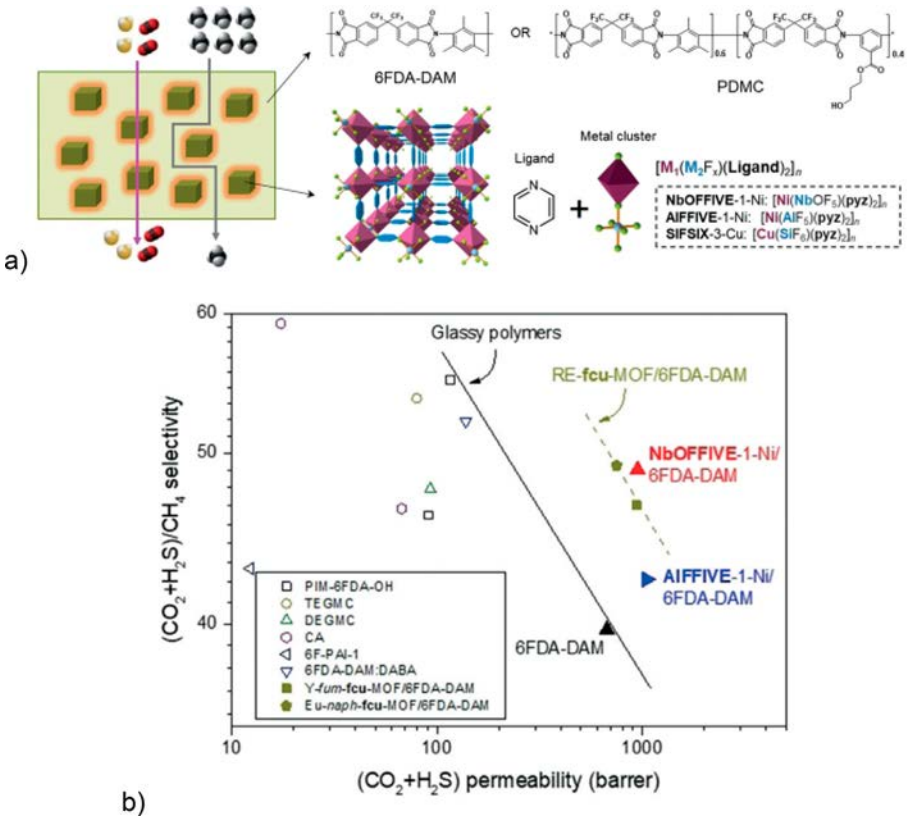

Figure 13. (a) Schematic of design approach using fluorinated MOF-based membranes for selective permeation of CO_2 and H_2S over CH_4. (b) Separation performance of 6FDA-DAM membrane, NbOFFIVE-1-Ni/6FDA-DAM MMM, and AlFFIVE-1-Ni/6FDA-DAM MMM for $H_2S/CO_2/CH_4$. Reprinted with from permission ref 84. Copyright 2018 Wiley Publishing Company.

pipeline specifications (<2% CO_2 and 4 ppm of H_2S), and this process consumes a sizable amount of energy.[83] H_2S removal from natural gas is especially challenging because of the close molecular kinetic diameter of H_2S (0.36 nm) and CH_4 (0.38 nm). Furthermore, this separation requires membranes with durability against the corrosive nature of H_2S and high feed pressures (30−60 bar). However, as the raw natural gas comes with high pressure, membrane separations do not require large compression energy to pressurize the feed gas stream. As such, membrane separation for natural gas separation has a potential to reduce the amount of energy needed compared to the abundantly consuming conventional process.

In the development of membranes for this application, Eddaoudi and Koros et al. reported MMMs containing rare earth MOFs and fluorinated MOFs for the removal of H_2S and CO_2 from raw natural gas.[83,84] Fluorinated MOFs such as SIFSIX $[Cu(SiF_6)(pyz)_2]_n$, NbOFFIVE $[Ni(NbOF_5)(pyz)_2]_n$, and AlFFIVE $[Ni(AlF_5)(pyz)_2]_n$ were combined with 4,4′-hexafluoroisopropylidene (6-FDA) polyimides (Figure 13). To improve the molecular interaction between the MOF and polymer matrix, the MOF particles were functionalized with 4-cyanopyridine. When comparing the various MOF composites (Figure 13) the NbOFFIVE-1-Ni/6FDA-DAM (DAM = 2,4,6-trimethyl-1,3-diaminobenzene) MMM showed far superior separation performance for total acid gas (CO_2+H_2S) removal from natural gas when compared to the existing glassy polymer-based membranes (e.g., cellulose acetate membranes). This study shows an efficient way to separate similar-sized molecules using a MOF-based MMM.

3.1.2. CO_2 Separation for Carbon Capture and Sequestration (CCS). CO_2 is a known greenhouse gas that contributes to the greenhouse effect, causing global warming. A huge amount of CO_2 gas is exhausted from power plants as a gas mixture of CO_2 and other gases. In order to reduce CO_2 emissions, CO_2 capture and sequestration (CCS) projects have been proposed, in which CO_2 gas is separated from gas mixtures and stored in geological rock formations that are typically located several kilometres below the Earth's surface. This method prevents CO_2 from entering the atmosphere; however, a major limiting factor of CCS is the cost of CO_2 separation. The current technology are liquid-phase adsorptions with aqueous ethanolamine that can be regenerated with heat, resulting in an extremely energy-intensive process. If this "amine scrubbing" approach was applied to every power station in the United States, CO_2 capture alone could amount to ∼30% of the country's growth in gross domestic product (GDP) each year.[82]

Combustion in powerplants results in a CO_2 containing flue gas making it one of the most sought after separations because the process can be retrofitted to existing units that generate two-thirds of the CO_2 emissions in the power sector.[85] In postcombustion, CO_2 needs to be separated from N_2 under humid conditions. As the gas has a low CO_2 partial pressure (CO_2 < 15% at atmospheric pressure), highly permeable CO_2 membranes are required in order to reduce the separation cost.[85−87] As such, a variety of studies regarding MMMs with MOFs have been reported for this application. Sivaniah et al. synthesized MMMs with gas permeable PIM-1 polymer and functionalized UiO-66 particles. The study highlighted the importance of particle size and functionalization of the MOFs, ultimately achieving improved CO_2 permeability and CO_2/N_2 selectivity.[86] For example, MMMs with 5−10 wt % loading of

DOI: 10.1021/acs.chemrev.9b00575
Chem. Rev. XXXX, XXX, XXX−XXX

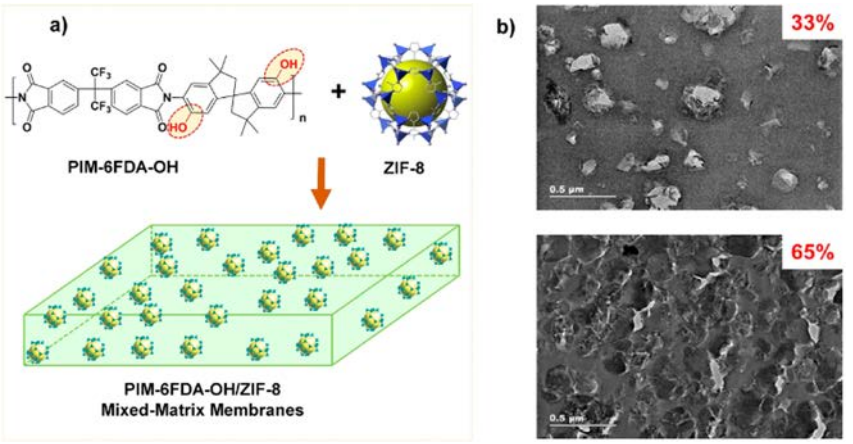

Figure 14. (a) Preparation of PIM-6FDA-OH/ZIF-8 based MMMs. (b) TEM images of PIM-6FDA-OH-based MMMs containing 33 and 65 wt %. Reprinted from ref 97. Copyright 2018 American Chemical Society.

small UiO-66-NH_2 particles (20−30 nm) showed improved CO_2/N_2 separation above the 2008 Robeson upper bound. Webley and Qiao et al. also proposed MOF scaffold/polymer membranes (MSPs) composed of an interconnected MOF scaffold and cross-linked polymer on the porous substrate, obtaining high MOF-loaded MMMs (47 wt % MOF) without defects.[88] To fabricate MSPs, MOF fibers were prepared on a filter paper surface by secondary growth where $Al(OH)_3$ particles and NH_2-benzene dicarboxylic acid (NH_2-bdc) ligand are used as seeds. After introducing α-bromoisobutyryl bromide (BiBB) to the MOF scaffold as an ATRP initiator, defect-free MSPs were fabricated through ATRP with poly(ethylene glycol)dimethacrylate which enabled the formation of the polymer matrix. MMMs with 47 wt % MOF loading displayed a CO_2/N_2 selectivity of 35 and CO_2 permeability of 2700 barrer, surpassing the 2008 Robeson upper bound and demonstrating 18-fold permeability enhancement as compared to pristine PEG membranes without compromising selectivity.

3.1.3. Propylene/Propane Separation. Propylene is one of the most important organic chemicals as it is a starting material for the synthesis of organic compounds and polymers such as polypropylene, propylene oxide, acrylonitrile, cumene, acrylic acid, and isopropanol.[89] Polypropylene is one of the most widely used synthetic plastics, and demand for polypropylene has been rising.[90] The physical properties of propylene are similar to those of propane, and the current method of separation is cryogenic distillation which requires a significant amount of energy.[82] Separation by membranes is expected to be an energy-efficient alternative method to cryogenic distillation as separation membranes do not require energy intensive phase changing steps. Various MOFs have been studied for propylene/propane separation, specifically ZIF-8 and ZIF-67 have demonstrated particularly good results for this application. The effective pore size of ZIF-8 is 0.40−0.42 nm (taking into account framework flexibility), which is suitable for separating propylene and propane.[91−93] To date, pure MOF membranes with ZIF-8 have demonstrated excellent permeability and selectivity for propylene/propane separation, beyond the 2008 Robeson upper bound.[94,95] As MMMs improve the processability of MOF membranes, MMMs with ZIF materials have potential for propylene/propane separation.

Koros et al. fabricated MMMs with ZIF-8 and the aforementioned 6FDA-DAM polyimide (Figure 13), showing that 48 wt % ZIF-loaded MMMs displayed a 258% improvement in permeability and a 150% improvement in selectivity compared to a pure 6FDA-DAM, polymer-only membrane.[96] Pinnau et al. synthesized MMMs with ZIF-8 particles and hydroxyl-functionalized microporous polyimide (PIM-6FDA−OH) in order to improve of compatibility between ZIF particles and the polymer matrix (Figure 14).[97] Though there was substantial aggregation, resulting in MOF clusters in the MMMs (Figure 14), no interfacial gaps in the MMMs were apparent. MMMs with 65 wt % ZIF-8 loading showed propylene permeability of 30 barrer and a propylene/propane selectivity of 31 in mixed gas permeation test, placing the performance above the 2003 Robeson upper bound.

ZIF-67 has proven to be intrinsically more efficient than ZIF-8 for propylene/propane separation due to the less dynamic Co−N bond compared to the Zn−N bond of ZIF-8. Therefore, to obtain MMMs with improved propylene/propane selectivity, ZIF-67 MMMs have been studied.[98] This smaller aperture size for ZIF-67 (3.31 Å) compared to ZIF-8 (3.42 Å) is suitable for propylene/propane separation.[99,100] Heseong et al. reported MMMs with 20 wt % ZIF-67-loaded MMMs with 6FDA-DAM, which showed higher propylene/propane selectivity and slightly lower propylene permeability compared to ZIF-8/6FDA-DAM MMMs.[98] This result suggests that ZIF-67 has a superior size sieving effect derived from its smaller aperture size compared to ZIF-8. The study further suggests that the selection of ZIF-8 and ZIF-67 can be optimized for this separation.

3.1.4. Hydrogen Gas Separations. Hydrogen (H_2) is desired as a potential clean energy alternative to fossil fuels, and high-purity H_2 gas is also wanted in the semiconductor, fine chemical, and optoelectronic industries.[101] For future energy production, H_2 gas also has an important role in an integrated gasification combined cycle (IGCC) process.[102] In these processes, H_2 gas needs to be isolated from a range of gas mixtures. Currently cryogenic distillation, pressure adsorption, and membrane separation are used to isolate H_2 gas. Among these techniques, separation of gas mixtures using membranes has been pursued as a more energy efficient process. For example, membranes have been used for the H_2/N_2 separation in the industrial ammonia synthesis process as well as for the H_2/CO_2 separation in an IGCC process. In the case of MMMs

DOI: 10.1021/acs.chemrev.9b00575
Chem. Rev. XXXX, XXX, XXX−XXX

for H_2 separation, selection of MOFs with relatively small pore size is required to obtain a size sieving effect due to the small molecular size of H_2 (kinetic diameter 0.29 nm).[103] Recently Zhu et al. reported MMMs with CAU-21-ODB (pore size ~0.33 nm) with PIM-1 as a polymer matrix.[103] Uniform CAU-21-ODB particles were synthesized using a microwave-assisted approach, showing good dispersibility in the polymer matrix. CAU-21-ODB/PIM-1 MMMs with ~15 wt % MOF loading showed improved H_2 permeability and H_2/N_2 selectivity of 7199 ± 117 Barrer and 127, respectively, for a H_2/N_2 mixed gas permeation test (Figure 15). The separation performance

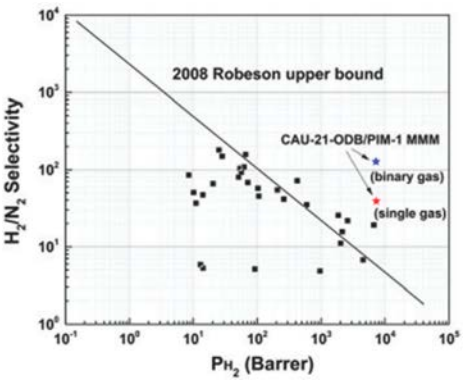

Figure 15. H_2 permeability and H_2/N_2 selectivity of CAU-21-ODB/PIM-1 MMM and reported relevant MMMs (squares show the single gas permeation data. Reproduced with permission from ref 103. Copyright 2019 The Royal Society of Chemistry.

far surpassed the 2008 Robeson upper bound. The H_2/CO_2 separation by CAU-21-ODB/PIM-1b MMMs was also studied, showing 7218 Barrer of H_2 permeability and H_2/CO_2 selectivity of 4. Another interesting approach to enhance the membrane performance of MMMs has been reported with ZIFs. Most MMMs with ZIFs show an increase in gas permeability but lack in gas selectivity because the ZIF pore size (effective pore size of ZIF-8 is 0.40−0.42 nm) is not small enough to have a size-sieving effect on H_2. Recently, a new ZIF material (named ZIF-L) was reported, showing selective H_2 permeation over CO_2 due to strong CO_2 adsorption to the ZIF-L.[104] Wang et al. reported MMMs with ZIF-L and a highly gas permeable hydroxyl group-containing polyimide, showing the improved H_2/CO_2 selectivity of 13.4 and maintaining the H_2 permeability of 260 Barrer in a single gas permeability test.[105] In contrast, the pristine polyimide membrane that displayed H_2/CO_2 selectivity and H_2 permeability of 1.8 and 220, respectively. The study suggests that MOF selection is crucial to further improve the separation capabilities of MMMs.

3.2. Water Purification

Gas separation has been the primary focus for application of MOF-based MMMs; however, these MMMs also provide an opportunity to address other important separation problems. Currently, about 780 million people worldwide lack access to clean water resources and data suggests this number is growing.[106] New materials for achieving water purification has captivated the attention of many researchers.[107,108] The synthesis of water stable MOFs (i.e., UiO-66, ZIFs) has enabled the use of MOF-based MMMs for the treatment of water.[109] MOF-based MMMs, through the tunability of MOF particles, presents an opportunity to purify water from contaminants of varying sizes and chemical properties.

3.2.1. Dye Separations. Dye separations are the most studied form of liquid separations with MOFs due to the facile nature of these experiments and potential relevance to the removal or separation of organic pollutants from water.[110] The use of dyes has grown exponentially over the last half century in many industries such as textiles, paper manufacturing, and the food industry; however, efficient methods of separating dyes from aqueous sources are lagging behind.[111] As such, dyes oftentimes end up in water streams and have been deemed harmful toward the environment. This has motivated studies on MOF-based MMMs as a potential method to remove dyes from aqueous sources.[34,66,112−114]

Engineering of MOF-based MMMs for dye separations have been based on either size or charge.[32,34,66,112,113,115,116] Zhang et al. developed the use of ZIF-8 poly(sodium 6-styrene-sulfonate) (PSS) MMMs for the separation of dyes from aqueous media based on size.[112] Retention of larger dyes such as methyl blue (MB) was exhibited by these membranes, whereas smaller dyes such as methyl orange (MO) displayed less retention. Building off this work, the same group synthesized ZIF-8 PEI MMMs and screened a wider range of dyes, such as Congo Red (CR) and Acid Fusion (AF). The MMMs showed a higher retention of dyes based on the size of the molecules (MB > CR > AF > MO).[117] Other groups have also used the ZIF-8 polyamide MMMs for the separation of dyes, such as Reactive Blue 2 (RB2) and Reactive Black 5 (RB5), based on electrostatic charge.[118] Other groups have separated Coomassie blue (CB) and MO using UiO-66 in a PVDF or polystyrene-*block*-polybutadiene (SBS) based MMM, where 99% removal of CB from a mixture of the two dyes was achieved (Figure 16).[32,34]

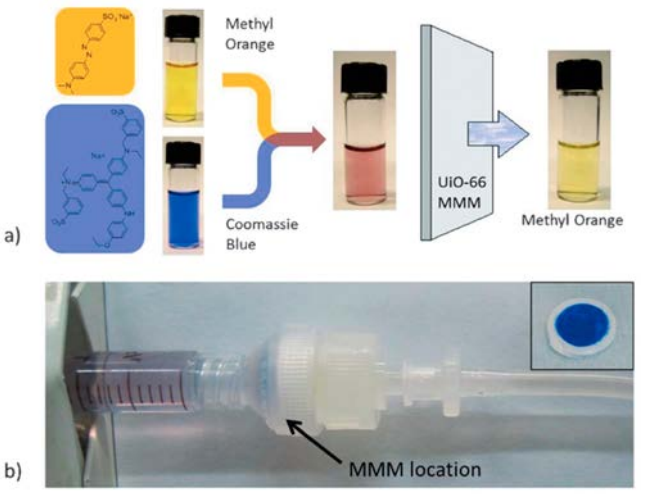

Figure 16. (a) Pictorial depiction of the separation of MO and CB dyes using a UiO-66 PVDF MMM. (b) Image of the separation filter housing set up and retention of CB dye on MMM. Reprinted with permission from ref 34. Copyright 2015 Wiley Publishing Company.

3.2.2. Toxic Heavy Metal Separations. The design of materials for the sequestration of heavy metal ions in aqueous media is sought for the removal of dangerous metals, such as lead, from drinking water. Such membranes could also be useful for recycling and recovering precious metals from waste streams or the recycling of radioactive materials from nuclear

DOI: 10.1021/acs.chemrev.9b00575
Chem. Rev. XXXX, XXX, XXX−XXX

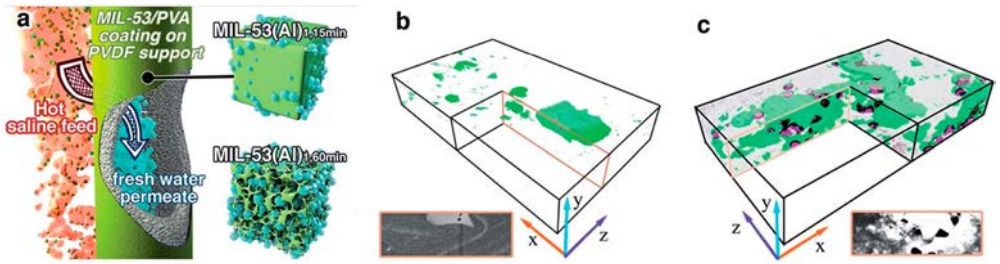

Figure 17. (a) Diagram of desalination via MIL-53 (Al) PVDF MMMs. (b) Surface-rendered views of segmented FIB-SEM tomograms of MIL-53 (Al) MMMs. (c) Surface-rendered views of segmented FIB-SEM tomograms of defective MIL-53 (Al) MMMs. Reprinted with permission from ref 134. Copyright 2018 The Royal Society of Chemistry.[134]

energy production.[109] Due to their inherent porosity, large surface areas and chemical tunability, MOFs and MOF-based MMMs have emerged as a potential candidate for this application.[115,119−123] Wu and Tang et al. synthesized an IRMOF-3 graphene oxide composite material with a maximum adsorption amount of Cu^{2+} of 254 mg g^{-1}.[124] This material was then embedded into a polydopamine-coated membrane and displayed 90% rejection of Cu^{2+} ions from aqueous media. Rana et al. used electrospinning to synthesize composite membranes with Zr^{4+}-based MOF-808 and tested it for the sequestration of two divalent metals, Cd^{2+} and Zn^{2+}, from aqueous media.[125] These materials showed ∼55% removal for Cd^{2+} with a maximum adsorption capacity of 225 mg g^{-1} and ∼70% removal for Zn^{2+} with a maximum adsorption capacity of 287 mg g^{-1}. Wang et al. used UiO-66-NH_2 PSP MMMs to extract Cr^{4+} ions from water and the PSP-derived membrane (60 wt % MOF) displayed 80% removal of Cr^{4+} with a maximum separation capacity of 8 mg g^{-1}, whereas the physically mixed MOF polymer membrane displayed 41% removal of Cr^{4+} with a maximum sorption capacity of 5 mg g^{-1}.[59] Recently, Queen et al. synthesized a MIL-100(Fe) and polydopamine (PDA) where dopamine monomers are polymerized through an anaerobic oxidation of dopamine from the redox active Fe^{3+} SBU sites.[126] These membranes displayed 99.8% removal of both Hg^{2+} and Pb^{2+} extracting 1634 mg and 394 mg per gram of composite, respectively. Building off of this work, the same group showed that their technology could be used to recycle precious metals such as Au^{3+} from an aqueous solution.[127] Queen et al. used the redox active MIL-100(Fe) and PpPDA polymer (PpPDA = poly-(para-phenylenediamine)) membrane to sequester Au^{3+} from aqueous solutions at record breaking rates (934 mg g^{-1}) with 99% removal each cycle for up to four cycles.

3.2.3. Desalination. Worldwide shortages in fresh water have motivated researchers to develop technologies for the desalination of ocean water.[128] Development of a nonenergy intensive method for the separations of salts would lead to an advancement toward bringing fresh water resources to countries across the world.[129,130] MOF-based MMMs offer new opportunities to address this problem.[131,132] Li et al. fabricated UiO-66 based membranes using an in situ solvothermal synthesis methods to grow MOFs on alumina hollow fibers.[133] Desalination experiments were conducted on these materials, and the results indicate that these membranes exhibit multivalent ion separation by rejecting ∼85% Ca^{2+}, ∼99% Mg^{2+}, and ∼99% Al^{3+}. Membrane stability was also tested, and the membranes showed no degradation upon exposure to saline for 170 h as evidenced by PXRD. Recently, D'Alessandro et al. reported the use of poly(vinyl alcohol) (PVA, Figure 2) and MIL-53(Al) composite materials for desalination studies.[134] The MIL-53(Al) synthesis was varied to modulate the amount of defects in the material and develop a hierarchical pore structure. The MIL-53(Al) and PVA were blended together as a physical mixture and subsequently coated on the surface of PVDF hollow fibers. Membranes prepared with defective MOFs were shown to significantly increase the water flux across the material leading to higher water transport efficiency (Figure 17). Desalination experiments indicate an essentially perfect salt rejection rate (99.99%) when tested for the desalination of a 100 g L^{-1} solution.

3.3. MOF-Polymer Composites for Toxic Chemical Protection

One of the many application areas where MOF-polymer composites have made an impact is in the mitigation of toxic chemicals, including sorption of toxic industrial chemicals (TICs) and sorption and neutralization of chemical warfare agents (CWAs), such as mustards and nerve agents. Outlined in a review on this topic,[135] MOFs have had considerable success in the sorption and catalytic breakdown of nerve and blister agents, the two highest risk classes of CWAs, as well as a number of TICs such as NH_3, H_2S, and Cl_2. MOFs are a promising solution to this problem, but development of MOF-based composites that are compatible with soldier and civilian protection (in the form of membranes and textiles) is essential to the successful implementation of MOFs for this application. The challenge is designing a MOF-polymer system that preserves MOF sorption and catalysis and can be readily applied to gas masks, suits, and shelters. A range of polymer support strategies, including atomic layer deposition (ALD) coated fibers,[136−142] MMMs,[33,143−145] electrospinning,[146−151] and others,[61,152−156] have been investigated to move MOFs toward field-ready use. The goal of providing protection from acutely toxic chemicals has inspired some unique MOF-polymer combinations that outperform the traditional activated carbon-based materials.

For this particular application, the composites are evaluated on three basic merits: effectiveness of MOF incorporation into polymer form, ability of composite to provide protection, and readiness of composite to be incorporated into a garment. As the field develops, the literature highlights new and effective forms of composites with an emphasis on those with high MOF content and accessibility. Tied to this first goal, is the availability of MOF for mitigation usually assessed by N_2 accessible surface area, TIC sorption, and CWA hydrolysis rates. Early development of MOFs for CWA simulant and agent degradation is outlined in detail in two recent reviews.[157,158] The last merit of MOF-polymer composites is

DOI: 10.1021/acs.chemrev.9b00575
Chem. Rev. XXXX, XXX, XXX−XXX

the most difficult to quantify (garment suitability), but mechanical properties of composites have been reported as a proxy for strength and moisture vapor transport rate (MVTR) and aerosol filtration efficiency have been studied as well. High MVTR and aerosol filtration efficiency allow more evaporative cooling and protection, respectively, both important metrics for composites as suitable materials for prolonged protection. As MOF-polymer composites progress in this emerging application, the emphasis must shift from discovery to comparisons to current technology and establishing performance metrics.

In 2014, Parsons et al. demonstrated that atomic layer deposition (ALD) could be used to coat a range of polymer fibers with metal oxides to serve as MOF nucleation sites. The original work demonstrated the deposition of Al_2O_3 onto polypropylene fibers and the subsequent growth of HKUST-1 with access to MOF microporosity and improved performance for the sorption of NH_3 gas.[136] Subsequent work showed the application of this technique for the growth of a series of Zr^{4+}-MOFs (UiO-66, UiO-66-NH_2, UiO-67) on polyamine (PA-6) fibers with TiO_2 as the ALD nucleation coating layer (Figure 18).[137] SEM and TEM images showed a conformal coating of the MOF on the fibers with all three MOFs. The ability of these MOF fibers to fight nerve agents was evaluated first by hydrolysis of dimethyl 4-nitrophenylphosphate (DMNP), then the nerve agent GD, both of which are effectively degraded by these composites. The same group also investigated the role of different oxides and noncovalent attachment methods to explore their effect on composite properties and DMNP hydrolysis but found improvement over TiO_2/PA-6 system performance in the hydrogen-bonded system.[138,139,141] While this is a more general method for MOF-polymer coupling, and the DMNP hydrolysis rates are the highest for ALD fibers, it relies on noncovalent interaction for MOF attachment that is not tested for strength. ALD coating has also been used to grow MOF sheets that can absorb both NH_3 gas and the sulfur mustard simulant 2-chloroethyl sulfide (2-CEES) under humid conditions.[142] A follow-up study of this work explored the performance of ALD fiber MOF hybrids against these threats as well as their MVTR and aerosol filtration efficiency. This study showed that MOF composites maintain MVTR of polypropylene and flame resistant textiles MOFs are grown and outperform the base textiles in terms of NH_3 and 2-CEES protection. In addition, the MOF textiles were compared to commercial textiles for aerosol protection and outcompete sorptive carbon materials and fall short of best aerosol protective textile, but MOF composites top this aerosol textile for MVTR. This is the first comprehensive study of MOF composites as true candidates for combat textiles and serves as a model for future reports that seek to make an impact in this space. ALD-coated fibers with MOF attached show promise for CWA mitigation textiles but are limited mostly by difficulties in large-scale processing of ALD fiber mats and generality of composites to a wide range of MOFs. The future of this work will rely on the continued expansion of versatility of MOF growth from metal oxide layers and these ALD fibers outcompeting composite structures with fewer processing steps.

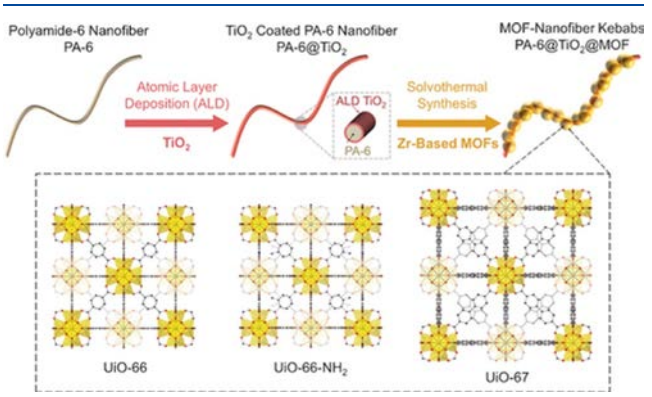

Figure 18. Schematic of ALD coating of fibers and subsequent MOF growth. Reprinted with permission from ref 137. Copyright 2016 Wiley Publishing Group.

MOF-based MMMs have been examined for the sorption and deactivation of TICs and CWAs. A proof-of-concept study used HKUST-1 MMMs for the sorption of NH_3 under humid conditions.[33] In this report, DeCoste et al. demonstrated that HKUST-1/PVDF MMMs with 30, 50, and 67 wt % MOF gave

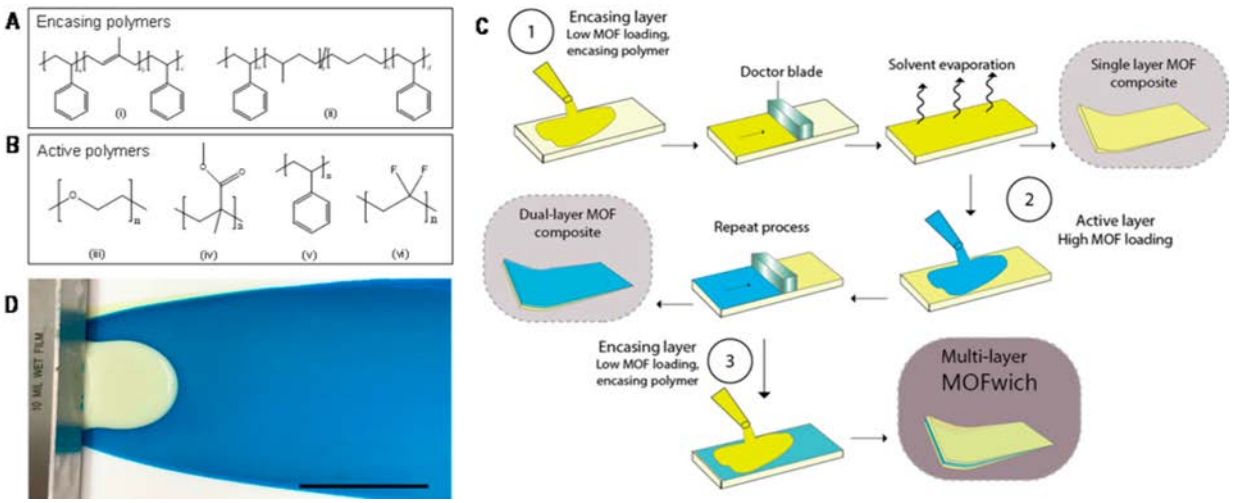

Figure 19. (A,B) Polymers used for encasing. (C) Step-by-step method used for multilayer MOF MMM synthesis, and (D) photograph of multilayer MOF MMMs (MOFwich). Reprinted from ref 144. Copyright 2018 American Chemical Society.

DOI: 10.1021/acs.chemrev.9b00575
Chem. Rev. XXXX, XXX, XXX−XXX

increasing NH_3 sorption with MOF loading. Equally important, the MMM form factor protected the HKUST-1 from humid conditions that decomposed the HKUST-1 free powder but allowed for consistent uptake of NH_3 in the MMM over a four-week test period with the MMM exposed to 90% relative humidity. In another interesting application of MOF MMMs for TIC sorption, the Qian group used MIL-53-NO_2(Al)/PVDF MMMs as sensors for H_2S.[145] MMMs with up to 70 wt % were fabricated where the reduction of nitro groups on the MOF ligands (to amines) by H_2S resulted in a detectable fluorescence from MIL-53-NH_2(Al). It was found that the MMMs showed selectivity for H_2S over acid and halogen salts as well as other reducing agents and 3 orders of magnitude lower detection limit than the free MOF powder (92 nM for the MMM vs 70 μM for the MOF alone) attributed to the availability of MOF in membrane over aggregated powder. Peterson and co-workers expanded upon the use of MMMs to bring MOF composites even closer to field applications. Using a polystyrene-*block*-polyisoprene (SIS) as a thick, rubbery polymer for HKUST-1 MMMs, a composite was formed that had both enhanced chemical protection and moisture-transport properties.[143] The MMMs, up to 50 wt % MOF, demonstrated orders of magnitude longer breakthrough times for the sulfur mustard simulant 2-chloroethyl ethyl sulfide (2-CEES) while allowing for increased water vapor transport when compared to pure SIS only membranes. However, this study also highlighted a decrease in mechanical properties of the membrane due to incorporation of MOF, demonstrating the need for further optimization. The same authors also developed multilayer MOF MMMs (so-called "MOFwich" membranes) that were synthesized with multiple layers of differing polymer and MOF combinations (Figure 19).[144] Membranes consisting of outer layers of flexible polymers and low MOF loading with an inner layer of high-MOF loading MMM were fabricated to address multiple threats in a single material. One example effectively combined HKUST-1 and UiO-66-NH_2 into two layers of polystyrene-*block*-poly(ethylene-*ran*-butylene)-*block*-polystyrene (SEBS) polymer for sorption of 2-CEES and breakdown of nerve agents. The clever and effective use of a layered system reinforces that MOF composites for protection do not necessitate a single solution but can be a multicomponent form and can be tailored to specific area protection and is needed. For practical applications, solution cast thin films have slightly poorer moisture transport than other composites highlighted here (ALD and electrospun fibers) but represent a simple and general method to make a diverse set of high MOF wt % composites. Because the form factor for protective equipment is varied (i.e., gas mask, gloves, clothing), solution processed MOF-polymer hybrids have great potential to be applied as flexible layers or coatings in these protective products.

Several methods are available to move away from the membrane format to obtain other MOF-polymer hybrid form factors. Electrospinning is one of the most common strategies for incorporating additive particles into polymer fibers for a range of applications.[159] Electrospun fibers are often collected as mats with fabric-like properties. In 2011, two concurrent reports applied this method to MOF-polymer fibers with MOF loadings of 50 wt % or greater and retention of crystallinity and microporosity.[160,161] UiO-66 was cosprayed onto a silk polymer mat, entrapping the particles in the mesh.[148] These fibers were then evaluated for their hydrolysis of nerve agent simulants diisopropylfluorophosphate (DIFP) and dimethyl methylphosphonate (DMMP), as well as mustard simulant 2-CEES. The electrospun fibers maintained much of the degradation kinetics of the neat MOF powders, indicating good mass transfer properties. In subsequent studies, UiO-66-NH_2 was spun directly in and on the surface of polymer fibers by suspending the MOF powders in the casting solution of PS, PVDF, or polyacrylonitrile (PAN).[146,151,162,163] Each of these systems provided additional information to the practical understanding of MOF-polymer composites for toxin mitigation. The first explores PVDF fibers with up to 33 wt % MOF were evaluated for Cl_2 sorption and *O*-pinacolyl methylphosphonofluoride (GD) degradation (UiO-66-NH_2 is known to be reactive with both of these agents).[162] In the next study, UiO-66-NH_2/PS composites showed higher loading (50 wt %) and methods for both trapping MOF inside or outside polymer resulting in slightly better for Cl_2 and GD mitigation.[146] Tighter junctions between MOF and polymer was achieved by direct growth of UiO-66-NH_2 particles onto polyacrylonitrile (PAN) fibers electrospun with 2-amino-terethphalic acid and resulting in higher Cl_2 loading.[163] Finally, in an effort to assist in the mitigation of nerve agents, groups have cospun additives. Jones et al. reported a PVDF/TiO_2/UiO-66-NH_2/triethanol amine composite that improves on previous PVDF electrospun fibers but also reported a MVTR that is on par with commercial protective fabrics.[151] Taking advantage of the photothermal catalytic enhancement from reported for dopamine-melanine particles in sunlight,[164] UiO-66-NH_2 was coated on these photosensitive microparticles and then electrospun in 55 wt % PAN/MOF fibers increased DMNP hydrolysis rates.[150] Another report of growing MOFs from electrospun fibers takes this idea a step further by first spinning a mixture of polyvinylpyrrolidone and zirconium(IV) acetate into fibers and calcining the polymer away. The resultant ZrO_2 fiber mats were used as the metal precursor for synthesis of UiO-66, UiO-67, and UiO-66-NH_2 films, resulting in a strikingly high MOF content of >90 wt % (Figure 20).[149] These MOF dominant films were self-standing mesoporous

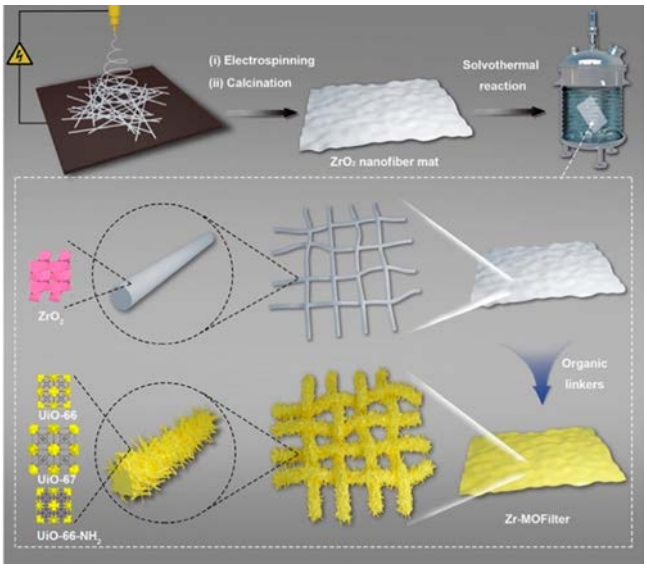

Figure 20. Fabrication method of high MOF mats derived from electrospun fibers. Reprinted with permission from ref 149. Copyright 2018 American Chemical Society.

DOI: 10.1021/acs.chemrev.9b00575
Chem. Rev. XXXX, XXX, XXX−XXX

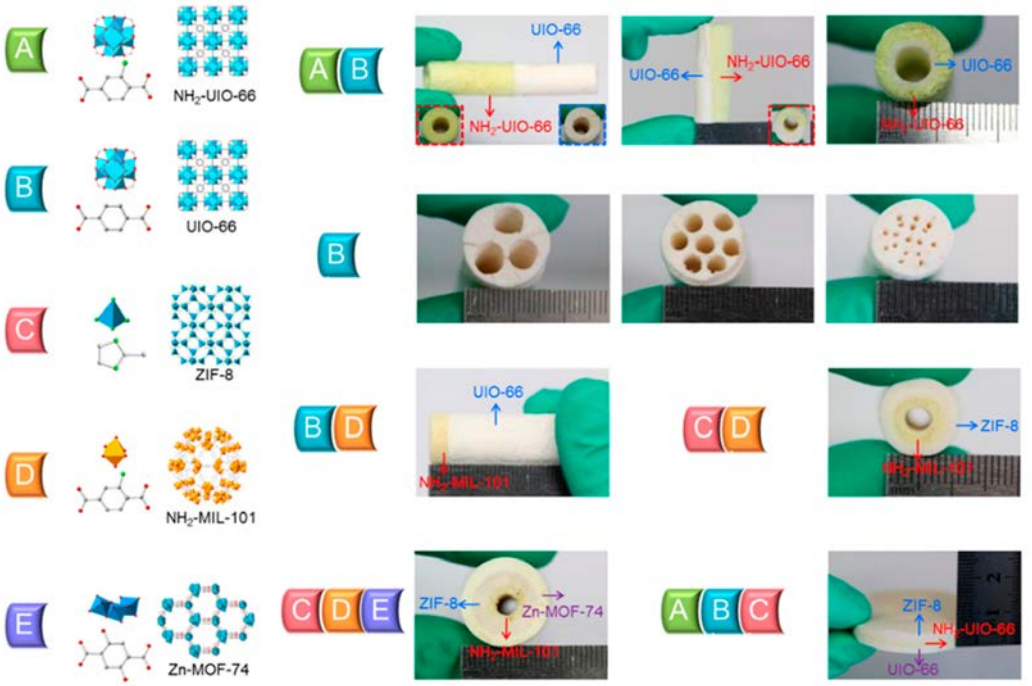

Figure 21. Chemical structures of MOFs used for MOF foam synthesis. Photographic images of multicomponent MOF hollow tube composites. Reprinted from ref 174. Copyright 2017 American Chemical Society.

mats with higher BET surface areas than MOF powders and tensile strengths only an order of magnitude lower than >50% UiO-66 MOF MMMs.[34] The MOF fiber mats were top performers as materials for DMNP hydrolysis when compared to other studies. Overall, electrospun MOF composites described here are a relatively simple process compared to ALD-MOF fibers but require specialized equipment for scale up. These composites have only been tested on a narrow subset of MOFs (mostly UiO-66-NH_2) but have real promise for making practical filtration and textile materials.

While MOF composites with ALD fibers, MMMs, and electrospun fibers have driven discovery, these composites have matured to address specific goals of protection. There are still studies are pushing the boundaries of MOF-polymer composites with new techniques by focusing on discovery of new materials that approach the problem in unique ways. For example, surface-functionalized cotton to facilitate UiO-66-NH_2 growth with the goal of making a simple wearable garment for protection have been reported.[153,154] Ryu and Jung et al. tested MOF/cotton materials as a barrier for the CWAs GD and sulfur mustard and observed an order of magnitude decrease in permeation of the agents over bare cotton. Unfortunately, this direct CWA permeance is not benchmarked to state-of-the-art materials or other MOF-polymer materials. Another creative form factor for MOF-polymer composites is additive manufacturing, which is an emerging application of MOFs. Using commercial acrylates mixed with a photoinitiator and UiO-66, it was shown that a simple free-standing composite with 74 wt % MOF that was accessible to degrade DMNP.[156] In another study, PSP was used by Cohen et al. to make covalent composites of polyamide-6,6 (PA-66) and UiO-66-NH_2 in the form of ∼30 wt % fibers.[61] The MOF, with its reactive amine groups, is used as a cross-linker in the PA-66 synthesis, so MOF was evenly incorporated into fiber growth and allowed higher hydrolysis rates than UiO-66/PA-66 physical mixtures.

3.4. Applicable MOF-Polymer Form Factors

Other approaches to synthesizing MOF-polymer composites to produce materials in form factors other than membranes have been reported. The motivation for this work is focused on bringing MOFs closer to an industry application by implementing already well developed and scalable engineering-based techniques such as extrusion, pressing, granulation, and freeze-drying. Pressing, extrusion, and granulation MOF powder into pellets has been previously explored; however, these materials are outside the scope of this review as they do not use polymer binders.[165−171]

Wang et al. designed a continuous phase transformation process where a series of MOFs (HKUST-1, ZIF-8, MOF-74, UiO-66) were molded into porous foam materials.[172,173] This method uses a core−shell approach where, for example, HKUST-1@Fe_3O_4 nanoparticles are prepared through a secondary growth method, sonicated in acetone, and subsequently added to a carboxymethylcellulose (CMC) solution and stirred at a high speed. The resulting solution is then freeze-dried into a cylindrical shape resulting in light foams of varying MOF incorporation based on loading (25−45 wt %). The standalone foams display good retention of MOF crystallinity but low retention in MOF porosity. The HKUST-1 foam was also used to test whether the MOF was catalytically active in this form factor, and the HKUST-1 foam displays excellent performance for C−H oxidation of diphenylmethane to benzophenone to with 92% conversion, as compared to 58% for a polymer-free pressed MOF pellet. Building from this work, Wang and co-workers prepared various hollow tube (e.g., Janus, coaxial, and cellular) MOF polymer composites with sodium alginate as a polymer binder (Figure 21).[174] These materials are prepared by freezing an aqueous suspension of MOF particles and sodium alginate around a cylindrical template used to create the hollow cavity. The template is then removed, and the resultant material is

DOI: 10.1021/acs.chemrev.9b00575
Chem. Rev. XXXX, XXX, XXX−XXX

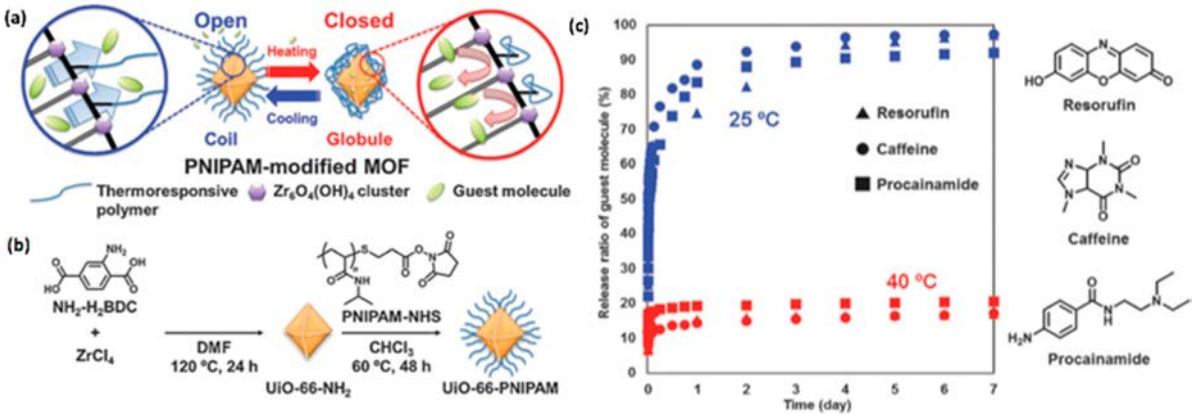

Figure 22. (a) On−off gating of surface grafted PNIPAM for controlled release of guest molecules, and (b) kinetics of guest release above and below the LCST. Reproduced with permission from ref 186. Copyright 2015 The Royal Society of Chemistry.

sublimed through the aforementioned freeze-drying technique. Interestingly, these materials can be prepared with high MOF loadings (up to 70 wt %), while controlling for the hole diameters of the tubes and maintaining almost all MOF porosity. Hollow tube composites were made with a range of MOFs (UiO-66, UiO-66-NH_2, ZIF-8, MIL-101-NH_2, and MOF-74(Zn)) and with multicomponent systems where two or more MOFs were incorporated into the same composite (Figure 21). These multicomponent composite materials maintained the properties of all incorporated MOF components as demonstrated through heavy metal and dye extraction experiments. The hybridization of MOFs and polymers through MMMs or other MOF-polymer form factors has shown promise in making MOFs a more useful material. However, most of the applications reported to date remain proof-of-concept studies, and the field will benefit more by moving toward application studies with actual field conditions.

4. POLYMER-GRAFTED MOF SURFACES

Covalent attachment of polymer chains to MOF surfaces have been investigated to provide robust material properties or compatibility with matrix components. In general, there are two common routes toward polymer-functionalized surfaces: grafting-to and grafting-from.[175−180] In the grafting-to approach, presynthesized polymers are end-functionalized with a reactive group complementary to the surface functionality to which the chain is grafted. A significant advantage of this approach is the ability to fully characterize the polymer prior to surface grafting; however, grafting-to suffers from poor grafting density, which limits the mass fractions of polymer that can be achieved. In contrast, the grafting-from technique begins by functionalizing the surface with initiator groups from which polymer is grown. This technique allows for highly dense brushes and consequently, high mass fractions of polymer. However, characterization of the polymer brushes is challenging, as cleavage and isolation of polymer chains from the surface is required for most analytical techniques.

The current literature on the topic of covalent attachment of polymer chains to MOF particles is predominately focused on grafting-to and grafting-from methodologies. That stated, other pioneering studies on MOF-polymer hybrids often relied on simple adsorption or layer-by-layer deposition of polymer chains on MOF surfaces. While a detailed discussion of these earlier works is outside the scope of this review, we highlight some important examples. In 2008, Kaskel and co-workers successfully incorporated Cu_3(benzene tricarboxylate)$_2$ MOFs into the pores of polymerized high internal phase emulsions (polyHIPEs) by loading the MOF precursor materials into the polyHIPE pores followed by solvothermal MOF synthesis.[181] Following the study by Kaskel, Bradshaw and co-workers reported in 2010 the growth of HKUST-1 and CPO-27 MOFs inside millimeter-sized microporous polyacrylamide (PAM) beads.[182] MOF growth in the bead pores was accomplished by adding the PAM beads to a typical synthesis of HKUST-1 or CPO-27. This simple method worked because the PAM beads contain terminal amide functionalities that can serve as anchoring points for the growing MOFs. In 2013, the Qui group used sulfonated PS particles to grow highly monodisperse, spherical, and hollow MIL100-Fe MOFs in a step-by-step fashion.[57] The same year, Bradshaw, Huo, and co-workers also constructed hollow spherical MOFs using Pickering emulsions to locate preformed MOFs (e.g., ZIF-8, MIL-101) on the droplet exterior followed by polymerization of the droplet exterior.[183] These examples highlight some of the possibilities for creating MOF-polymer hybrids, but these methods generally lack specificity and control at the MOF−polymer interface. The rational design of either anchoring points for polymers to attach (grafting-to) or initiating sites on MOFs from which to controllably grow polymers (grafting-from) allows for more precise control of composite structure and is the focus of the following section.

4.1. Grafting-to Methodologies

In general, the grafting-to strategy is simpler, as grafting-from surface-initiated polymerizations have inherent challenges, such as difficult characterization of the initiator-functionalized surfaces and the resulting polymer brushes. As such, the first examples of the covalent attachment of polymer chains to MOF surfaces utilized the grafting-to method. Some of the earliest examples of grafting polymers to MOF surfaces involved the attachment of various polymers to Gd-based MOFs for medical imaging applications. Boyes and co-workers[184] synthesized a functionalized polymer using reversible addition−fragmentation chain-transfer (RAFT) polymerization, containing a thermally responsive, poly(*N*-isopropylacrylamide) (PNIPAM) block, a pentapeptide targeting block or methotrexate functionalized block, and a fluorescently tagged block. Aminolysis of the RAFT trithiocarbonate group allowed for anchoring to a Gd^{3+}-MOF surface via

DOI: 10.1021/acs.chemrev.9b00575
Chem. Rev. XXXX, XXX, XXX−XXX

Gd^{3+}-thiolate ligation. These functional MOF-polymer hybrids were shown to have excellent properties for magnetic resonance imaging (MRI) contrast, with T1 relaxation times on the same order as current clinically used Gd^{3+}-based contrast agents. In a follow up report by the same group, a wide variety of homopolymers synthesized via RAFT polymerization including poly(*N*-(2-hydroxypropyl) methacrylamide), poly(*N*-isopropylacrylamide), PS, poly(2-(dimethylamino)-ethyl acrylate), poly(((poly)ethylene glycol) methyl ether acrylate), and PAA were grafted-to Gd^{3+}-MOFs.[185] Attachment of this suite of polymers allowed for tuning of the T1 relaxation times, where hydrophilic polymers gave increasing long relaxation times as the polymer molecular weight was increased.

Several studies have also utilized the grafting-to method to attach functional or stimuli-responsive polymers to MOF surfaces. The first example to explicitly demonstrate thermally responsive behavior in polymer-grafted MOFs was accomplished by Sada and co-workers, who grafted PNIPAM to the surface of UiO-66 particles (Figure 22).[186] PNIPAM is known for stimuli-responsive applications as it displays a lower critical solution temperature (LCST) near physiological conditions, making it particularly attractive for biomedical applications.[187] PNIPAM was synthesized by RAFT polymerization and functionalized with an *N*-hydroxy succinimide activated-ester end group, which was subsequently coupled to exposed amino groups on UiO-66-NH_2. Analysis by ^1H NMR revealed that about 11% of the ligands were functionalized with the polymer, suggesting that polymer grafting occurred primarily on the particle surface. After showing that small molecules could still enter the MOF interior of the polymer-grafted materials, the MOFs were loaded with guest molecules, including resorufin, caffeine, and procainamide. Due to the LCST behavior of the PNIPAM chains, internalized cargo loaded in the polymer-grafted MOFs could be controllably released by adjusting the solution temperature. Above the LCST, the polymer is desolvated and collapsed on the MOF surface, trapping the guest molecules. When the solution temperature was cooled to below the LCST, the polymer becomes solvated and extends from the MOF surface, allowing for escape of the guest molecules.

Wuttke, Lächelt, and co-workers grafted fluorescently tagged polymers selectively to the surface-exposed carboxylate linkers of MIL-100(Fe).[188] Both amino-functionalized PEG and Stp10-C, an oligoamino amide containing a terminal thiol, were grafted to the MIL-100(Fe) surface via carbodiimide coupling in aqueous conditions. Particle size measurements by dynamic light scattering (DLS) confirmed the high colloidal stability of the polymer-functionalized particles, and BET isotherms indicated a modest drop in surface area due to pore blockage by the polymer surfaces. Because the Stp10-C polymer contained a terminal thiol, a fluorescent label Cy5 was attached via thiol-maleimide conjugation to give dye labeled MIL-100(Fe) surfaces. Fluorescence correlation spectroscopy (FCS) was then used to measure the diffusion coefficient of the dye molecules and confirm the surface grafting. When nonsurface grafted Stp10-C*Cy5 was measured with FCS, an effective hydrodynamic radius of 1.1 nm was found. In contrast, when the dye-labeled MOFs were measured, an effective size of 56 nm was found, which agreed well with measurements from DLS. The authors went on the explore the cellular uptake of the polymer grafted MOFs, which were found to be taken up effectively in N2A cells with virtually no cytotoxicity at loadings as high as 300 μg/mL. Lei and co-workers also utilized grafting-to strategies for biomedical applications, creating poly(methacrylic acid) functionalized UiO-66 particles with immobilized pectinase.[189] In this example, poly(*tert*-butyl methacrylate) was synthesized using an azide functional ATRP initiator and grafted to the surface of alkyne functional UiO-66 using copper-mediated azide−alkyne click chemistry. Following hydrolysis of the *tert*-butyl esters, poly(methacrylic acid) polymers were exposed on the MOF surface to which pectinase was immobilized by mixing in a citrate buffer. The authors showed that the surface-tethered enzymes maintained high activity in a much wider range of pH and temperature than the free enzyme, highlighting the utility of polymer/MOF hybrid materials.

4.2. Grafting-From Methodologies

Grafting-from methodologies are a versatile route toward MOF-polymer hybrid materials, as a wide variety of polymers can be formed on the particle surfaces at high grafting densities. Polymer grafting can enable fully aqueous dispersible MOFs as demonstrated by Webley, Qiao, and co-workers.[190] To accomplish this, UiO-66-NH_2 was synthesized and subsequently functionalized with an ATRP initiator, bromoisobutyryl bromide. Following MOF functionalization, poly(ethylene glycol) methyl ether methacrylate (PEGMA) was polymerized from the surface under ARGET-ATRP (activators regenerated by electron transfer) conditions (Figure 23).[191]

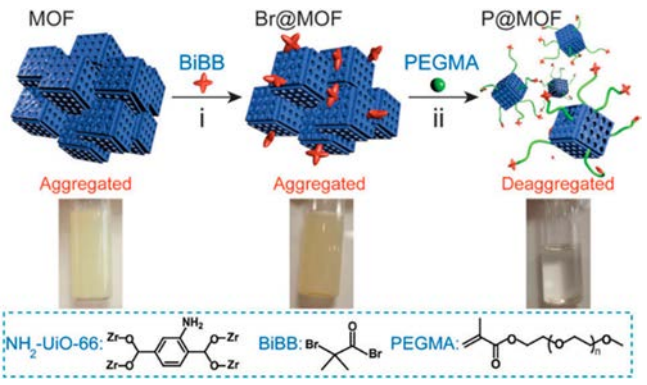

Figure 23. Grafting of PEGMA via surface-initiated ATRP for highly dispersible MOFs in aqueous conditions. Reproduced with permission from ref 190. Copyright 2015 The Royal Society of Chemistry.[190]

PEG is an ideal polymer to attach to MOF surfaces for improving the material dispersibility as PEG is soluble in a wide variety of solvents, both hydrophilic and hydrophobic, and has numerous secondary benefits such as being highly inert and biologically compatible.[192] Prior to polymer functionalization, both the native UiO-66-NH_2 (~20−70 nm particles as determined by SEM) and the ATRP-functionalized UiO-66-NH_2 particles were highly aggregated when attempts were made to disperse the particles in water, with hydrodynamic radii exceeding 1 μm as measured with DLS. However, upon grafting of PEGMA to the MOF surface, aqueous dispersibility was easily achieved and the particles displayed hydrodynamic radii equal to that measured by SEM. At high loadings of PEGMA in the grafting-from polymerization, sufficiently long brushes were grown such that the particles were dispersible over a wide pH range. In contrast, when small loadings of PEGMA were used in the polymer-

DOI: 10.1021/acs.chemrev.9b00575
Chem. Rev. XXXX, XXX, XXX−XXX

ization, only short brushes were obtained which caused particle aggregation in pH neutral water. When the pH was raised to 9, the particles disaggregated and returned to the original 20−70 nm size, demonstrating the stimuli-responsive behavior of the particles. While this example demonstrated the pH-responsive properties of PEGMA-grafted MOFs, the unique thermal properties of this polymer (LCST) were not explored.

The field of functional or stimuli-responsive polymers has rapidly expanded in the previous two decades[193,194] and has naturally extended to the realm of MOF-polymer composites.[195,196] Thermally responsive polymers are of significant interest as their behavior does not require physiochemical activation (i.e., unlike pH-responsive polymers that require protons or hydroxide ions to alter their properties). In one of the earliest reports of thermally responsive polymers conjugated to MOF surfaces via a grafting-from route, Zhu and co-workers grafted 2-(2-methoxyethoxy)ethyl methacrylate and oligo(ethylene glycol) methacrylate to the surface of MIL-101(Al)-NH_2 particles using ATRP.[197] The resulting particles were shown to easily disperse at room temperature, rapidly precipitate at temperatures above 45 °C, and dispersed again upon cooling in a process that could be repeatedly cycled. Related work by Dong and co-workers demonstrating the grafting-from of poly(urea)s for the synthesis of standalone membranes in discussed in further detail in section 2.3.[66]

Early efforts for achieving MOF-polymer hybrids often suffered from pore clogging by surface grafted chains, resulting in significantly reduced surface areas. To overcome this issue, Matzger and co-workers designed a core−shell MOF in which the outer shell provided both initiating sites and mitigated pore blockage.[68] In this example, IRMOF-1 (a.k.a., MOF-5) was synthesized, followed by growth of an IRMOF-3 shell, which was subsequently functionalized with 2-bromoisobutyric anhydride to give ATRP initiator groups (Figure 24). Following polymerization of poly(methyl methacrylate) (PMMA), the surface area was measured to be >2,800 m^2g^{-1}, corresponding to a modest 15% drop compared to the initiator-functional MOF. Polymer grafted, core−shell single crystals were isolated, mechanically cleaved, and characterized by Raman microspectroscopy to determine the extent to which the polymer penetrates the MOF. This experiment revealed that the polymer was only located in the IRMOF-3 crystal shell, with the MOF-5 layer being free of polymeric material.

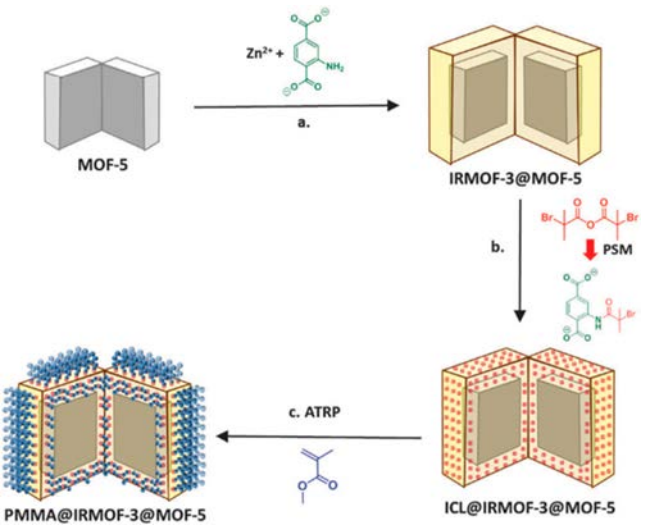

Figure 24. Grafting-from core−shell IRMOF-3@MOF-5 particles with poly(methyl methacrylate). Reproduced with permission from ref 68. Copyright 2015 The Royal Society of Chemistry.[68]

Very recently, Li and co-workers developed a highly generalizable strategy for attachment of ATRP initiators to a wide variety of MOFs including UiO-66, ZIF-8, ZIF-67, MIL-96(Al), and MIL-101(Cr).[78] The authors first synthesized a random copolymer containing methacrylic acid (MAA) and an ATRP-functional monomer 2-(2-bromoisobutyryloxy) ethyl methacrylate in an 8.5:1 ratio with a molecular weight of 10.3 kDa. The MAA units allowed for strong anchoring to the MOF surfaces, after which a thin shell of cross-linked polystyrene was grown from the surface of the MOFs, locking the initiating groups onto the particle surface for further functionalization (Figure 25). The authors elegantly demonstrated the robustness of their strategy by growing a layer of poly(4-chlorostyrene), microtoming ultrathin sections of the MOF, and imaging the slices with STEM. EDX of the ultrathin sections, clearly showed the Zr^{4+} ions in the MOF core and Cl atoms in the outer polymer shell, confirming the precise placement expected for the surface-initiated polymer grafting. Furthermore, it was demonstrated that a thin shell of polystyrene (7 nm) was capable of fully shielding UiO-66 particles from degradation by both 1 M H_2SO_4 or 1 M NaOH, both of which would significantly digest the free, unfunctionalized MOF.

4.3. Grafting-Through Methodologies

A third type of grafting reaction for polymer surface functionalization is known as grafting-through. In this method, similar to PSP, the surface is functionalized with a monomeric group that can become incorporated into a growing, exogenously initiated polymer chain that then becomes covalently linked to the surface. A simple, but illustrative example of grafting-through to create covalent MOF-polymer hybrids was performed by Shojaei and co-workers.[71] UiO-66-NH_2 was functionalized with glycidyl methacrylate, followed by dispersion in a methyl methacrylate (MMA) solution and subsequent polymerization to give covalently grafted PMMA. The resulting polymer-grafted MOFs were cast into MMMs at 28 wt % loadings, which showed a nearly doubled Young's modulus over pure PMMA films. In a separate study also using methacrylate functionalized UiO-66-NH_2, Dong, Yao, and co-workers grafted poly(diethylaminoethyl methacrylate) (PDEAEMA) from the MOF surface using a redox initiator system in aqueous solution.[198] Following grafting of PDEAEMA brushes, the particles were loaded with Pd nanoparticles which were shown to be highly effective at catalyzing the Knoevenagel condensation. Additionally, because of the pH-responsive properties of PDEAEMA, stable aqueous suspensions could be formed under acidic conditions due to the protonated amine side chains. Pickering emulsions were formed when an organic layer was present after the pH of the aqueous layer was increased. Work by Li and co-workers demonstrating the covalent immobilization of MOFs on nylon fibers is an interesting and novel approach to covalent MOF-polymer hybrids.[199] In this example, MIL-101 was grafted to nylon surfaces by gamma-ray induced copolymerization with 2-hydroxyethyl acrylate. The gamma-ray irradiation produced radicals on the aromatic rings of the MIL-101 as well as the nylon chains, which can both propagate through the growing chains of the poly(2-hydroxyethyl acrylate). The authors showed that the resulting fibers were capable of withstanding

DOI: 10.1021/acs.chemrev.9b00575
Chem. Rev. XXXX, XXX, XXX−XXX

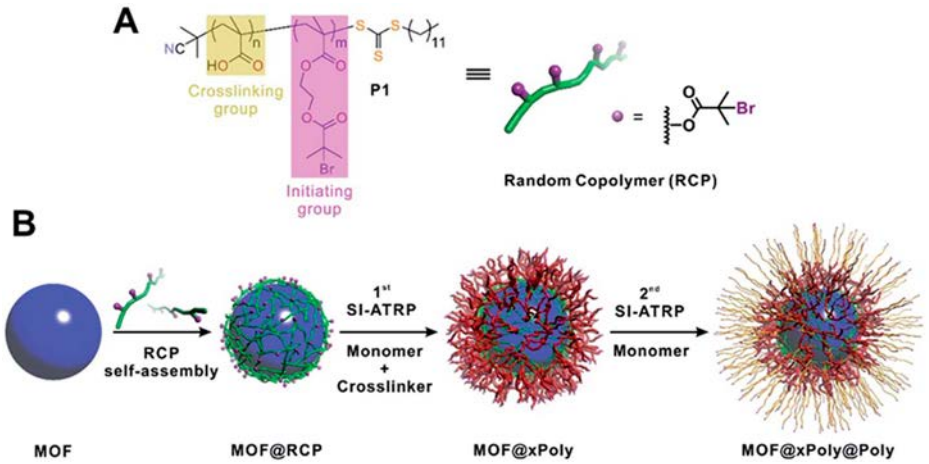

Figure 25. (A,B) General strategy to introduce ATRP initiators on a wide variety of MOFs. Reprinted with permission from ref 78. Copyright 2019 The Royal Society of Chemistry.[78]

30 h of laundering while maintaining surface attachment of the MOF particles. A particularly well-executed example by Wang and co-workers regarding photoinduced polymerization of poly(butyl methacrylate) through UiO-66-NH_2 is discussed extensively in section 2.4.[59] Polymer-grafted MOFs are an important class of MOF-polymer hybrid materials that combine the exciting properties of both MOFs and polymers into a single system. While significant strides have been taken in the past decade toward advancing these materials, much work remains to provide better control in these systems as well as more universal approaches toward polymer-grafted MOFs. Specifically, broadening the scope of controlled radical polymerizations from MOF surfaces, both in terms of polymerization mechanism (ring opening metathesis, reversible-addition−fragmentation chain transfer, etc.) as well as expanded MOF and monomer scope will greatly enhance the feasibility for real-world implementation of these materials.

5. POLYMERIZATION OF MONOMERS WITHIN MOFS

The tunable chemistry and porosity inherent in MOFs offer a unique chemical environment for performing polymerization reactions. The molecular scale of these channels has been used to control the arrangement and reactivity of guest monomers that when polymerized give polymers with structures and topologies different than those prepared in the bulk, solution phase. MOFs have been used to alter the primary structure of polymers, including stereo- and regiochemical outcomes, and more recent applications as templates for the synthesis of precisely structured, noncrystalline materials show that MOFs have a versatile place in the field of polymer chemistry.

5.1. Dispersity and Molecular Weight

The dispersity of molecular weights in a given polymer sample is an important factor to consider particularly for the application being explored and is often the main variable affecting physical properties of polymers with the same chemical structure.[200] Free radical polymerizations are among the simplest of polymerization techniques, but the high reactivity of the propagating chain end leads to high rates of termination and transfer resulting in a wide variety of molecular weights in a single sample. Over the past two decades, tremendous advances have been made in the field of controlled radical polymerization (CRP), but recent work using MOFs to control the chain properties of polymers offers promise as an alternative route toward accessing well-defined polymers. The first polymerization of a monomer within the pores of a MOF framework was done using a free-radical polymerization of styrene and $[M_2(BDC)_2(ted)]_n$ (M = Zn^{2+} or Cu^{2+}), (bdc = benzenedicarboxylate; ted = triethylenediamine) (Figure 26).[201] The one-dimensional channels were

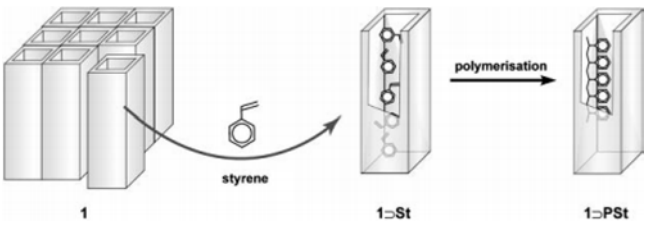

Figure 26. Scheme for the polymerization of styrene in the linear channels of a metal−organic framework. Reproduced with permission from ref 201. Copyright 2005 The Royal Society of Chemistry.[201]

filled with a mixture of monomer and initiator. After careful removal of nonpore occupied monomer under vacuum, the polymerization was initiated by heating under an inert atmosphere. Dissolution of the MOF structure allowed for analysis of the resulting polymer, which revealed that the dispersity of the MOF-templated polymer was much lower than traditional bulk phase synthesis (1.6 vs 4.6). Electron spin resonance of the MOF before dissolution showed the persistence of the chain-end radical, even after 3 days at 70 °C. These results indicate that the MOF protects the radical from termination, giving it a "living" character. The extent of this space-effect was analyzed by changing the organic linkers to alter the pore size of the MOF to be longer and narrower. In this case, almost no polymerization occurred. NMR experiments revealed that the monomer has no free movement in the smaller MOF pores and cannot adopt the orientation necessary to propagate the reaction to the next monomer. The molecular weight dispersity of the polymer was inversely related to this, showing that control over the polymerization was subject to the narrow pores protecting the radical from termination events.

5.2. Stereocontrol

Free-radical polymerizations of vinyl monomers generally result in achiral polymers due to the prochiral and racemic

DOI: 10.1021/acs.chemrev.9b00575
Chem. Rev. XXXX, XXX, XXX−XXX

nature of the vinyl group and propagating radical, respectively.[200] However, polymers that have been synthesized with stereochemical control usually have higher packing density and stronger mechanical properties. Because of this, control over the formation of stereocenters along the backbones of vinyl polymers is a long-sought goal of polymer chemists. The main difficulty is the formation of a chiral environment around the propagating radical. While some stereocontrolled radical polymerizations do exist, they are typically limited to very bulky or carbonyl bearing monomers in the presence of fluoroalcohols or Lewis acids, and the produced tacticity is usually syndiotactic rather than the often preferred isotacticity.[202−204]

MOFs provide a sterically confined space for both the propagating radical and approaching monomer, and the chemical structures of the organic linkers can be modified to force a commonly atactic polymerization to show some degree of tacticity under otherwise similar conditions.[205] By altering the substituents of both the chemical and isomeric derivatives of BDC in a $[Cu_2(L)_2(ted)]_n$ MOF on the polymerization of MMA, a clear increase in the formation of meso diads was shown, indicating increasing isotacticity, when a 2,5-dimethoxyterephthalate ligand was used and showing an 18% increase compared to bulk polymerization. Interestingly, the 2,3-dimethoxyterephthalate isomer showed almost no increase in tacticity from the bulk. Further investigation using simulations of linker conformations indicated that the 2,5-substitution pattern was more likely to reside in a specific steric environment than the 2,3-substituted ligand. This effect allowed the propagating polymer to remain in the necessary conformation, preventing a switch in the local environment and resulting in a higher amount of meso diads.

The presence of unsaturated metal sites within the MOF channels was also able to give some control over tacticity in the polymerization of MMA through complexation (Figure 27).[206]

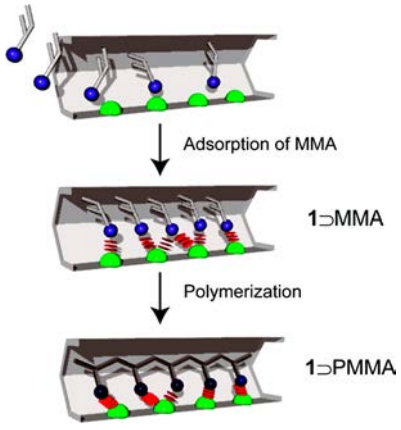

Figure 27. Scheme for the coordination and subsequent radical polymerization of methyl methacrylate. Reprinted from ref 206. Copyright 2011 American Chemical Society.

With the use of a series of metals (Al^{3+}, Eu^{3+}, Nd^{3+}, Y^{3+}, La^{3+}, and Tb^{3+}) as the metal ions in the MOF, increasing Lewis acidity of the metal center resulted in increasing tacticity at the expense of decreasing conversion. The Tb^{3+} ion, which as a discrete complex shows no control over the tacticity of MMA, showed the highest increase, and statistical analysis of the tacticity values indicated a penultimate effect as the most likely mechanism for this control.

RAFT, a commonly used CRP technology that generally gives low dispersities (<1.2), was used by Hwang and coworkers to explore the effect of monomer size of a variety of acetates on the dispersity and tacticity of polymers synthesized in the pores of a $[Cu_2(L)_2(ted)]_n$ MOF.[207] In the case of the free radical polymerization, as monomer size increased from vinyl acetate to vinyl butyrate, both conversion and dispersity decreased while the isotacticity increased, with vinyl pivolate being too large to polymerize. When RAFT conditions were used, the same effect was noticed but the dispersities were significantly lower than in the case of free radical. A hallmark of CRP is the ability of the polymer chain to be reinitiated and extended using another monomer to create a block copolymer. The recovered isotactic polyvinylpropionate (*iso*PVPr) was extended with vinyl acetate in solution to give *iso*PVPr-*b*-*at*PVA. The authors note it is unclear whether the RAFT polymerization is undergoing the same chain-transfer mechanism in the MOF as in solution and further analysis is needed.

Controlled radical polymerization using ARGET ATRP further expanded the tools available to control polymerizations in MOFs. Polymerizations were performed with both free initiator and initiator physically installed into the MOF pores, and in both cases, the polymers had high molecular weights, low dispersity, and an increase in overall tacticity depending on the size of the monomer. The use of free initiator resulted in high molecular weights regardless of the amount of initiator present, indicating an increase in polymerization rate due to the confinement effect. However, the initiator-functionalized MOF showed better control over the molecular weight and decreasing the amount of initiator by half resulted in polymers of roughly double the molecular weight, as expected in a controlled polymerization. Livingness was evaluated by chain extensions of the synthesized polymers to form block copolymers, and a clean shift in the GPC traces indicated that the polymers all contain dormant chain ends even at high molecular weights, indicating that the MOF host decreased the rate of termination as well.

5.3. Sequence Control

Controlling either the location or distribution of repeat units, as well as the inter- and intramolecular connections within the polymer structure can completely change the physical properties of the resulting material. Monomer sequence is precisely controlled in nature as a fundamental component of complex biomacromolecules, but the ability to control such structure in synthetic polymer systems is comparable; if polymer technology is ever to reach such advanced levels, generally applicable precision in monomer sequence must be developed.

The well-defined, periodic spacing of organic linkers and metal clusters in MOFs can be used to control the placement of monomers along the backbone of a polymer if they are designed to position one of the monomers in place along the narrow pores. To achieve this, open metal sites of a coordinatively unsaturated MOF framework can be used to selectively complex one monomer over another at specific intervals and create a controlled copolymer with a non-complexing ligand. For example, a lanthanide-based MOF, $[Tb(btb)]_n$ (btb = 1,3,5-benzenetrisbenzoate), was infiltrated with a mixture of MMA and styrene and the monomer ratio was tuned in the resulting copolymer by varying the polymerization conditions.[208] Interestingly, when the copolymer was synthesized at 70 °C, the ratio of incorporation of the

DOI: 10.1021/acs.chemrev.9b00575
Chem. Rev. XXXX, XXX, XXX−XXX

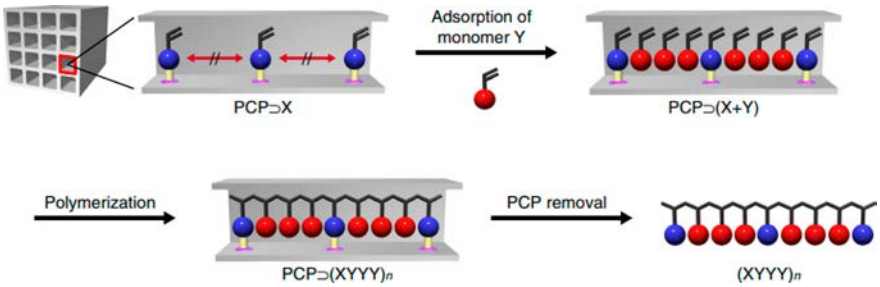

Figure 28. Schematic showing the infiltration of MOF pores with free monomer and the ordered spacing leading to the sequence-controlled polymerization. Reprinted from ref 209 under Creative Commons License. Copyright 2018 Nature Publishing Group (https://creativecommons.org/licenses/by/4.0/).

two monomers did not differ from the bulk polymerization, but light-initiated polymerization at room temperature gave consistently high ratios of MMA to styrene over a wide range of initial feed ratios. Variable-temperature IR of the monomer-infiltrated MOF indicated that at above 40 °C the MMA dissociated from the coordination sites and negated the influence of the MOF on the polymerization. However, it was also shown that while an increase in the MMA fraction compared to the bulk was achieved, no control over the final sequence was observed.

In a similar example, the organic linkers of a MOF were modified into a monomer that could be incorporated into a copolymer at regular intervals (Figure 28).[209] Isoterephthalic acid was synthesized as a styrene derivative and the Cu^{2+}-based MOF formed from this ligand contained one-dimensional channels with the vinyl groups projecting into the pores at regular intervals. The space between each ligand was bridged with acrylamide as the comonomer and polymerized, which was shown to be a poly(acrylamide-*co*-vinylisoterephthalic acid) copolymer with an isoterephthalic acid group at every fourth repeat unit. Modeling of the acrylamide monomer present in the MOF during the polymerization showed that the propagating radical was sterically favored to contact the MOF vinyl group after polymerizing exactly three acrylamide monomers, giving a precise $(AAAS)_n$ repeat unit along the backbone.

5.4. MOFs as Templates for Materials

The synthesis of well-defined polymeric particles with controlled morphologies or intrinsic porosity is generally performed using hard, inorganic templates such as porous silica particles or zeolites.[210,211] The drawbacks of these templates are the harsh conditions necessary to remove the templates, as well as the general meso- or microporous nature of the polymeric products which can result in pore collapse of less rigid polymers. MOFs offer a well-defined template with nanoscale pores that can be easily removed under mild conditions, increasing the range of polymers that can be used and improving the final porosity and stability of the polymer particles.

The morphology of simple polymer particle shapes was controlled by using MOFs as a template for styrene and MMA polymerizations.[212] By first synthesizing MOFs of different shapes (rods, cubes, and hexagons) and polymerizing monomer within these structures, dissolution of the framework kept the polymer chains in the macroscopic shape of the MOF particle (Figure 29). The retention of these forms was accessible due to the mild isolation techniques, which could be performed at room temperature below the glass-transition

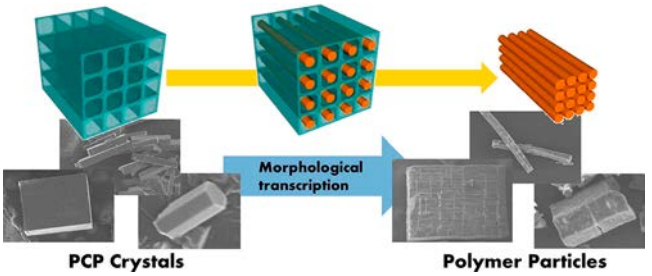

Figure 29. Scheme showing SEM of MOF crystals before polymerization and of polymeric monoliths formed after dissolution. Reprinted from ref 212. Copyright 2013 American Chemical Society.[212]

temperature (T_g) of the polymer, and heat treatment of the polymer monolith above its T_g resulted in a loss of form as observed by SEM.

Adsorption of 3,4-dihydroxy-L-phenylalanine (L-DOPA), a chiral monomer, into a HKUST-1 SURMOF and subsequent photopolymerization created a chiral, poly(L-DOPA) gel after dissolution of the MOF.[213] This chiral gel thin film showed a 32% increase in adsorption of *S*-naproxen over its enantiomer, demonstrating its use for chiral separation technology, and this methodology could be applied generally to synthesize homochiral polymer thin films. Another biologically compatible gel was prepared by the cationic polymerization of glucose within the pores of HKUST-1.[214] This gel was permanently porous, showing a BET surface area of 153 m^2 g^{-1}, and decreasing polymerization time and conversion could create gels with wider pores and lower surface area. Uptake and release experiments were performed with ibuprofen and BSA, with ibuprofen releasing faster from the gel than from the pure crystal and BSA releasing slower as the pore size decreased.

Polypyrrole was synthesized into two different morphologies depending on the template used.[215,216] Redox-active, two-dimensional coordination nanosheets of $\{Ni(dmen)_2\}_2\{Fe^{III}(CN)_6\}]PhBSO_3$ (dmen = 1,1-dimethylethylenediamine; $PhBSO_3$ = p-phenylbenzenesulfonate) were intercalated with pyrrole and oxidatively polymerized by the framework structure. Following the removal of the framework materials, the polymers clearly showed intercalated sheets, unlike the amorphous structures of solution polymerized pyrrole. Changing the MOF to a three-dimensional $[Cu_3(BTC)_2]_n$ (BTC = benzene-1,3,5-tricarboxylate) template, the isolated polypyrrole retained a fully integrated 3-dimensional structure with permanent porosity.

A fully porous, conductive polymeric monolith was achieved by the polymerization of aniline within the pores of HKUST-1

DOI: 10.1021/acs.chemrev.9b00575
Chem. Rev. XXXX, XXX, XXX−XXX

on the surface of a platinum electrode.[217] Deposition of a thin layer of HKUST-1 onto the surface of a platinum electrode, followed by electropolymerization of aniline within the pores, created a microporous polyaniline structure with a surface area of 986 m^2 g^{-1}, indicating a highly rigid polymer, and an electrical conductivity of 0.125 S cm^{-1} which is significantly higher than any MOF or COF to date.

The orientation of polymer chains, especially conjugated polymers, has a significant effect on the physical properties of the material. Several processing techniques such as mechanical stress or electrospinning have been used to force polymer chains into different alignments, but these methods are only applicable for a limited number of polymers. Polymerizations conducted in MOFs can use the regular array of nanochannels to precisely align polymer chains, and removal of the MOF leaves the polymers in their polymerized state. Polythiophene was prepared in the linear channels of a MOF through oxidative polymerization of the adsorbed monomers.[218] Dissolution of the framework did not disturb the aligned polymer chains, yielding a monolith of polymer chains that showed an increase in conductivity 3 orders of magnitude higher than traditional polythiophene.

The organizing properties of the MOF can also be extended to the side chains. Poly(*N*-vinylcarbazole) (PVCz) is the most widely studied organic polymeric photoconductor due to its ability to form radical cations under irradiation, and the charge transport abilities of this polymer are strongly affected by the π-stacking of the pendant group. Uemura et al.[219] was able to show that first loading the *N*-vinylcarbazole into the MOF caused the monomers to stack prior to polymerization, and the polymers in the MOF showed hole mobilities close to the ideal values calculated for this polymer. Dissolution of the MOF led to a decrease in this mobility as the polymer chains were able to relax, but the polymers still showed higher mobilities than the bulk polymer.

5.4.1. Gels from Cross-linked MOF Ligands. Functionalization of MOF ligands with multiple polymerizable group allows the organic linker to act as either a cross-linking agent in the case of radical polymerization or as a monomer in step growth polymerization. For example, in contrast to the sequence control example above where a single vinyl group incorporated the ligand into a linear polymer, a difunctional monomer 2,5-divinyl-terephthalic acid incorporated in small percentages into a MOF lattice acted as a cross-linking agent when copolymerized with adsorbed styrene.[220] The recovered polymer gel showed both crystallinity by PXRD and permanent porosity, indicating that the MOF could organize and template the gel into a purely organic mirror image of itself.

Noncrystalline, swellable polymer gels were synthesized using click chemistry between azide difunctionalized organic ligands in a MOF that were cross-linked by an external multifunctional alkyne.[221,222] These gels still retained the macroscopic shape of the parent MOF crystal but lost all crystallinity after cleavage of the metal–ligand bonds. The Sada group used this methodology on a MOF that contained large pore windows along specific axes.[223] When the external alkyne was added, it preferentially cross-linked the ligands along these axes, giving anisotropic cross-linking density. Removal of the metal ions created an anisotropic gel which could swell in along a single axis (Figure 30). The Wöll group applied this gel synthesis to surface-mounted MOFs (SURMOFs) that were used as biocompatible substrates for

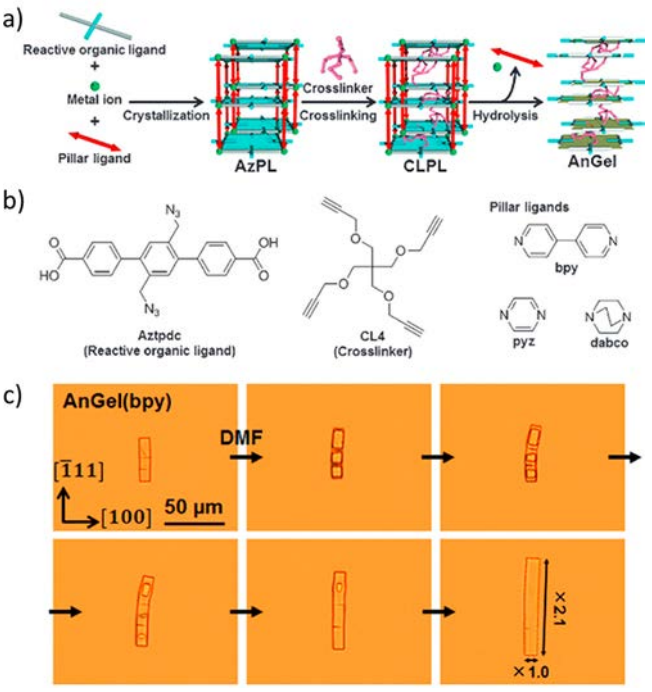

Figure 30. (a) Scheme of cross-linking and hydrolysis leading to anisotropic gel (b) ligands and cross-linker used in the study. (c) DMF swelling experiment showing the anisotropic growth of the gel along a specific axis. Reprinted with permission from ref 223. Copyright 2017 Wiley Publishing Group.

small molecule release and cell adhesion and modification.[224] Using the interior of MOF crystals to control polymerizations is an exciting route toward highly controlled polymers. While the field of controlled radical polymerizations has blossomed in the previous two decades, facile routes toward stereospecific polymers and, in particular, sequence-defined polymers remains largely elusive. Because of the highly controlled and tunable pore environment of MOFs, polymers with well-defined tactility and sequence control can be achieved. MOFs with variable pores, such as breathing MOFs, may offer methodologies to even more complex polymer topologies, and increasing the yield of polymer in pore-controlled polymerizations will be highly important for future research in this field.

6. POLYMERS TEMPLATING MOFS

Controlling the crystal habit (i.e., crystalline phase, shape, size, and mesoporosity) of MOFs using organic polymers is an intriguing strategy for hybridizing MOFs and polymers. In contrast to templating MOFs using small molecules or inorganic substrates, organic polymers have the advantage of containing many coordination sites, having an ability to self-assemble, and are highly tunable for different applications. Although the literature is rich with examples of the use of polymers to template the morphologies of a wide variety of metal oxides, minerals, and soft matter structures, the use of polymers to template and control the growth of MOFs is still in its infancy. This section assesses how polymers have been used to template MOF materials and highlights important areas for which future endeavors may be particularly fruitful.

DOI: 10.1021/acs.chemrev.9b00575
Chem. Rev. XXXX, XXX, XXX−XXX

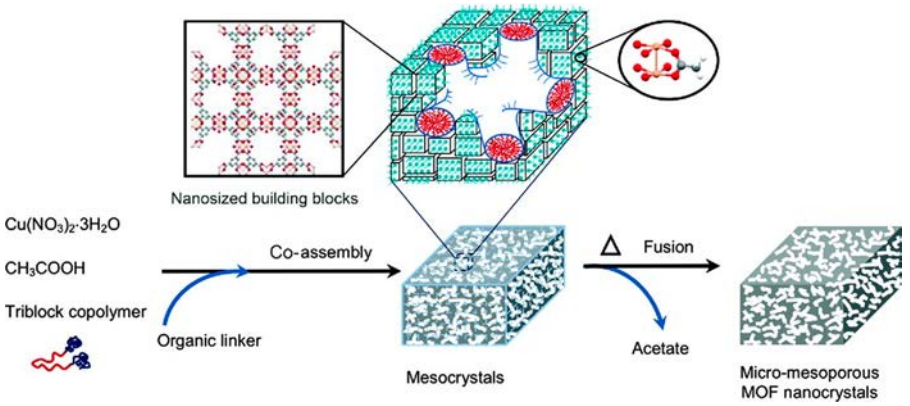

Figure 31. Synthetic strategy to achieve HKUST-1 with hierarchical porosity using block polymer self-assembled templates. Reprinted from ref 226. Copyright 2012 American Chemical Society.

6.1. Polymers as Soft Templates for MOFs

In an earlier review, Bradshaw and co-workers discussed the importance of using nonionic polymers to produce hierarchical porosity in MOF materials.[225] Nonionic polymers do not contain any coordinating groups but are able to spontaneously self-assemble in solution to direct the structures of MOFs through electrostatic interactions. A common class of these nonionic polymers include Pluronic type polymers, which are composed of PEO and poly(propylene oxide) (PPO) blocks. For example, Do and co-workers used the polymer F127 ($PEO_{97}PPO_{69}PEO_{97}$) and acetic acid in situ during synthesis of HKUST-1 to obtain crystalline MOF materials with 4 nm mesopores (Figure 31).[226] The triblock copolymer spontaneously self-assembled into hierarchical superstructures of micelles in solution, producing mesosized channels and pores with polar surfaces for the growing MOF to nucleate. Following the synthesis of HKUST-1, the assembled polymer template was removed to yield a MOF with a high abundance of both micro- and meso-sized pores. In another example, Wang and co-workers synthesized ZIF-67 and ZIF-8 using stoichiometric amounts of metal and ligand in the presence of P-123 ($PEO_{20}PPO_{70}PEO_9$) and ammonium hydroxide.[227] In both examples, the Pluronic type polymers form micelles in solution, which also have the ability to solubilize metal ions in solution. However, in both of the previous examples an exogeneous small molecule modulator was required to maximize crystallinity in the resulting MOFs.

Another common polymer used for templating MOFs is polyvinylpyrrolidone (PVP). Like Pluronic polymers, PVP can act as a surfactant in solution, but PVP has the additional benefit of containing amide groups which can further stabilize metal ions in solution via metal-amide interactions. However, like Pluronic polymers, PVP is typically used in combination with small molecule modulators to control morphologies and sizes of the resulting MOF crystals. Eddaoudi and co-workers demonstrated that PVP could be used to control the size of Fe^{3+}, In^{3+}, and Ga^{3+} square-octahedral (soc) MOFs to prepare cubic, truncated cubic, and colloidosome MOFs (Figure 32).[228−230] Additional modulators such as tetramethylammonium nitrate (TMAN) or *tert*-butylamine were required to regulate the shape of the MOF materials, but the presence of PVP was critical to control the particle morphology. Eddaoudi and co-workers found that the resultant Ga-soc-MOFs were irregular in shape and size in the absence of PVP and

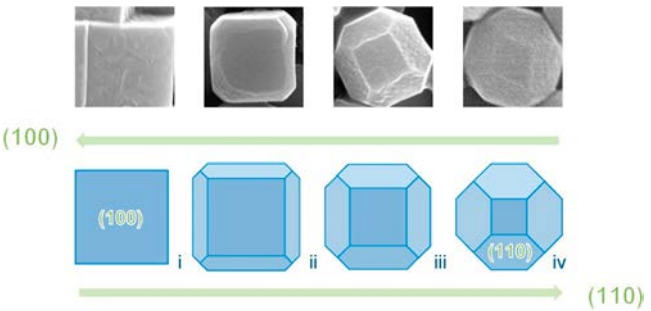

Figure 32. A representative scheme depicting the use of polyvinylpyrrolidone (PVP) in combination with surface-directing agents to modulate MOF growth. Increasing concentration of PVP allowed for selective tuning of the size of 100 facet. Reprinted from ref 228. Copyright 2012 American Chemical Society.[228]

modulator, demonstrating the importance of using polymers as soft templates for regular MOF growth.[230]

In a report by Wang and co-workers, it was shown that IRMOF-1 with highly uniform shapes and sizes could be synthesized with the use of PVP and triethylamine (TEA).[231] By changing the concentration of TEA and keeping the concentration of PVP constant, the authors were able to obtain IRMOF-1 particles in sizes ranging from 50 nm to 2.5 μm. Conversely, increasing the concentration of PVP under diluted IRMOF-1 conditions revealed that the shape of the materials varied from cubes to truncated cubes to truncated octahedron and finally to octahedron. It was proposed that the PVP directs the MOF growth by blocking the 111 face of the crystals, producing the observed shapes. Using Fourier-transform infrared (FTIR) spectroscopy and thermogravimetric analysis (TGA), Wang and co-workers determined that a minimum amount of PVP remains in the product, but the IRMOF-1 retains its porosity (2500−2700 m^2/g), highlighting the value of this technique to create polymer-templated MOFs.

6.2. Polymers as Modulators for MOF Crystal Growth

Although templating of MOFs has been possible with nonionic polymers, the ability to prepare polymers with coordinating groups provides additional control in MOF templating that can potentially provide access to a wider variety of MOF sizes and morphologies. Early work with ionic polymers to template MOFs was demonstrated by Kitagawa and co-workers, wherein polyvinyl sulfonic acid was used to control the size of a MOF $[Cu_2pzdc_2(pyz)_n]$ (pzdc = pyrazine-2,3-dicarboxylate; pyz =

DOI: 10.1021/acs.chemrev.9b00575
Chem. Rev. XXXX, XXX, XXX−XXX

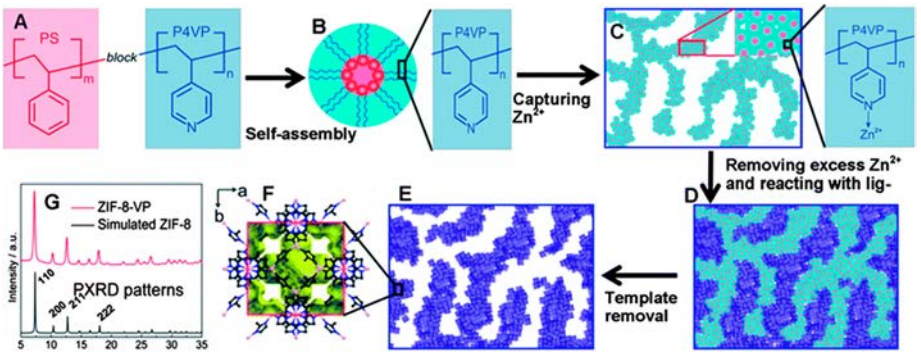

Figure 33. Polystyrene-*co*-polyvinylpyridine were self-assembled and loaded with zinc to be used as templates for the synthesis of ZIF-8. Reproduced with permission from ref 233. Copyright 2013 The Royal Society of Chemistry.

pyrazine) from 2 μm platelets to 70 μm platelets.[232] Since then, a combination of coordinative block copolymers have been prepared for controlling the crystal habit of MOFs. In a particularly elegant example, block polymers of poly(styrene-*b*-(acrylic acid)) and poly(styrene-*b*-vinylpyridine) were prepared as sacrificial templates for the preparation of ZIF-8 and HKUST-1.[233] By introducing the block polymers to metal ions (Zn^{2+} or Cu^{2+}), Cheetam and co-workers were able to prepare block polymer micelles containing a source of metal ions for MOF nanoparticles to grow (Figure 33), which in turn directed the morphology of the MOF. The block polymers were then removed by washing, leaving mesoporous MOF materials behind. It must be noted that the MOFs themselves were not mesoporous, but instead the mesoporosity was attributed to the voids left by removal or block copolymer. This result demonstrates a promising way to template MOFs using organic polymers.

Cohen and co-workers prepared a poly((isophthalic acid)-*b*-(ethylene oxide)) polymer to control the morphology of metal–organic polyhedra (MOPs).[234] The polymer design included isophthalic acid moieties interconnected by ethylene oxide trimers, both of which proved to be important for control of MOP morphology (Figure 34). MOP-1, composed

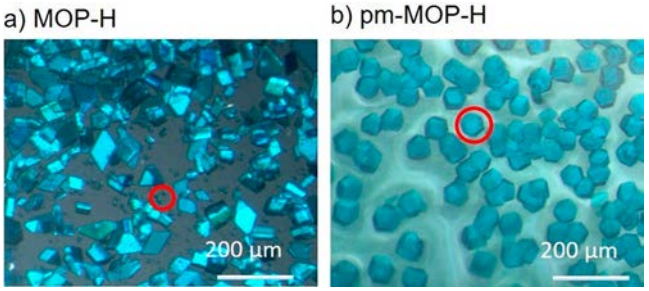

Figure 34. Optical images of as synthesized (a) MOP-H (small cubic c-MOP-H crystals are circled in red) and (b) pm-MOP-H (large cubic c-MOP-H crystal circled in red), where "pm" indicates "polymer modulated". Reprinted from ref 234. Copyright 2016 American Chemical Society.

of isophthalic acid and Cu^{2+} paddlewheel structures, was used as a prototype for morphology control of MOPs. MOP-1 typically forms heterogeneously sized crystallites in two different phases (triclinic and cubic). Use of the poly-((isophthalic acid)-*b*-(ethylene oxide)) polymer during the synthesis resulted in the successful isolation of only large, cubic crystals of MOP-1. Demonstrating the importance of one of the defining features of synthetic polymers, namely high molecular weight, oligomer derivatives of the polymer alone were unable to control the morphology of these MOP materials. Furthermore, morphology control was still achieved when MOPs containing ligand derivatives of isophthalic acid were used as well, showcasing the generality of this approach. Finally, the polymer was shown to be useful for growing MOPs on glass substrates, opening opportunities in macro-scale material fabrication.

Recently, Schmidt and co-workers developed a double-hydrophilic block polymer (DHBC), poly(ethylene oxide)-*block*-poly(methacrylic acid) ($PEO_{68}MAA_8$), to control the crystal habit of MOFs that display multiple crystalline phases.[235] In contrast to amphiphilic block polymers, the DHBC does not spontaneously self-assemble into a micellar structure in solution. The morphology control produced by the DHBC is not caused by phase separation of the block copolymer, rather, morphology control of the MOF occurs through coordination-modulation exhibited by the carboxylic acid groups in DHBC, while the ethylene oxide block induces particle stabilization by controlled aggregation during nucleation of MOFs (Figure 35). For this study,

Figure 35. A DHBC used to modulate a MOF that experiences two different phases. Reprinted from ref 235. Copyright 2018 American Chemical Society.

$[M_2(bdc)_2dabco]_n$ (where "M" is Zn^{2+} or Cu^{2+}, "bdc" is benzene-1,4-dicarboxylic acid, and "dabco" is 1,4-diazabicyclo[2.2.2]octane) was chosen because it produces two crystalline topologies, kinetically favored hexagonal plates and thermodynamically favored cubic crystals. Using $PEO_{68}MAA_8$ as a modulator, Schmidt and co-workers were able to trap the kinetic hexagonal phase, yielding hexagonal

DOI: 10.1021/acs.chemrev.9b00575
Chem. Rev. XXXX, XXX, XXX−XXX

mesocrystal rods. By varying the ratio of $[CO_2H$ of $EO_{68}MAA_8]/[Zn^{2+}]$, $PEO_{68}MAA_8$ kinetically trapped the hexagonal phase of the material by preferentially coordinating from the Zn-bdc surfaces of the materials. Furthermore, modifying the ratios of ethylene oxide:methacrylic acid in the polymer demonstrates the importance of both components acting together to control the shape and size of the MOF mesocrystals. By understanding the mechanism of nucleation for these MOF mesocrystals, the authors demonstrated the ability to transform hexagonal rods into thermodynamically stable cubic rods by submerging mesocrystals into methanol to slowly dissolve $PEO_{68}MAA_8$. Additionally, Schmidt and co-workers demonstrated the ability to grow hexagonal nanorods of $[Cu_2(bdc)_2dabco]_n$ onto the surfaces of $[Zn_2(bdc)_2dabco]_n$ cubic crystals using $PEO_{68}MAA_8$ as a modulator, demonstrating the power of using polymers to modulate the growth of MOFs.

Another recent, spectacular example of polymer control over MOF morphology was reported by Johnson and co-workers.[236] In this study, a polymer comprised of a long PEG block and a 1,4-benzenedicarboxylic acid (H_2bdc) tetramer (see below) were used as modulators for the synthesis of IRMOF-1 and UiO-66 particles. The result was the production of MOF nanoparticles with sizes as small as ~20 nm (Figure 36). These

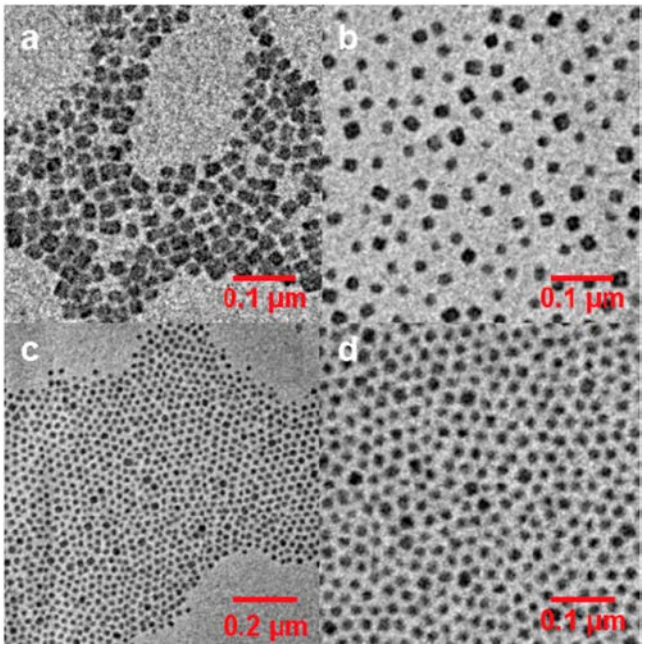

Figure 36. (a) TEM image of polyMOF-5 NPs (28 ± 2 nm in diameter) formed using PEG5k-L_4. (b) TEM image of polyMOF-5 (20 ± 1 nm in diameter) formed using PEG10k-L_4. (c and d) TEM images of PEG 10k-L_4 modulated polyMOF-5 NPs. Reprinted with permission from ref 236. Copyright 2019 Wiley Publishing group.

MOF nanoparticles were also extremely stable. For example, the IRMOF-1 particles, which are typically quite unstable in water, were found to form stable colloids in DMF for up to 7 months and were stable to ambient conditions for as long as 6 weeks.[236] The use of polymers containing a H_2bdc block has proven a rich area of chemistry beyond nanoparticles, making new MOF hybrids in their own right.

7. BOTTOM-UP MOF/POLYMER COMPOSITES: POLYMOFS AND POLYMOPS

PolyMOFs are a unique class of MOF-polymer materials where the framework is composed polymers (instead of molecular organic linkers) and metal ion SBUs. This approach is remarkable as amorphous polymers fold into highly crystalline MOFs simply by undergoing interaction with a variety of metal salts, such as Zn^{2+} and Zr^{4+}.[237] This bottom-up approach to synthesizing MOF-polymer hybrids is unique as it integrates organic polymers as part of the MOF lattice. PolyMOFs possess both the crystalline, porous capacities of MOFs and the potential to behave like polymers. Additionally, polyMOFs break the dogma that linear, one-dimensional amorphous polymers cannot be transformed into highly crystalline, porous materials. Studies on polyMOFs to date have focused on structural relationships to match MOF formation between MOF scaffolds (e.g., formation of different MOFs such as IRMOF-1,[237] UiO-66,[238] or pillared-MOF structures[239]) with polymer architecture (e.g., spacer-length, isoreticular expansion,[240] and the use of block copolymers).[241,242] Combining these materials to form block polymers has opened the possibility to produce polyMOFs as a material with functional properties like membrane formation, conductivity, solubility, and stimuli-responsiveness. This section will examine the strengths and shortcomings of polyMOFs as a method that integrates processable polymers with functional MOFs.

In the first report, Cohen and co-workers successfully prepared a polyMOF of the IRMOF-1 type architecture (Figure 37).[237] A linear, one-dimensional polymer was

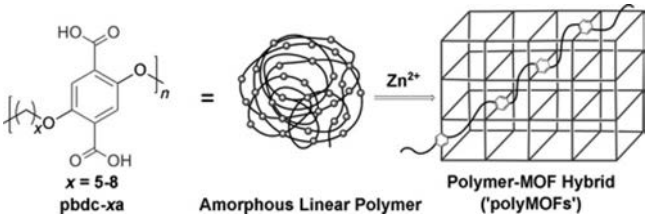

Figure 37. A representation of preparing a polyMOF using a linear, one-dimensional, amorphous polymer ligand is presented. Reprinted with permission from ref 237. Copyright 2015 Wiley Publishing group.

synthesized (using a Williamson ether synthesis polycondensation) containing H_2bdc units within the backbone of the polymer; the spacing between the H_2bdc units could be varied by using methylene spacers of different lengths. It was determined that with appropriate methylene spacing (CH_2 = 5−8), materials with high crystallinity could be prepared (Figure 37). Although IRMOF-1 typically produces cubic crystals, using polymer ligands changed the morphology of these materials from intergrown to spherical crystallites. IRMOF-1 is typically not stable under ambient conditions but using a polymer ligand also increased the stability of the structure, whereby the MOF could be left in ambient air for up to 3 days. In fact, even upon decomposition due to ambient moisture, polyIRMOF-1 could be regenerated by immersing the material in DMF at 60 °C for 1 h. In general, using a polymer ligand could be used to tune and improve the properties of an established MOF.

Having established the possibility to make a linear, one-dimensional polymer ligand into a MOF, Cohen and co-workers sought to investigate the compatibility of polyMOFs

DOI: 10.1021/acs.chemrev.9b00575
Chem. Rev. XXXX, XXX, XXX−XXX

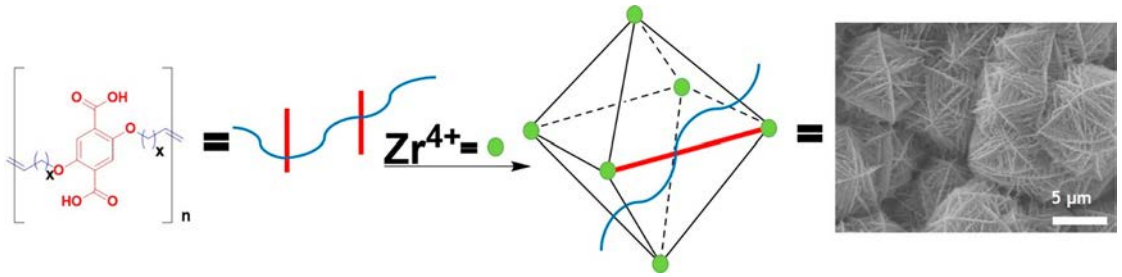

Figure 38. Preparation of UiO-66 polyMOF with a unique, mesoporous, interlaced morphology is presented. Reproduced with permission from ref 238. Copyright 2017 The Royal Society of Chemistry.[238]

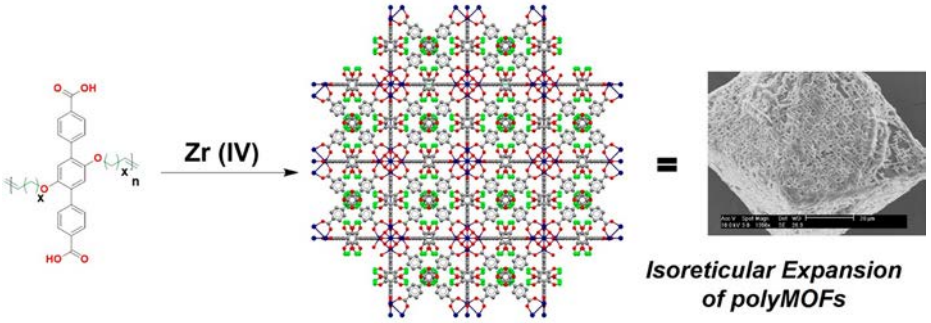

Figure 39. Axially extended polymer ligands were used to prepare polyMOFs with greater surface areas. Reproduced with permission from ref 240. Copyright 2017 The Royal Society of Chemistry.

with other framework architectures (Figure 38). Using pillaring ligands such as 4,4′-bipyridine, a coligand strategy could be developed to synthesize new polyMOFs.[239] In another example, Zr^{4+}-based UiO-66 polyMOFs were also prepared.[238] Acyclic diene metathesis (ADMET) polymerization was used to synthesize polymers with well-defined end-groups and higher molecular weights, both of which could not be achieved with Williamson ether polycondensation. Linear polymers with varied spacer-lengths, molecular weights, and dispersities were prepared to determine the extent to which they affected properties of the UiO-66 polyMOF. A hierarchically mesoporous UiO-66 polyMOF was obtained with an unprecedented, interlaced morphology when an appropriate spacer-length between the H_2bdc monomer units was used. In both examples, the use of polymer ligands serves to modify the properties of MOF materials.

Although reports have demonstrated the ability to synthesize polyMOFs of various MOF architectures, there have been fewer reports on varying the architectures of the polymer. In one report, isoreticular chemistry was applied to the linear, one-dimensional polymers used to synthesize polyMOFs (Figure 39).[240] Axially extended polymer ligands containing 1,4-biphenyl dicarboxylic acid (H_2bpdc) and 1,4-terphenyl dicarboxylic acid (H_2tpdc) were prepared to investigate both the UiO-polyMOF series and the polyIRMOF series. The results demonstrated that extended polyMOFs increase the surface area when compared to the parent MOFs. In a more recent report, ortho-substituted benzene dicarboxylic acid ligands (o-H_2bdc) were used to determine the importance of positioning the organic linker.[243] Although polyMOFs of the IRMOF-1 architecture could be achieved using polymers containing o-H_2bdc, the same ligands could not form the previously reported Zr^{4+}-based polyUiO-66 MOFs, highlighting the importance of polymer architecture in affecting or limiting the formation of polyMOFs.

Block copolymers hold a promising future for the preparation of functional polyMOFs, with two recent reports on block co-polyMOFs (BCPMOFs).[236] In the first report, Johnson and co-workers prepared dimeric or tetrameric (H_2bdc) ligands using a synthetic strategy called iterative exponential growth (IEG); the oligomers were then coupled to a PS block using copper "click" chemistry (Figure 40).[242]

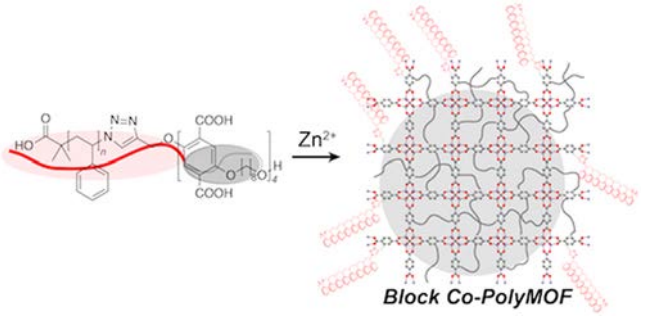

Figure 40. A block copolymer, synthesized by iterative growth, was used to prepare polyRIMOF-1. Reprinted with permission from ref 242. Copyright 2017 The Royal Society of Chemistry.

Interestingly, their results demonstrated that the number of repeating units of (H_2bdc) were crucial to BCPMOF formation, as the (H_2bdc) dimer was unable to yield a crystalline material. Using various methods (TEM, SAXS, and WAXS), Johnson and co-workers observed that IRMOF-1 prepared from the block polymer ligand undergoes nanophase-separation between the MOF component and the PS component. Their results demonstrate that these materials have the potential to behave like block copolymers, which could hold as a promising way to make processable materials.

To take advantage of block copolymer function, the Cohen group reported that block polymer ligands containing non-

DOI: 10.1021/acs.chemrev.9b00575
Chem. Rev. XXXX, XXX, XXX−XXX

coordinating blocks combined with MOF-forming blocks can be used to control the morphology of resultant polyMOFs (Figure 41).[241] Using ADMET polymerization, block copolymers composed of H_2bdc blocks and either PEG or poly(cyclooctadiene) (polyCOD) were used to prepare BCPMOFs. The non-MOF forming blocks could be varied by size as a basis to direct the BCPMOF morphology and size. Morphology control of the BCPMOFs affected the porous properties of these materials, transforming block-polyUiO-66 from a mesoporous material to a microporous material. In addition, the method was applicable to two different MOF scaffolds, IRMOF-1 and UiO-66, suggesting that the technique can be applied to various polyMOF scaffolds. PolyMOFs are a unique class of bottom-up MOF-polymer hybrid materials because the MOFs are prepared from polymer macromolecules. The field is still in its infancy as there is limited knowledge as to how the architectures of MOFs and polymers interplay to develop functional polyMOF materials. Efforts to understand polyMOFs, their structure, and properties should produce interesting composites with exceptional properties.

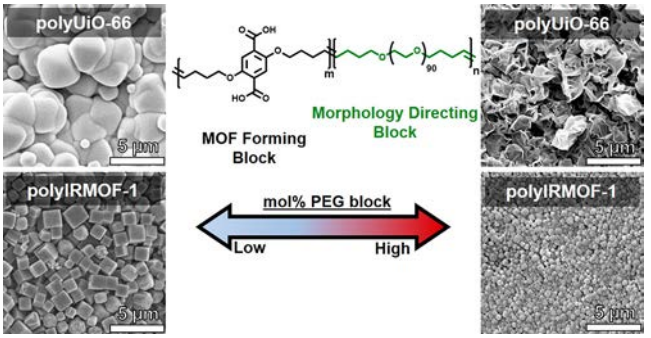

Figure 41. A block copolymer was used to direct the morphology of two different classes of polyMOFs. By varying the amount of the morphology directing block, the shape of UiO-66 polyMOFs could be controlled (top left and right SEM). Varying the amount of the morphology directing block, the size of polyIRMOF-1 could be varied. Reprinted with permission from ref 241. Copyright 2019 The Royal Society of Chemistry.

8. CONCLUDING REMARKS AND FUTURE DIRECTIONS

The hybridization of MOFs and polymers has become an increasingly explored area over the past decade. Unique and elegant approaches have been developed in an attempt to understand the interactions and interplay between these hard (MOF) and soft (polymer) materials, and to bring MOFs closer to implementation for applications. These new materials have been synthesized using top-down approaches, wherein MOF particles are postsynthetically incorporated into a hybrid composite, as well as by bottom-up approaches where MOF particles are synthesized from polymer-based ligands. However, synthesis of MOF-polymer hybrid materials requires careful consideration and characterization of both materials to ensure the material contains the desired properties of the MOF, the polymer, or both.

New approaches and significant advancements of MOF-polymer composites are expected in the next several years as MOFs increasingly gain attention for commercial applications. Achievement of single component MOF MMMs that combine the precision of inorganic membranes with the flexibility and processability of polymer membranes will be breakthrough materials for gas separations. Synthesizing MOFs from polymer-based ligands in which the resulting structure of the MOF can be determined a priori is likely to become more significant in designing multifunctional materials with complex domain structures. The use of MOF-polymer hybrids as catalytic membranes has rarely been reported and may find use in future studies of flow- or continuous-synthesis systems. Finally, the use of MOF-polymer composites has been reported in several studies ranging from gas separations to chemical warfare agent degradation in many proof-of-concept experiments. While these findings are valuable, applications that more accurately mimic field conditions are certain to be important in developing the utility of MOFs in a variety of technologies. We look forward to the many discoveries to come in this exciting frontier of MOF-polymer hybrid materials chemistry.

AUTHOR INFORMATION

Corresponding Author

*E-mail: scohen@ucsd.edu.

ORCID

Mark Kalaj: 0000-0001-7139-7517

Seth M. Cohen: 0000-0002-5233-2280

Notes

The authors declare no competing financial interest.

Biographies

Mark Kalaj was born in Shkoder, Albania, before moving to a suburb of Detroit, Michigan, with his family. He received his B.S. in Chemistry from The George Washington University in 2016, performing research with Prof. Christopher L. Cahill on structure property relationships of novel actinide- and lanthanide-based compounds and coordination polymers. He then joined the graduate program at U.C. San Diego, where he is currently a DoD NDSEG and ARCS fellow in the laboratory of Prof. Seth M. Cohen. His research includes integration of polymers and MOFs, as well as the use of MOFs and MOF-polymer hybrid materials for the catalytic degradation of chemical warfare agents.

Kyle C. Bentz received his B.S. in Chemistry as well as his M.S. in Polymers and Coatings from California Polytechnic State University, San Luis Obispo, in 2011. He then completed his Ph.D. in Chemistry at the University of Florida in 2017, where he focused on polymer nanostructures and gel rheology with Prof. Daniel A. Savin. Kyle is currently a postdoctoral scholar at U.C. San Diego in the Department of Chemistry and Biochemistry in the laboratory of Prof. Seth M. Cohen. His current research interests involve the hybridization of traditional metallopolymers and metal−organic frameworks.

Sergio Ayala, Jr. grew up in Southern California. He received his B.S. in chemistry from the University of California, Irvine, in 2014, where he performed undergraduate research on the synthesis of bioinspired dynamic soft materials in the laboratory of Prof. Zhibin Guan. He then joined the graduate program at U.C. San Diego in 2014, where he is currently a doctoral candidate in the laboratory of Prof. Seth M. Cohen. His current research includes the synthesis and characterization of a unique class of polymer-MOF hybrid materials (polyMOFs).

Joseph M. Palomba grew up in Shrewsbury, MA, and earned his B.S. in chemistry from Boston College in 2015, where he performed studies on porous materials with Prof. Chia-Kuang (Frank) Tsung. He

DOI: 10.1021/acs.chemrev.9b00575
Chem. Rev. XXXX, XXX, XXX−XXX

is currently a graduate student at U.C. San Diego in the department of Chemistry and Biochemistry in the laboratory of Prof. Seth M. Cohen. His research interests include using inorganic, materials, and analytical chemistry to investigate MOFs as heterogeneous catalysts particularly for defense applications.

Kyle S. Barcus grew up in Tollhouse, California. He received his B.S. in Biochemistry from California Polytechnic State University, San Luis Obispo, in 2017, where he performed research on stimuli-responsive polymer architectures with Prof. Phillip J. Costanzo. He then joined the graduate program at U.C. San Diego in 2017, where he is currently a graduate researcher in the laboratory of Prof. Seth M. Cohen. His current research includes developing new polymers for the synthesis of polyMOFs in the field of polymer and materials chemistry.

Yuji Katayama was born and raised in Saitama, a suburb of Tokyo, Japan. He received his B.S. degree from Tokyo Institute of Technology, Tokyo, Japan, in 2006. He earned his M.S. degree in Chemistry in 2008 at Tokyo Institute of Technology under the supervision of Prof. Yuichi Kobayashi in the field of organic chemistry. He then joined Asahi Kasei Corporation in Shizuoka, Japan, working on separation membranes. He has been a visiting scholar with Prof. Seth M. Cohen at U.C. San Diego since September 2017, working on MMMs with MOFs. His research interests are primarily in the area of functional materials for separation membranes.

Seth M. Cohen was born and raised in the San Fernando Valley of Los Angeles, California. He received a B.S. in Chemistry and B.A. in Political Science from Stanford University in 1994. He completed his Ph.D. in Chemistry at U.C. Berkeley under the direction of Prof. Kenneth N. Raymond and performed postdoctoral studies with Prof. Stephen J. Lippard at M.I.T. He started his independent career at U.C. San Diego in 2001, served as Chair of the Department of Chemistry and Biochemistry at U.C. San Diego from 2012−2015. His research interests are in the areas of inorganic, bioinorganic, medicinal, materials, and supramolecular chemistry.

ACKNOWLEDGMENTS

S.M.C. would like to thank a long, unnamed group of co-workers, colleagues, and collaborators, past, present, and future, that have contributed to his laboratory's contributions to MOF chemistry. Work on polymer-MOF composites for toxic chemical protection has been supported by the Army Research Office, Department of Army Material command, under Award W911NF-16-2-0106. Work on corona-MOFs and polyMOFs has been supported by a grant from the Department of Energy, Office of Basic Energy Sciences, Division of Materials Science and Engineering under Award DE-FG02-08ER46519. Fundamental studies on the synthesis and characterization of MOF MMMs has been supported by the National Science Foundation, Division of Materials Research (DMR-1506059). Studies on MOF catalysis has been supported by the National Science Foundation, Division of Chemistry (CHE-1661655). S.A. was supported, in part, by the United States Department of Education GAANN Fellowship (P200A150251). M.K. is supported by the Department of Defense (DoD) through the National Defense Science and Engineering Graduate (NDSEG) Fellowship Program and is the recipient of an Achievement Rewards for College Scientists (ARCS) Foundation Fellowship. J.M.P. is supported by the USD/R&E (The Under Secretary of Defense-Research and Engineering), National Defense Education Program (NDEP)/BA-1, Basic Research in the Science Mathematics and Research for Transformation (SMART) Scholarship Program. Y.K was supported by the Asahi Kasei Corporation.

ABBREVIATIONS

ALD	atomic layer deposition
ATRP	atom transfer radical polymerization
BDC	benzene dicarboxylic acid
CBC	carboxymethylcellulose
CCS	carbon capture and sequestration
CRP	controlled radical polymerization
CWA	chemical warfare agent
DHBC	double hydrophilic block polymer
DLS	dynamic light scattering
DMNP	dimethyl-4-nitrophenyl phosphate
EDX	energy-dispersive X-ray spectroscopy
FCS	fluoresence correlation spectroscopy
FTIR	Fourier transform infrared spectroscopy
GD	*o*-pinacolyl methylphosphonofluoride
HIPE	high internal phase emulsions
IL	ionic liquid
LCST	lower critical solution temperature
MMM	mixed-matrix membrane
MOF	metal−organic framework
MOP	metal−organic polyhedron
MSP	MOF scaffold polymer membrane
MVTR	moisture vapor transport rate
NMR	nuclear magnetic resonance spectroscopy
NP	nanoparticle
PAN	polyacrylonitrile
PA-6	polyamide-6
PBI	polybenzimidazole
PDMS	polydimethylsiloxane
PEG	polyethylene glycol
PEI	polyethylenimine
PI	polyimide
PIM	polymer of intrinsic microporosity
PMA	poly(methyl acrylate)
PPG	polypropylene glycol
PS	polystyrene
PSE	postsynthetic exchange
PSF	polysulfone
PSM	postsynthetic modification
PSP	postsynthetic polymerization
PXRD	powder X-ray iffraction
PVA	poly(vinyl alcohol)
PVC	polyvinyl chloride
PVCz	poly(*N*-vinylcarbazole)
PVDF	polyvinylidene fluoride
PVP	polyvinylpyrrolidone
RAFT	reversible addition−fragmentation chain-transfer
ROMP	ring opening metathesis polymerization
SEM	scanning electron microscopy
SURMOF	surface-mounted MOF
TEA	triethylamine
TEM	transmission electron microscopy
TGA	thermogravimetric analysis
TIC	toxic industrial chemical

REFERENCES

(1) Eddaoudi, M.; Kim, J.; Rosi, N.; Vodak, D.; Wachter, J.; O'Keeffe, M.; Yaghi, O. M. Systematic Design of Pore Size and Functionality in Isoreticular MOFs and Their Application in Methane Storage. *Science* **2002**, *295*, 469−472.

DOI: 10.1021/acs.chemrev.9b00575
Chem. Rev. XXXX, XXX, XXX−XXX

(2) Yaghi, O. M.; O'Keeffe, M.; Ockwig, N. W.; Chae, H. K.; Eddaoudi, M.; Kim, J. Reticular Synthesis and the Design of New Materials. *Nature* **2003**, *423*, 705−714.
(3) Li, J.-R.; Sculley, J.; Zhou, H.-C. Metal−Organic Frameworks for Separations. *Chem. Rev.* **2012**, *112*, 869−932.
(4) Suh, M. P.; Park, H. J.; Prasad, T. K.; Lim, D.-W. Hydrogen Storage in Metal−Organic Frameworks. *Chem. Rev.* **2012**, *112*, 782−835.
(5) Khan, N. A.; Hasan, Z.; Jhung, S. H. Adsorptive Removal of Hazardous Materials Using Metal-Organic Frameworks (MOFs): A Review. *J. Hazard. Mater.* **2013**, *244*−*245*, 444−456.
(6) Yuan, S.; Feng, L.; Wang, K.; Pang, J.; Bosch, M.; Lollar, C.; Sun, Y.; Qin, J.; Yang, X.; Zhang, P.; et al. Stable Metal−Organic Frameworks: Design, Synthesis, and Applications. *Adv. Mater.* **2018**, *30*, 1704303.
(7) Denny, M. S., Jr.; Moreton, J. C.; Benz, L.; Cohen, S. M. Metal-Organic Frameworks for Membrane-Based Separations. *Nat. Rev. Mater.* **2016**, *1*, 16078.
(8) Gascon, J.; Kapteijn, F. Metal-Organic Framework Membranes—High Potential, Bright Future? *Angew. Chem., Int. Ed.* **2010**, *49*, 1530−1532.
(9) Seoane, B.; Coronas, J.; Gascon, I.; Benavides, M. E.; Karvan, O.; Caro, J.; Kapteijn, F.; Gascon, J. Metal−Organic Framework Based Mixed Matrix Membranes: A Solution for Highly Efficient CO2 Capture? *Chem. Soc. Rev.* **2015**, *44*, 2421−2454.
(10) Friebe, S.; Diestel, L.; Knebel, A.; Wollbrink, A.; Caro, J. MOF-Based Mixed-Matrix Membranes in Gas Separation − Mystery and Reality. *Chem. Ing. Tech.* **2016**, *88*, 1788−1797.
(11) Shah, M.; McCarthy, M. C.; Sachdeva, S.; Lee, A. K.; Jeong, H.-K. Current Status of Metal−Organic Framework Membranes for Gas Separations: Promises and Challenges. *Ind. Eng. Chem. Res.* **2012**, *51*, 2179−2199.
(12) Tanh Jeazet, H. B.; Staudt, C.; Janiak, C. Metal−Organic Frameworks in Mixed-Matrix Membranes for Gas Separation. *Dalton Trans* **2012**, *41*, 14003−14027.
(13) Zhang, Y.; Feng, X.; Yuan, S.; Zhou, J.; Wang, B. Challenges and Recent Advances in MOF−Polymer Composite Membranes for Gas Separation. *Inorg. Chem. Front.* **2016**, *3*, 896−909.
(14) Kitao, T.; Zhang, Y.; Kitagawa, S.; Wang, B.; Uemura, T. Hybridization of MOFs and polymers. *Chem. Soc. Rev.* **2017**, *46*, 3108−3133.
(15) Chung, T.-S.; Jiang, L. Y.; Li, Y.; Kulprathipanja, S. Mixed Matrix Membranes (MMMs) Comprising Organic Polymers with Dispersed Inorganic Fillers for Gas Separation. *Prog. Polym. Sci.* **2007**, *32*, 483−507.
(16) Bastani, D.; Esmaeili, N.; Asadollahi, M. Polymeric Mixed Matrix Membranes Containing Zeolites as a Filler for Gas Separation Applications: A review. *J. Ind. Eng. Chem.* **2013**, *19*, 375−393.
(17) Zimmerman, C. M.; Singh, A.; Koros, W. J. Tailoring Mixed Matrix Composite Membranes for Gas Separations. *J. Membr. Sci.* **1997**, *137*, 145−154.
(18) Kusakabe, K.; Kuroda, T.; Morooka, S. Separation of Carbon Dioxide from Nitrogen using Ion-Exchanged Faujasite-Type Zeolite Membranes Formed on Porous Support Tubes. *J. Membr. Sci.* **1998**, *148*, 13−23.
(19) Ackley, M. W.; Rege, S. U.; Saxena, H. Application of Natural Zeolites in the Purification and Separation of Gases. *Microporous Mesoporous Mater.* **2003**, *61*, 25−42.
(20) Li, S.; Falconer, J. L.; Noble, R. D. SAPO-34 Membranes for CO2/CH4 Separation. *J. Membr. Sci.* **2004**, *241*, 121−135.
(21) Kita, H.; Fuchida, K.; Horita, T.; Asamura, H.; Okamoto, K. Preparation of Faujasite Membranes and Their Permeation Properties. *Sep. Purif. Technol.* **2001**, *25*, 261−268.
(22) Mahajan, R.; Koros, W. J. Mixed Matrix Membrane Materials with Glassy Polymers. Part 1. *Polym. Eng. Sci.* **2002**, *42*, 1420−1431.
(23) Ismail, A. F.; David, L. I. B. A Review on the Latest Development of Carbon Membranes for Gas Separation. *J. Membr. Sci.* **2001**, *193*, 1−18.
(24) Koros, W. J.; Mahajan, R. Pushing the Limits on Possibilities for Large Scale Gas Separation: Which Strategies? *J. Membr. Sci.* **2000**, *175*, 181−196.
(25) García, M. G.; Marchese, J.; Ochoa, N. A. High Activated Carbon Loading Mixed Matrix Membranes for Gas Separations. *J. Mater. Sci.* **2012**, *47*, 3064−3075.
(26) Vu, D. Q.; Koros, W. J.; Miller, S. J. Mixed Matrix Membranes Using Carbon Molecular Sieves: I. Preparation and Experimental Results. *J. Membr. Sci.* **2003**, *211*, 311−334.
(27) Vu, D. Q.; Koros, W. J.; Miller, S. J. High Pressure CO2/CH4 Separation Using Carbon Molecular Sieve Hollow Fiber Membranes. *Ind. Eng. Chem. Res.* **2002**, *41*, 367−380.
(28) Mellot-Draznieks, C.; Cheetham, A. K. Encoding Evolution of Porous Solids. *Nat. Chem.* **2017**, *9*, 6−8.
(29) Semino, R.; Moreton, J. C.; Ramsahye, N. A.; Cohen, S. M.; Maurin, G. Understanding the Origins of Metal-Organic Framework/Polymer Compatibility. *Chem. Sci.* **2018**, *9*, 315−324.
(30) Robeson, L. M.; Liu, Q.; Freeman, B. D.; Paul, D. R. Comparison of Transport Properties of Rubbery and Glassy Polymers and the Relevance to the Upper Bound Relationship. *J. Membr. Sci.* **2015**, *476*, 421−431.
(31) Katayama, Y.; Bentz, K. C.; Cohen, S. M. Defect-Free MOF-Based Mixed-Matrix Membranes Obtained by Corona Cross-Linking. *ACS Appl. Mater. Interfaces* **2019**, *11*, 13029−13037.
(32) Moreton, J. C.; Denny, M. S.; Cohen, S. M. High MOF Loading in Mixed-Matrix Membranes Utilizing Styrene/Butadiene Copolymers. *Chem. Commun.* **2016**, *52*, 14376−14379.
(33) DeCoste, J. B.; Denny, M. S., Jr.; Peterson, G. W.; Mahle, J. J.; Cohen, S. M. Enhanced Aging Properties of HKUST-1 in Hydrophobic Mixed-Matrix Membranes for Ammonia Adsorption. *Chem. Sci.* **2016**, *7*, 2711−2716.
(34) Denny, M. S., Jr.; Cohen, S. M. In Situ Modification of Metal-Organic Frameworks in Mixed-Matrix Membranes. *Angew. Chem., Int. Ed.* **2015**, *54*, 9029−9032.
(35) Erucar, I.; Yilmaz, G.; Keskin, S. Recent Advances in Metal−Organic Framework-Based Mixed Matrix Membranes. *Chem. - Asian J.* **2013**, *8*, 1692−1704.
(36) Jia, Z.; Wu, G. Metal-Organic Frameworks Based Mixed Matrix Membranes for Pervaporation. *Microporous Mesoporous Mater.* **2016**, *235*, 151−159.
(37) Lin, R.; Villacorta Hernandez, B.; Ge, L.; Zhu, Z. Metal Organic Framework Based Mixed Matrix Membranes: An Overview on Filler/Polymer Interfaces. *J. Mater. Chem. A* **2018**, *6*, 293−312.
(38) Liu, J.; Wöll, C. Surface-Supported Metal−Organic Framework Thin Films: Fabrication Methods, Applications, and Challenges. *Chem. Soc. Rev.* **2017**, *46*, 5730−5770.
(39) Zhu, X.; Tian, C.; Do-Thanh, C.-L.; Dai, S. Two-Dimensional Materials as Prospective Scaffolds for Mixed-Matrix Membrane-Based CO2 Separation. *ChemSusChem* **2017**, *10*, 3304−3316.
(40) Zornoza, B.; Tellez, C.; Coronas, J.; Gascon, J.; Kapteijn, F. Metal Organic Framework Based Mixed Matrix Membranes: An Increasingly Important Field of Research with a Large Application Potential. *Microporous Mesoporous Mater.* **2013**, *166*, 67−78.
(41) Shen, J.; Liu, G.; Huang, K.; Li, Q.; Guan, K.; Li, Y.; Jin, W. UiO-66-Polyether Block Amide Mixed Matrix Membranes for CO2 Separation. *J. Membr. Sci.* **2016**, *513*, 155−165.
(42) Furukawa, H.; Cordova, K. E.; O'Keeffe, M.; Yaghi, O. M. The Chemistry and Applications of Metal-Organic Frameworks. *Science* **2013**, *341*, 1230444.
(43) Deng, H.; Doonan, C. J.; Furukawa, H.; Ferreira, R. B.; Towne, J.; Knobler, C. B.; Wang, B.; Yaghi, O. M. Multiple Functional Groups of Varying Ratios in Metal-Organic Frameworks. *Science* **2010**, *327*, 846−850.
(44) Cao, L.; Tao, K.; Huang, A.; Kong, C.; Chen, L. A Highly Permeable Mixed Matrix Membrane Containing CAU-1-NH2 for H2 and CO2 Separation. *Chem. Commun.* **2013**, *49*, 8513−8515.
(45) Su, N. C.; Sun, D. T.; Beavers, C. M.; Britt, D. K.; Queen, W. L.; Urban, J. J. Enhanced Permeation Arising From Dual Transport

DOI: 10.1021/acs.chemrev.9b00575
Chem. Rev. XXXX, XXX, XXX−XXX

Pathways in Hybrid Polymer−MOF Membranes. *Energy Environ. Sci.* **2016**, *9*, 922−931.
(46) Feijani, E. A.; Mahdavi, H.; Tavasoli, A. Poly(vinylidene fluoride) Based Mixed Matrix Membranes Comprising Metal Organic Frameworks for Gas Separation Applications. *Chem. Eng. Res. Des.* **2015**, *96*, 87−102.
(47) Wang, Z.; Cohen, S. M. Postsynthetic Modification of Metal-Organic Frameworks. *Chem. Soc. Rev.* **2009**, *38*, 1315−1329.
(48) Cohen, S. M. The Postsynthetic Renaissance in Porous Solids. *J. Am. Chem. Soc.* **2017**, *139*, 2855−2863.
(49) Tanabe, K. K.; Cohen, S. M. Postsynthetic Modification of Metal-Organic Frameworks-A Progress Report. *Chem. Soc. Rev.* **2011**, *40*, 498−519.
(50) Cohen, S. M. Postsynthetic Methods for the Functionalization of Metal−Organic Frameworks. *Chem. Rev.* **2012**, *112*, 970−1000.
(51) Wang, Z.; Cohen, S. M. Postsynthetic Covalent Modification of a Neutral Metal−Organic Framework. *J. Am. Chem. Soc.* **2007**, *129*, 12368−12369.
(52) Kim, M.; Cahill, J. F.; Su, Y.; Prather, K. A.; Cohen, S. M. Postsynthetic Ligand Exchange as a Route to Functionalization of Metal-Organic Frameworks. *Chem. Sci.* **2012**, *3*, 126−130.
(53) Kim, M.; Cahill, J. F.; Fei, H.; Prather, K. A.; Cohen, S. M. Postsynthetic Ligand and Cation Exchange in Robust Metal-Organic Frameworks. *J. Am. Chem. Soc.* **2012**, *134*, 18082−18088.
(54) Denny, M. S.; Kalaj, M.; Bentz, K. C.; Cohen, S. M. Multicomponent Metal−Organic Framework Membranes for Advanced Functional Composites. *Chem. Sci.* **2018**, *9*, 8842−8849.
(55) Troyano, J.; Carné-Sánchez, A.; Pérez-Carvajal, J.; León-Reina, L.; Imaz, I.; Cabeza, A.; Maspoch, D. A Self-Folding Polymer Film Based on Swelling Metal−Organic Frameworks. *Angew. Chem., Int. Ed.* **2018**, *57*, 15420−15424.
(56) Troyano, J.; Carné-Sánchez, A.; Maspoch, D. Programmable Self-Assembling 3D Architectures Generated by Patterning of Swellable MOF-Based Composite Films. *Adv. Mater.* **2019**, *31*, 1808235.
(57) Chen, X. Y.; Hoang, V.-T.; Rodrigue, D.; Kaliaguine, S. Optimization of Continuous Phase in Amino-functionalized Metal−Organic Framework (MIL-53) Based co-polyimide Mixed Matrix Membranes for CO2/CH4 Separation. *RSC Adv.* **2013**, *3*, 24266−24279.
(58) Wang, H.; He, S.; Qin, X.; Li, C.; Li, T. Interfacial Engineering in Metal−Organic Framework-Based Mixed Matrix Membranes Using Covalently Grafted Polyimide Brushes. *J. Am. Chem. Soc.* **2018**, *140*, 17203−17210.
(59) Zhang, Y.; Feng, X.; Li, H.; Chen, Y.; Zhao, J.; Wang, S.; Wang, L.; Wang, B. Photoinduced Postsynthetic Polymerization of a Metal-Organic Framework toward a Flexible Stand-Alone Membrane. *Angew. Chem., Int. Ed.* **2015**, *54*, 4259−4263.
(60) Anjum, M. W.; Vermoortele, F.; Khan, A. L.; Bueken, B.; De Vos, D. E.; Vankelecom, I. F. J. Modulated UiO-66-Based Mixed-Matrix Membranes for CO2 Separation. *ACS Appl. Mater. Interfaces* **2015**, *7*, 25193−25201.
(61) Kalaj, M.; Denny, M. S., Jr; Bentz, K. C.; Palomba, J. M.; Cohen, S. M. Nylon−MOF Composites through Postsynthetic Polymerization. *Angew. Chem., Int. Ed.* **2019**, *58*, 2336−2340.
(62) Nam, D.; Huh, J.; Lee, J.; Kwak, J. H.; Jeong, H. Y.; Choi, K.; Choe, W. Cross-Linking Zr-Based Metal−Organic Polyhedra via Postsynthetic Polymerization. *Chem. Sci.* **2017**, *8*, 7765−7771.
(63) Chin, J. M.; Reithofer, M. R.; Tan, T. T. Y.; Menon, A. G.; Chen, E. Y.; Chow, C. A.; Hor, A. T. S.; Xu, J. Supergluing MOF Liquid Marbles. *Chem. Commun.* **2013**, *49*, 493−495.
(64) Satheeshkumar, C.; Yu, H. J.; Park, H.; Kim, M.; Lee, J. S.; Seo, M. Thiol−ene Photopolymerization of Vinyl-Functionalized Metal−Organic Frameworks Towards Mixed-Matrix Membranes. *J. Mater. Chem. A* **2018**, *6*, 21961−21968.
(65) Jiang, W.-L.; Ding, L.-G.; Yao, B.-J.; Wang, J.-C.; Chen, G.-J.; Li, Y.-A.; Ma, J.-P.; Ji, J.; Dong, Y.; Dong, Y.-B. A MOF-membrane Based on the Covalent Bonding Driven Assembly of a NMOF with an Organic Oligomer and its Application in Membrane Reactors. *Chem. Commun.* **2016**, *52*, 13564−13567.
(66) Yao, B.-J.; Jiang, W.-L.; Dong, Y.; Liu, Z.-X.; Dong, Y.-B. Post-Synthetic Polymerization of UiO-66-NH2 Nanoparticles and Polyurethane Oligomer toward Stand-Alone Membranes for Dye Removal and Separation. *Chem. - Eur. J.* **2016**, *22*, 10565−10571.
(67) Yao, B.-J.; Ding, L.-G.; Li, F.; Li, J.-T.; Fu, Q.-J.; Ban, Y.; Guo, A.; Dong, Y.-B. Chemically Cross-Linked MOF Membrane Generated from Imidazolium-Based Ionic Liquid-Decorated UiO-66 Type NMOF and Its Application toward CO2 Separation and Conversion. *ACS Appl. Mater. Interfaces* **2017**, *9*, 38919−38930.
(68) McDonald, K. A.; Feldblyum, J. I.; Koh, K.; Wong-Foy, A. G.; Matzger, A. J. Polymer@MOF@MOF: "Grafting From" Atom Transfer Radical Polymerization for the Synthesis of Hybrid Porous Solids. *Chem. Commun.* **2015**, *51*, 11994−11996.
(69) Sun, H.; Tang, B.; Wu, P. Development of Hybrid Ultrafiltration Membranes with Improved Water Separation Properties Using Modified Superhydrophilic Metal−Organic Framework Nanoparticles. *ACS Appl. Mater. Interfaces* **2017**, *9*, 21473−21484.
(70) Gao, X.; Zhang, J.; Huang, K.; Zhang, J. ROMP for Metal−Organic Frameworks: An Efficient Technique toward Robust and High-Separation Performance Membranes. *ACS Appl. Mater. Interfaces* **2018**, *10*, 34640−34645.
(71) Molavi, H.; Shojaei, A.; Mousavi, S. A. Improving mixed-matrix membrane performance via PMMA grafting from functionalized NH2−UiO-66. *J. Mater. Chem. A* **2018**, *6*, 2775−2791.
(72) Xie, K.; Fu, Q.; Kim, J.; Lu, H.; He, Y.; Zhao, Q.; Scofield, J.; Webley, P. A.; Qiao, G. G. Increasing Both Selectivity and Permeability of Mixed-Matrix Membranes: Sealing the External Surface of Porous MOF Nanoparticles. *J. Membr. Sci.* **2017**, *535*, 350−356.
(73) Marti, A. M.; Venna, S. R.; Roth, E. A.; Culp, J. T.; Hopkinson, D. P. Simple Fabrication Method for Mixed Matrix Membranes with in Situ MOF Growth for Gas Separation. *ACS Appl. Mater. Interfaces* **2018**, *10*, 24784−24790.
(74) Rodenas, T.; Luz, I.; Prieto, G.; Seoane, B.; Miro, H.; Corma, A.; Kapteijn, F.; Llabrés i Xamena, F. X.; Gascon, J. Metal−Organic Framework Nanosheets in Polymer Composite Materials for Gas Separation. *Nat. Mater.* **2015**, *14*, 48−55.
(75) Smith, Z. P.; Bachman, J. E.; Li, T.; Gludovatz, B.; Kusuma, V. A.; Xu, T.; Hopkinson, D. P.; Ritchie, R. O.; Long, J. R. Increasing M2(dobdc) Loading in Selective Mixed-Matrix Membranes: A Rubber Toughening Approach. *Chem. Mater.* **2018**, *30*, 1484−1495.
(76) Sabetghadam, A.; Seoane, B.; Keskin, D.; Duim, N.; Rodenas, T.; Shahid, S.; Sorribas, S.; Guillouzer, C. L.; Clet, G.; Tellez, C.; et al. Metal Organic Framework Crystals in Mixed-Matrix Membranes: Impact of the Filler Morphology on the Gas Separation Performance. *Adv. Funct. Mater.* **2016**, *26*, 3154−3163.
(77) Benzaqui, M.; Semino, R.; Menguy, N.; Carn, F.; Kundu, T.; Guigner, J.-M.; McKeown, N. B.; Msayib, K. J.; Carta, M.; Malpass-Evans, R.; et al. Toward an Understanding of the Microstructure and Interfacial Properties of PIMs/ZIF-8 Mixed Matrix Membranes. *ACS Appl. Mater. Interfaces* **2016**, *8* (40), 27311−27321.
(78) He, S.; Wang, H.; Zhang, C.; Zhang, S.; Yu, Y.; Lee, Y.; Li, T. A Generalizable Method for the Construction of MOF@Polymer Functional Composites Through Surface-Initiated Atom Transfer Radical Polymerization. *Chem. Sci.* **2019**, *10*, 1816−1822.
(79) Semino, R.; Ramsahye, N. A.; Ghoufi, A.; Maurin, G. Microscopic Model of the Metal−Organic Framework/Polymer Interface: A First Step toward Understanding the Compatibility in Mixed Matrix Membranes. *ACS Appl. Mater. Interfaces* **2016**, *8*, 809−819.
(80) Benzaqui, M.; Semino, R.; Carn, F.; Tavares, S. R.; Menguy, N.; Giménez-Marqués, M.; Bellido, E.; Horcajada, P.; Berthelot, T.; Kuzminova, A. I.; et al. Covalent and Selective Grafting of Polyethylene Glycol Brushes at the Surface of ZIF-8 for the Processing of Membranes for Pervaporation. *ACS Sustainable Chem. Eng.* **2019**, *7*, 6629−6639.

DOI: 10.1021/acs.chemrev.9b00575
Chem. Rev. XXXX, XXX, XXX−XXX

(81) Duan, P.; Moreton, J. C.; Tavares, S. R.; Semino, R.; Maurin, G.; Cohen, S. M.; Schmidt-Rohr, K. Polymer Infiltration into Metal−Organic Frameworks in Mixed-Matrix Membranes Detected in Situ by NMR. *J. Am. Chem. Soc.* **2019**, *141*, 7589−7595.
(82) Sholl, D. S.; Lively, R. P. Seven Chemical Separations to Change the World. *Nature* **2016**, *532*, 435−437.
(83) Liu, G.; Chernikova, V.; Liu, Y.; Zhang, K.; Belmabkhout, Y.; Shekhah, O.; Zhang, C.; Yi, S.; Eddaoudi, M.; Koros, W. J. Mixed Matrix Formulations with MOF Molecular Sieving for Key Energy-Intensive Separations. *Nat. Mater.* **2018**, *17*, 283−289.
(84) Liu, G.; Cadiau, A.; Liu, Y.; Adil, K.; Chernikova, V.; Carja, I.-D.; Belmabkhout, Y.; Karunakaran, M.; Shekhah, O.; Zhang, C.; et al. Enabling Fluorinated MOF-Based Membranes for Simultaneous Removal of H2S and CO2 from Natural Gas. *Angew. Chem., Int. Ed.* **2018**, *57*, 14811−14816.
(85) Figueroa, J. D.; Fout, T.; Plasynski, S.; McIlvried, H.; Srivastava, R. D. Advances in CO2 Capture Technology—The U.S. Department of Energy's Carbon Sequestration Program. *Int. J. Greenhouse Gas Control* **2008**, *2*, 9−20.
(86) Ghalei, B.; Sakurai, K.; Kinoshita, Y.; Wakimoto, K.; Isfahani, A. P.; Song, Q.; Doitomi, K.; Furukawa, S.; Hirao, H.; Kusuda, H.; Kitagawa, S.; Sivaniah, E. Enhanced Selectivity in Mixed Matrix Membranes for CO2 Capture Through Efficient Dispersion of Amine-Functionalized MOF Nanoparticles. *Nat. Energy* **2017**, *2*, 17086.
(87) Ebadi Amooghin, A.; Mashhadikhan, S.; Sanaeepur, H.; Moghadassi, A.; Matsuura, T.; Ramakrishna, S. Substantial Breakthroughs on Function-Led Design of Advanced Materials Used in Mixed Matrix Membranes (MMMs): A New Horizon for Efficient CO2 Separation. *Prog. Mater. Sci.* **2019**, *102*, 222−295.
(88) Xie, K.; Fu, Q.; Webley, P. A.; Qiao, G. G. MOF Scaffold for a High-Performance Mixed-Matrix Membrane. *Angew. Chem., Int. Ed.* **2018**, *57*, 8597−8602.
(89) Eldridge, R. B. Olefin/Paraffin Separation Technology: A Review. *Ind. Eng. Chem. Res.* **1993**, *32*, 2208−2212.
(90) Martins, V. F. D.; Ribeiro, A. M.; Plaza, M. G.; Santos, J. C.; Loureiro, J. M.; Ferreira, A. F. P.; Rodrigues, A. E. Gas-Phase Simulated Moving Bed: Propane/Propylene Separation on 13X Zeolite. *J. Chromatogr. A* **2015**, *1423*, 136−148.
(91) Fairen-Jimenez, D.; Moggach, S. A.; Wharmby, M. T.; Wright, P. A.; Parsons, S.; Düren, T. Opening the Gate: Framework Flexibility in ZIF-8 Explored by Experiments and Simulations. *J. Am. Chem. Soc.* **2011**, *133*, 8900−8902.
(92) Bennett, T. D.; Cheetham, A. K.; Fuchs, A. H.; Coudert, F.-X. Interplay Between Defects, Disorder and Flexibility in Metal-Organic Frameworks. *Nat. Chem.* **2017**, *9*, 11−16.
(93) Zhang, C.; Lively, R. P.; Zhang, K.; Johnson, J. R.; Karvan, O.; Koros, W. J. Unexpected Molecular Sieving Properties of Zeolitic Imidazolate Framework-8. *J. Phys. Chem. Lett.* **2012**, *3*, 2130−2134.
(94) Lee, M. J.; Abdul Hamid, M. R.; Lee, J.; Kim, J. S.; Lee, Y. M.; Jeong, H.-K. Ultrathin Zeolitic-Imidazolate Framework ZIF-8 Membranes on Polymeric Hollow Fibers for Propylene/Propane Separation. *J. Membr. Sci.* **2018**, *559*, 28−34.
(95) Kwon, H. T.; Jeong, H.-K. In Situ Synthesis of Thin Zeolitic−Imidazolate Framework ZIF-8 Membranes Exhibiting Exceptionally High Propylene/Propane Separation. *J. Am. Chem. Soc.* **2013**, *135*, 10763−10768.
(96) Zhang, C.; Dai, Y.; Johnson, J. R.; Karvan, O.; Koros, W. J. High Performance ZIF-8/6FDA-DAM Mixed Matrix Membrane for Propylene/Propane Separations. *J. Membr. Sci.* **2012**, *389*, 34−42.
(97) Ma, X.; Swaidan, R. J.; Wang, Y.; Hsiung, C.-e.; Han, Y.; Pinnau, I. Highly Compatible Hydroxyl-Functionalized Microporous Polyimide-ZIF-8 Mixed Matrix Membranes for Energy Efficient Propylene/Propane Separation. *ACS Appl. Nano Mater.* **2018**, *1*, 3541−3547.
(98) An, H.; Park, S.; Kwon, H. T.; Jeong, H.-K.; Lee, J. S. A New Superior Competitor for Exceptional Propylene/Propane Separations: ZIF-67 Containing Mixed Matrix Membranes. *J. Membr. Sci.* **2017**, *526*, 367−376.
(99) Kwon, H. T.; Jeong, H.-K.; Lee, A. S.; An, H. S.; Lee, J. S. Heteroepitaxially Grown Zeolitic Imidazolate Framework Membranes with Unprecedented Propylene/Propane Separation Performances. *J. Am. Chem. Soc.* **2015**, *137*, 12304−12311.
(100) Krokidas, P.; Castier, M.; Moncho, S.; Sredojevic, D. N.; Brothers, E. N.; Kwon, H. T.; Jeong, H.-K.; Lee, J. S.; Economou, I. G. ZIF-67 Framework: A Promising New Candidate for Propylene/Propane Separation. Experimental Data and Molecular Simulations. *J. Phys. Chem. C* **2016**, *120*, 8116−8124.
(101) Turner, J. A. Sustainable Hydrogen Production. *Science* **2004**, *305*, 972−974.
(102) Scholes, C. A.; Smith, K. H.; Kentish, S. E.; Stevens, G. W. CO2 Capture from Pre-Combustion Processes—Strategies for Membrane Gas Separation. *Int. J. Greenhouse Gas Control* **2010**, *4*, 739−755.
(103) Zhang, C.; Liu, B.; Wang, G.; Yu, G.; Zou, X.; Zhu, G. Small-Pore CAU-21 and Porous PIM-1 in Mixed-Matrix Membranes for Improving Selectivity and Permeability in Hydrogen Separation. *Chem. Commun.* **2019**, *55*, 7101−7104.
(104) Zhong, Z.; Yao, J.; Chen, R.; Low, Z.; He, M.; Liu, J. Z.; Wang, H. Oriented Two-Dimensional Zeolitic Imidazolate Framework-L Membranes and Their Gas Permeation Properties. *J. Mater. Chem. A* **2015**, *3*, 15715−15722.
(105) Kim, S.; Shamsaei, E.; Lin, X.; Hu, Y.; Simon, G. P.; Seong, J. G.; Kim, J. S.; Lee, W. H.; Lee, Y. M.; Wang, H. The Enhanced Hydrogen Separation Performance of Mixed Matrix Membranes by Incorporation of Two-Dimensional ZIF-L into Polyimide Containing Hydroxyl Group. *J. Membr. Sci.* **2018**, *549*, 260−266.
(106) UNICEF, W. H. O. a. *Progress on Drinking Water and Sanitation: 2012 Update*; WHO/UNICEF Joint Monitoring Programme for Water Supply and Sanitation: United States, 2012.
(107) Zhao, X.; Wang, D.; Xiang, C.; Zhang, F.; Liu, L.; Zhou, X.; Zhang, H. Facile Synthesis of Boron Organic Polymers for Efficient Removal and Separation of Methylene Blue, Rhodamine B, and Rhodamine 6G. *ACS Sustainable Chem. Eng.* **2018**, *6*, 16777−16787.
(108) Liu, H.; Sun, R.; Feng, S.; Wang, D.; Liu, H. Rapid Synthesis of a Silsesquioxane-Based Disulfide-Linked Polymer for Selective Removal of Cationic Dyes from Aqueous Solutions. *Chem. Eng. J.* **2019**, *359*, 436−445.
(109) Wang, C.; Liu, X.; Keser Demir, N.; Chen, J. P.; Li, K. Applications of Water Stable Metal−Organic Frameworks. *Chem. Soc. Rev.* **2016**, *45*, 5107−5134.
(110) Li, X.; Liu, Y.; Wang, J.; Gascon, J.; Li, J.; Van der Bruggen, B. Metal−Organic Frameworks Based Membranes for Liquid Separation. *Chem. Soc. Rev.* **2017**, *46*, 7124−7144.
(111) Wu, C.; Maurer, C.; Wang, Y.; Xue, S.; Davis, D. L. Water Pollution and Human Health in China. *Environ. Health Perspect.* **1999**, *107*, 251−256.
(112) Zhang, R.; Ji, S.; Wang, N.; Wang, L.; Zhang, G.; Li, J.-R. Coordination-Driven In Situ Self-Assembly Strategy for the Preparation of Metal−Organic Framework Hybrid Membranes. *Angew. Chem., Int. Ed.* **2014**, *53*, 9775−9779.
(113) Basu, S.; Maes, M.; Cano-Odena, A.; Alaerts, L.; De Vos, D. E.; Vankelecom, I. F. J. Solvent Resistant Nanofiltration (SRNF) Membranes Based on Metal-Organic Frameworks. *J. Membr. Sci.* **2009**, *344*, 190−198.
(114) Ordoñez, M. J. C.; Balkus, K. J.; Ferraris, J. P.; Musselman, I. H. Molecular Sieving Realized with ZIF-8/Matrimid® Mixed-Matrix Membranes. *J. Membr. Sci.* **2010**, *361*, 28−37.
(115) Li, J.; Gong, J.-L.; Zeng, G.-M.; Zhang, P.; Song, B.; Cao, W.-C.; Liu, H.-Y.; Huan, S.-Y. Zirconium-Based Metal Organic Frameworks Loaded on Polyurethane Foam Membrane for Simultaneous Removal of Dyes with Different Charges. *J. Colloid Interface Sci.* **2018**, *527*, 267−279.
(116) Li, Z.; Yang, P.; Gao, Z.; Song, M.; Fang, Q.; Xue, M.; Qiu, S. A New ZIF Molecular-Sieving Membrane for High-Efficiency Dye Removal. *Chem. Commun.* **2019**, *55*, 3505−3508.

DOI: 10.1021/acs.chemrev.9b00575
Chem. Rev. XXXX, XXX, XXX−XXX

(117) Yang, L.; Wang, Z.; Zhang, J. Zeolite Imidazolate Framework Hybrid Nanofiltration (NF) Membranes with Enhanced Permselectivity for Dye Removal. *J. Membr. Sci.* **2017**, *532*, 76−86.
(118) Zhu, J.; Qin, L.; Uliana, A.; Hou, J.; Wang, J.; Zhang, Y.; Li, X.; Yuan, S.; Li, J.; Tian, M.; et al. Elevated Performance of Thin Film Nanocomposite Membranes Enabled by Modified Hydrophilic MOFs for Nanofiltration. *ACS Appl. Mater. Interfaces* **2017**, *9*, 1975−1986.
(119) Bai, Z.-Q.; Yuan, L.-Y.; Zhu, L.; Liu, Z.-R.; Chu, S.-Q.; Zheng, L.-R.; Zhang, J.; Chai, Z.-F.; Shi, W.-Q. Introduction of Amino Groups into Acid-Resistant MOFs for Enhanced U(vi) Sorption. *J. Mater. Chem. A* **2015**, *3*, 525−534.
(120) Meng, X.; Zhong, R.-L.; Song, X.-Z.; Song, S.-Y.; Hao, Z.-M.; Zhu, M.; Zhao, S.-N.; Zhang, H.-J. A Stable, Pillar-Layer Metal−Organic Framework Containing Uncoordinated Carboxyl Groups for Separation of Transition Metal Ions. *Chem. Commun.* **2014**, *50*, 6406−6408.
(121) Fang, Q.-R.; Yuan, D.-Q.; Sculley, J.; Li, J.-R.; Han, Z.-B.; Zhou, H.-C. Functional Mesoporous Metal−Organic Frameworks for the Capture of Heavy Metal Ions and Size-Selective Catalysis. *Inorg. Chem.* **2010**, *49*, 11637−11642.
(122) Wang, C.; Liu, X.; Chen, J. P.; Li, K. Superior Removal of Arsenic from Water with Zirconium Metal-Organic Framework UiO-66. *Sci. Rep.* **2015**, *5*, 16613.
(123) Yin, N.; Wang, K.; Wang, L.; Li, Z. Amino-Functionalized MOFs Combining Ceramic Membrane Ultrafiltration for Pb (II) Removal. *Chem. Eng. J.* **2016**, *306*, 619−628.
(124) Rao, Z.; Feng, K.; Tang, B.; Wu, P. Surface Decoration of Amino-Functionalized Metal−Organic Framework/Graphene Oxide Composite onto Polydopamine-Coated Membrane Substrate for Highly Efficient Heavy Metal Removal. *ACS Appl. Mater. Interfaces* **2017**, *9*, 2594−2605.
(125) Efome, J. E.; Rana, D.; Matsuura, T.; Lan, C. Q. Insight Studies on Metal-Organic Framework Nanofibrous Membrane Adsorption and Activation for Heavy Metal Ions Removal from Aqueous Solution. *ACS Appl. Mater. Interfaces* **2018**, *10*, 18619−18629.
(126) Sun, D. T.; Peng, L.; Reeder, W. S.; Moosavi, S. M.; Tiana, D.; Britt, D. K.; Oveisi, E.; Queen, W. L. Rapid, Selective Heavy Metal Removal from Water by a Metal−Organic Framework/Polydopamine Composite. *ACS Cent. Sci.* **2018**, *4*, 349−356.
(127) Sun, D. T.; Gasilova, N.; Yang, S.; Oveisi, E.; Queen, W. L. Rapid, Selective Extraction of Trace Amounts of Gold from Complex Water Mixtures with a Metal−Organic Framework (MOF)/Polymer Composite. *J. Am. Chem. Soc.* **2018**, *140*, 16697−16703.
(128) Elimelech, M.; Phillip, W. A. The Future of Seawater Desalination: Energy, Technology, and the Environment. *Science* **2011**, *333*, 712−717.
(129) Greenlee, L. F.; Lawler, D. F.; Freeman, B. D.; Marrot, B.; Moulin, P. Reverse Osmosis Desalination: Water Sources, Technology, and Today's Challenges. *Water Res.* **2009**, *43*, 2317−2348.
(130) Zhou, M.; Nemade, P. R.; Lu, X.; Zeng, X.; Hatakeyama, E. S.; Noble, R. D.; Gin, D. L. New Type of Membrane Material for Water Desalination Based on a Cross-Linked Bicontinuous Cubic Lyotropic Liquid Crystal Assembly. *J. Am. Chem. Soc.* **2007**, *129*, 9574−9575.
(131) Liang, B.; He, X.; Hou, J.; Li, L.; Tang, Z. Membrane Separation in Organic Liquid: Technologies, Achievements, and Opportunities. *Adv. Mater.* **2019**, *31*, 1806090.
(132) Lee, T. H.; Park, I.; Oh, J. Y.; Jang, J. K.; Park, H. B. Facile Preparation of Polyamide Thin-Film Nanocomposite Membranes Using Spray-Assisted Nanofiller Predeposition. *Ind. Eng. Chem. Res.* **2019**, *58*, 4248−4256.
(133) Liu, X.; Demir, N. K.; Wu, Z.; Li, K. Highly Water-Stable Zirconium Metal−Organic Framework UiO-66 Membranes Supported on Alumina Hollow Fibers for Desalination. *J. Am. Chem. Soc.* **2015**, *137*, 6999−7002.
(134) Liang, W.; Li, L.; Hou, J.; Shepherd, N. D.; Bennett, T. D.; D'Alessandro, D. M.; Chen, V. Linking Defects, Hierarchical Porosity Generation and Desalination Performance in Metal−Organic Frameworks. *Chem. Sci.* **2018**, *9*, 3508−3516.
(135) DeCoste, J. B.; Peterson, G. W. Metal−Organic Frameworks for Air Purification of Toxic Chemicals. *Chem. Rev.* **2014**, *114*, 5695−5727.
(136) Zhao, J.; Losego, M. D.; Lemaire, P. C.; Williams, P. S.; Gong, B.; Atanasov, S. E.; Blevins, T. M.; Oldham, C. J.; Walls, H. J.; Shepherd, S. D.; et al. Highly Adsorptive, MOF-Functionalized Nonwoven Fiber Mats for Hazardous Gas Capture Enabled by Atomic Layer Deposition. *Adv. Mater. Interfaces* **2014**, *1*, 1400040.
(137) Zhao, J.; Lee, D. T.; Yaga, R. W.; Hall, M. G.; Barton, H. F.; Woodward, I. R.; Oldham, C. J.; Walls, H. J.; Peterson, G. W.; Parsons, G. N. Ultra-Fast Degradation of Chemical Warfare Agents Using MOF-Nanofiber Kebabs. *Angew. Chem., Int. Ed.* **2016**, *55*, 13224−13228.
(138) Lee, D. T.; Zhao, J.; Oldham, C. J.; Peterson, G. W.; Parsons, G. N. UiO-66-NH2Metal−Organic Framework (MOF) Nucleation on TiO2, ZnO, and Al2O3 Atomic Layer Deposition-Treated Polymer Fibers: Role of Metal Oxide on MOF Growth and Catalytic Hydrolysis of Chemical Warfare Agent Simulants. *ACS Appl. Mater. Interfaces* **2017**, *9*, 44847−44855.
(139) Lee, D. T.; Zhao, J.; Peterson, G. W.; Parsons, G. N. Catalytic "MOF-Cloth" Formed via Directed Supramolecular Assembly of UiO-66-NH2 Crystals on Atomic Layer Deposition-Coated Textiles for Rapid Degradation of Chemical Warfare Agent Simulants. *Chem. Mater.* **2017**, *29*, 4894−4903.
(140) Barton, H. F.; Davis, A. K.; Lee, D. T.; Parsons, G. N. Solvothermal Synthesis of MIL-96 and UiO-66-NH2 on Atomic Layer Deposited Metal Oxide Coatings on Fiber Mats. *J. Visualized Exp.* **2018**, *136*, No. e57734.
(141) Lemaire, P. C.; Zhao, J.; Williams, P. S.; Walls, H. J.; Shepherd, S. D.; Losego, M. D.; Peterson, G. W.; Parsons, G. N. Copper Benzenetricarboxylate Metal−Organic Framework Nucleation Mechanisms on Metal Oxide Powders and Thin Films formed by Atomic Layer Deposition. *ACS Appl. Mater. Interfaces* **2016**, *8*, 9514−9522.
(142) Lee, D. T.; Jamir, J. D.; Peterson, G. W.; Parsons, G. N. Water-Stable Chemical-Protective Textiles via Euhedral Surface-Oriented 2D Cu-TCPP Metal-Organic Frameworks. *Small* **2019**, *15*, 1805133.
(143) Peterson, G. W.; Browe, M. A.; Durke, E. M.; Epps, T. H. Flexible SIS/HKUST-1 Mixed Matrix Composites as Protective Barriers against Chemical Warfare Agent Simulants. *ACS Appl. Mater. Interfaces* **2018**, *10*, 43080−43087.
(144) Peterson, G. W.; Lu, A. X.; Hall, M. G.; Browe, M. A.; Tovar, T.; Epps, T. H. MOFwich: Sandwiched Metal−Organic Framework-Containing Mixed Matrix Composites for Chemical Warfare Agent Removal. *ACS Appl. Mater. Interfaces* **2018**, *10*, 6820−6824.
(145) Zhang, X.; Zhang, Q.; Yue, D.; Zhang, J.; Wang, J.; Li, B.; Yang, Y.; Cui, Y.; Qian, G. Flexible Metal−Organic Framework-Based Mixed-Matrix Membranes: A New Platform for H2S Sensors. *Small* **2018**, *14*, 1801563.
(146) Peterson, G. W.; Lu, A. X.; Epps, T. H. Tuning the Morphology and Activity of Electrospun Polystyrene/UiO-66-NH2Metal−Organic Framework Composites to Enhance Chemical Warfare Agent Removal. *ACS Appl. Mater. Interfaces* **2017**, *9*, 32248−32254.
(147) McCarthy, D. L.; Liu, J.; Dwyer, D. B.; Troiano, J. L.; Boyer, S. M.; DeCoste, J. B.; Bernier, W. E.; Jones, W. E., Jr. Electrospun Metal−Organic Framework Polymer Composites for the Catalytic Degradation of Methyl Paraoxon. *New J. Chem.* **2017**, *41*, 8748−8753.
(148) López-Maya, E.; Montoro, C.; Rodríguez-Albelo, L. M.; Aznar Cervantes, S. D.; Lozano-Pérez, A. A.; Cenís, J. L.; Barea, E.; Navarro, J. A. R. Textile/Metal−Organic-Framework Composites as Self-Detoxifying Filters for Chemical-Warfare Agents. *Angew. Chem., Int. Ed.* **2015**, *54*, 6790−6794.
(149) Liang, H.; Yao, A.; Jiao, X.; Li, C.; Chen, D. Fast and Sustained Degradation of Chemical Warfare Agent Simulants Using Flexible Self-Supported Metal−Organic Framework Filters. *ACS Appl. Mater. Interfaces* **2018**, *10*, 20396−20403.

DOI: 10.1021/acs.chemrev.9b00575
Chem. Rev. XXXX, XXX, XXX−XXX

(150) Yao, A.; Jiao, X.; Chen, D.; Li, C. Photothermally Enhanced Detoxification of Chemical Warfare Agent Simulants Using Bioinspired Core−Shell Dopamine−Melanin@Metal−Organic Frameworks and Their Fabrics. *ACS Appl. Mater. Interfaces* **2019**, *11*, 7927−7935.
(151) Dwyer, D. B.; Dugan, N.; Hoffman, N.; Cooke, D. J.; Hall, M. G.; Tovar, T. M.; Bernier, W. E.; DeCoste, J.; Pomerantz, N. L.; Jones, W. E. Chemical Protective Textiles of UiO-66-Integrated PVDF Composite Fibers with Rapid Heterogeneous Decontamination of Toxic Organophosphates. *ACS Appl. Mater. Interfaces* **2018**, *10*, 34585−34591.
(152) Moon, S.-Y.; Proussaloglou, E.; Peterson, G. W.; DeCoste, J. B.; Hall, M. G.; Howarth, A. J.; Hupp, J. T.; Farha, O. K. Detoxification of Chemical Warfare Agents Using a Zr6-Based Metal−Organic Framework/Polymer Mixture. *Chem. - Eur. J.* **2016**, *22*, 14864−14868.
(153) Bunge, M. A.; Davis, A. B.; West, K. N.; West, C. W.; Glover, T. G. Synthesis and Characterization of UiO-66-NH2Metal−Organic Framework Cotton Composite Textiles. *Ind. Eng. Chem. Res.* **2018**, *57*, 9151−9161.
(154) Kim, M.-K.; Kim, S. H.; Park, M.; Ryu, S. G.; Jung, H. Degradation of Chemical Warfare Agents Over Cotton Fabric Functionalized with UiO-66-NH2. *RSC Adv.* **2018**, *8*, 41633−41638.
(155) Chen, Z.; Islamoglu, T.; Farha, O. K. Toward Base Heterogenization: A Zirconium Metal−Organic Framework/Dendrimer or Polymer Mixture for Rapid Hydrolysis of a Nerve-Agent Simulant. *ACS Appl. Nano Mater.* **2019**, *2*, 1005−1008.
(156) Young, A. J.; Guillet-Nicolas, R.; Marshall, E. S.; Kleitz, F.; Goodhand, A. J.; Glanville, L. B. L.; Reithofer, M. R.; Chin, J. M. Direct Ink Writing of Catalytically Active UiO-66 Polymer Composites. *Chem. Commun.* **2019**, *55*, 2190−2193.
(157) Bobbitt, N. S.; Mendonca, M. L.; Howarth, A. J.; Islamoglu, T.; Hupp, J. T.; Farha, O. K.; Snurr, R. Q. Metal−Organic Frameworks for the Removal of Toxic Industrial Chemicals and Chemical Warfare Agents. *Chem. Soc. Rev.* **2017**, *46*, 3357−3385.
(158) Liu, Y.; Howarth, A. J.; Vermeulen, N. A.; Moon, S.-Y.; Hupp, J. T.; Farha, O. K. Catalytic Degradation of Chemical Warfare Agents and Their Simulants by Metal-Organic Frameworks. *Coord. Chem. Rev.* **2017**, *346*, 101−111.
(159) Greiner, A.; Wendorff, J. H. Electrospinning: A Fascinating Method for the Preparation of Ultrathin Fibers. *Angew. Chem., Int. Ed.* **2007**, *46*, 5670−5703.
(160) Rose, M.; Böhringer, B.; Jolly, M.; Fischer, R.; Kaskel, S. MOF Processing by Electrospinning for Functional Textiles. *Adv. Eng. Mater.* **2011**, *13*, 356−360.
(161) Ostermann, R.; Cravillon, J.; Weidmann, C.; Wiebcke, M.; Smarsly, B. M. Metal−Organic Framework Nanofibers via Electrospinning. *Chem. Commun.* **2011**, *47*, 442−444.
(162) Lu, A. X.; McEntee, M.; Browe, M. A.; Hall, M. G.; DeCoste, J. B.; Peterson, G. W. MOFabric: Electrospun Nanofiber Mats from PVDF/UiO-66-NH2 for Chemical Protection and Decontamination. *ACS Appl. Mater. Interfaces* **2017**, *9*, 13632−13636.
(163) Lu, A. X.; Ploskonka, A. M.; Tovar, T. M.; Peterson, G. W.; DeCoste, J. B. Direct Surface Growth Of UIO-66-NH2 on Polyacrylonitrile Nanofibers for Efficient Toxic Chemical Removal. *Ind. Eng. Chem. Res.* **2017**, *56*, 14502−14506.
(164) Liu, Y.; Ai, K.; Liu, J.; Deng, M.; He, Y.; Lu, L. Dopamine-Melanin Colloidal Nanospheres: An Efficient Near-Infrared Photothermal Therapeutic Agent for In Vivo Cancer Therapy. *Adv. Mater.* **2013**, *25*, 1353−1359.
(165) Dhainaut, J.; Avci-Camur, C.; Troyano, J.; Legrand, A.; Canivet, J.; Imaz, I.; Maspoch, D.; Reinsch, H.; Farrusseng, D. Systematic Study of the Impact of MOF Densification into Tablets on Textural and Mechanical Properties. *CrystEngComm* **2017**, *19*, 4211−4218.
(166) Peterson, G. W.; DeCoste, J. B.; Glover, T. G.; Huang, Y.; Jasuja, H.; Walton, K. S. Effects of Pelletization Pressure on the Physical and Chemical Properties of the Metal−Organic Frameworks Cu3(BTC)2 and UiO-66. *Microporous Mesoporous Mater.* **2013**, *179*, 48−53.
(167) Valekar, A. H.; Cho, K.-H.; Lee, U. H.; Lee, J. S.; Yoon, J. W.; Hwang, Y. K.; Lee, S. G.; Cho, S. J.; Chang, J.-S. Shaping of Porous Metal−Organic Framework Granules Using Mesoporous ρ-alumina as a Binder. *RSC Adv.* **2017**, *7*, 55767−55777.
(168) U. H. Lee, A. H. V., Hwang, Y. K.; Chang, J. S., Granulation and Shaping of Metal−Organic Frameworks. In *The Chemistry of Metal−Organic Frameworks*; Kaskel, S., Ed.; Wiley-VCH, 2016; pp 551−572.
(169) Grande, C. A.; Agueda, V. I.; Spjelkavik, A.; Blom, R. An Efficient Recipe for Formulation of Metal-Organic Frameworks. *Chem. Eng. Sci.* **2015**, *124*, 154−158.
(170) Küsgens, P.; Zgaverdea, A.; Fritz, H.-G.; Siegle, S.; Kaskel, S. Metal-Organic Frameworks in Monolithic Structures. *J. Am. Ceram. Soc.* **2010**, *93*, 2476−2479.
(171) Hong, W. Y.; Perera, S. P.; Burrows, A. D. Manufacturing of Metal-Organic Framework Monoliths and Their Application in CO2 Adsorption. *Microporous Mesoporous Mater.* **2015**, *214*, 149−155.
(172) Chen, Y.; Huang, X.; Zhang, S.; Li, S.; Cao, S.; Pei, X.; Zhou, J.; Feng, X.; Wang, B. Shaping of Metal−Organic Frameworks: From Fluid to Shaped Bodies and Robust Foams. *J. Am. Chem. Soc.* **2016**, *138*, 10810−10813.
(173) Ma, X.; Chai, Y.; Li, P.; Wang, B. Metal−Organic Framework Films and Their Potential Applications in Environmental Pollution Control. *Acc. Chem. Res.* **2019**, *52*, 1461−1470.
(174) Chen, Y.; Chen, F.; Zhang, S.; Cai, Y.; Cao, S.; Li, S.; Zhao, W.; Yuan, S.; Feng, X.; Cao, A.; et al. Facile Fabrication of Multifunctional Metal−Organic Framework Hollow Tubes To Trap Pollutants. *J. Am. Chem. Soc.* **2017**, *139*, 16482−16485.
(175) Hansson, S.; Trouillet, V.; Tischer, T.; Goldmann, A. S.; Carlmark, A.; Barner-Kowollik, C.; Malmstrom, E. Grafting Efficiency of Synthetic Polymers onto Biomaterials: A Comparative Study of Grafting-from versus Grafting-To. *Biomacromolecules* **2013**, *14*, 64−74.
(176) Dukes, D.; Li, Y.; Lewis, S.; Benicewicz, B.; Schadler, L.; Kumar, S. K. Conformational Transitions of Spherical Polymer Brushes: Synthesis, Characterization, and Theory. *Macromolecules* **2010**, *43*, 1564−1570.
(177) Bentz, K. C.; Ejaz, M.; Arencibia, S.; Sultan, N.; Grayson, S. M.; Savin, D. A. Hollow Amphiphilic Crosslinked Nanocapsules from Sacrificial Silica Nanoparticle Templates and Their Application as Dispersants for Oil Spill Remediation. *Polym. Chem.* **2017**, *8*, 5129−5138.
(178) Radhakrishnan, B.; Ranjan, R.; Brittain, W. J. Surface Initiated Polymerizations from Silica Nanoparticles. *Soft Matter* **2006**, *2*, 386−396.
(179) Bentz, K. C.; Savin, D. A. Chain Dispersity Effects on Brush Properties of Surface-Grafted Polycaprolactone-Modified Silica Nanoparticles: Unique Scaling Behavior in the Concentrated Polymer Brush Regime. *Macromolecules* **2017**, *50*, 5565−5573.
(180) Kango, S.; Kalia, S.; Celli, A.; Njuguna, J.; Habibi, Y.; Kumar, R. Surface Modification of Inorganic Nanoparticles for Development of Organic−Inorganic Nanocomposites—A Review. *Prog. Polym. Sci.* **2013**, *38*, 1232−1261.
(181) Schwab, M. G.; Senkovska, I.; Rose, M.; Koch, M.; Pahnke, J.; Jonschker, G.; Kaskel, S. MOF@PolyHIPEs. *Adv. Eng. Mater.* **2008**, *10*, 1151−1155.
(182) O'Neill, L. D.; Zhang, H.; Bradshaw, D. Macro-/Microporous MOF Composite Beads. *J. Mater. Chem.* **2010**, *20*, 5720−5726.
(183) Huo, J.; Marcello, M.; Garai, A.; Bradshaw, D. MOF-Polymer Composite Microcapsules Derived from Pickering Emulsions. *Adv. Mater.* **2013**, *25*, 2717−2722.
(184) Rowe, M. D.; Thamm, D. H.; Kraft, S. L.; Boyes, S. G. Polymer-Modified Gadolinium Metal-Organic Framework Nanoparticles Used as Multifunctional Nanomedicines for the Targeted Imaging and Treatment of Cancer. *Biomacromolecules* **2009**, *10*, 983−993.

DOI: 10.1021/acs.chemrev.9b00575
Chem. Rev. XXXX, XXX, XXX−XXX

(185) Rowe, M. D.; Chang, C.-C.; Thamm, D. H.; Kraft, S. L.; Harmon, J. F., Jr.; Vogt, A. P.; Sumerlin, B. S.; Boyes, S. G. Tuning the Magnetic Resonance Imaging Properties of Positive Contrast Agent Nanoparticles by Surface Modification with RAFT Polymers. *Langmuir* **2009**, *25*, 9487−9499.
(186) Nagata, S.; Kokado, K.; Sada, K. Metal−Organic Framework Tethering PNIPAM for ON−OFF Controlled Release in Solution. *Chem. Commun.* **2015**, *51*, 8614−8617.
(187) Hoffman, A. S. Stimuli-Responsive Polymers: Biomedical Applications and Challenges for Clinical Translation. *Adv. Drug Delivery Rev.* **2013**, *65*, 10−16.
(188) Zimpel, A.; Preiß, T.; Roder, R.; Engelke, H.; Ingrisch, M.; Peller, M.; Radler, J. O.; Wagner, E.; Bein, T.; Lachelt, U.; et al. Imparting Functionality to MOF Nanoparticles by External Surface Selective Covalent Attachment of Polymers. *Chem. Mater.* **2016**, *28*, 3318−3326.
(189) Li, Y.; Liu, J.; Zhang, K.; Lei, L.; Lei, Z. UiO-66-NH2@PMAA: A Hybrid Polymer−MOFs Architecture for Pectinase Immobilization. *Ind. Eng. Chem. Res.* **2018**, *57*, 559−567.
(190) Xie, K.; Fu, Q.; He, J.; Kim, J.; Goh, S. J.; Nam, E.; Qiao, G. G.; Webley, P. A. Synthesis of Well Dispersed Polymer Grafted Metal−Organic Framework Nanoparticles. *Chem. Commun.* **2015**, *51*, 15566−15569.
(191) Matyjaszewski, K.; Dong, H.; Jakubowski, W.; Pietrasik, J.; Kusumo, A. Grafting from Surfaces for "Everyone": ARGET ATRP in the Presence of Air. *Langmuir* **2007**, *23*, 4528−4531.
(192) Horcajada, P.; Gref, R.; Baati, T.; Allan, P. K.; Maurin, G.; Couvreur, P.; Ferey, G.; Morris, R. E.; Serre, C. Metal-Organic Frameworks in Biomedicine. *Chem. Rev.* **2012**, *112*, 1232−1268.
(193) Stuart, M. A. C.; Huck, W. T. S.; Genzer, J.; Muller, M.; Ober, C.; Stamm, M.; Sukhorukov, G. B.; Szleifer, I.; Tsukruk, V. V.; Urban, M.; et al. Emerging Applications of Stimuli-Responsive Polymer Materials. *Nat. Mater.* **2010**, *9*, 101−113.
(194) Wei, M.; Gao, Y.; Li, X.; Serpe, M. J. Stimuli-Responsive Polymers and Their Applications. *Polym. Chem.* **2017**, *8*, 127−143.
(195) Coudert, F.-X. Responsive Metal−Organic Frameworks and Framework Materials: Under Pressure, Taking the Heat, in the Spotlight, with Friends. *Chem. Mater.* **2015**, *27*, 1905−1916.
(196) Nagarkar, S. S.; Desai, A. V.; Ghosh, S. K. Stimulus-Responsive Metal-Organic Frameworks. *Chem. - Asian J.* **2014**, *9*, 2358−2376.
(197) Liu, H.; Zhu, H.; Zhu, S. Reversibly Dispersible/Collectable Metal- Organic Frameworks Prepared by Grafting Thermally Responsive and Switchable Polymers. *Macromol. Mater. Eng.* **2015**, *300*, 191−197.
(198) Jiang, W.-L.; Fu, Q.-J.; Yao, B.-J.; Ding, L.-G.; Liu, C.-X.; Dong, Y.-B. Smart pH-Responsive Polymer-Tethered and Pd NP-Loaded NMOF as the Pickering Interfacial Catalyst for One-Pot Cascade Biphasic Reaction. *ACS Appl. Mater. Interfaces* **2017**, *9*, 36438−36446.
(199) Yu, M.; Li, W.; Wang, Z.; Zhang, B.; Ma, H.; Li, L.; Li, J. Covalent Immobilization of Metal−Organic Frameworks onto the Surface of Nylon—A New Approach to the Functionalization and Coloration of Textiles. *Sci. Rep.* **2016**, *6*, 22796.
(200) Nunes, R. W.; Martin, J. R.; Johnson, J. F. Influence of Molecular Weight and Molecular Weight Distribution on Mechanical Properties of Polymers. *Polym. Eng. Sci.* **1982**, *22*, 205−228.
(201) Uemura, T.; Kitagawa, K.; Horike, S.; Kawamura, T.; Kitagawa, S.; Mizuno, M.; Endo, K. Radical Polymerisation of Styrene in Porous Coordination Polymers. *Chem. Commun.* **2005**, 5968−5970.
(202) Satoh, K.; Kamigaito, M. Stereospecific Living Radical Polymerization: Dual Control of Chain Length and Tacticity for Precision Polymer Synthesis. *Chem. Rev.* **2009**, *109*, 5120−5156.
(203) Liu, W.; Koike, Y.; Okamoto, Y. Stereochemistry of the Radical Polymerization of Vinyl Pentafluorobenzoate. *Polymer* **2004**, *45*, 5491−5495.
(204) Yamada, K.; Nakano, T.; Okamoto, Y. Stereochemistry of Radical Polymerization of Vinyl Esters in the Presence of Lewis Acid. *Polym. J.* **2000**, *32*, 707−710.
(205) Uemura, T.; Ono, Y.; Kitagawa, K.; Kitagawa, S. Radical Polymerization of Vinyl Monomers in Porous Coordination Polymers: Nanochannel Size Effects on Reactivity, Molecular Weight, and Stereostructure. *Macromolecules* **2008**, *41*, 87−94.
(206) Uemura, T.; Uchida, N.; Higuchi, M.; Kitagawa, S. Effects of Unsaturated Metal Sites on Radical Vinyl Polymerization in Coordination Nanochannels. *Macromolecules* **2011**, *44*, 2693−2697.
(207) Hwang, J.; Lee, H.-C.; Antonietti, M.; Schmidt, B. V. K. J. Free Radical and RAFT Polymerization of Vinyl Esters in Metal Organic Frameworks. *Polym. Chem.* **2017**, *8*, 6204−6208.
(208) Uemura, T.; Mochizuki, S.; Kitagawa, S. Radical Copolymerization Mediated by Unsaturated Metal Sites in Coordination Nanochannels. *ACS Macro Lett.* **2015**, *4*, 788−791.
(209) Mochizuki, S.; Ogiwara, N.; Takayanagi, M.; Nagaoka, M.; Kitagawa, S.; Uemura, T. Sequence-Regulated Copolymerization Based on Periodic Covalent Positioning of Monomers Along One-Dimensional Nanochannels. *Nat. Commun.* **2018**, *9*, 329.
(210) Thomas, A.; Goettmann, F.; Antonietti, M. Hard Templates for Soft Materials: Creating Nanostructured Organic Materials. *Chem. Mater.* **2008**, *20*, 738−755.
(211) Wang, Y.; Liu, Z.; Han, B.; Li, J.; Gao, H.; Wang, J.; Zhang, J. Fabrication of Flowerlike Polymer Superstructures Using Polymer/Zeolite Composites Prepared with Supercritical CO2. *J. Phys. Chem. B* **2005**, *109*, 2605−2609.
(212) Uemura, T.; Kaseda, T.; Kitagawa, S. Controlled Synthesis of Anisotropic Polymer Particles Templated by Porous Coordination Polymers. *Chem. Mater.* **2013**, *25*, 3772−3776.
(213) Gu, Z.-G.; Fu, W.-Q.; Liu, M.; Zhang, J. Surface-Mounted MOF Templated Fabrication of Homochiral Polymer Thin Film for Enantioselective Adsorption of Drugs. *Chem. Commun.* **2017**, *53*, 1470−1473.
(214) Kobayashi, Y.; Honjo, K.; Kitagawa, S.; Uemura, T. Preparation of Porous Polysaccharides Templated by Coordination Polymer with Three-Dimensional Nanochannels. *ACS Appl. Mater. Interfaces* **2017**, *9*, 11373−11379.
(215) Yanai, N.; Uemura, T.; Ohba, M.; Kadowaki, Y.; Maesato, M.; Takenaka, M.; Nishitsuji, S.; Hasegawa, H.; Kitagawa, S. Fabrication of Two-Dimensional Polymer Arrays: Template Synthesis of Polypyrrole between Redox-Active Coordination Nanoslits. *Angew. Chem., Int. Ed.* **2008**, *47*, 9883−9886.
(216) Uemura, T.; Kadowaki, Y.; Yanai, N.; Kitagawa, S. Template Synthesis of Porous Polypyrrole in 3D Coordination Nanochannels. *Chem. Mater.* **2009**, *21*, 4096−4098.
(217) Lu, C.; Ben, T.; Xu, S.; Qiu, S. Electrochemical Synthesis of a Microporous Conductive Polymer Based on a Metal−Organic Framework Thin Film. *Angew. Chem., Int. Ed.* **2014**, *53*, 6454−6458.
(218) Kitao, T.; MacLean, M. W. A.; Le Ouay, B.; Sasaki, Y.; Tsujimoto, M.; Kitagawa, S.; Uemura, T. Preparation of Polythiophene Microrods with Ordered Chain Alignment Using Nanoporous Coordination Template. *Polym. Chem.* **2017**, *8*, 5077−5081.
(219) Uemura, T.; Uchida, N.; Asano, A.; Saeki, A.; Seki, S.; Tsujimoto, M.; Isoda, S.; Kitagawa, S. Highly Photoconducting π-Stacked Polymer Accommodated in Coordination Nanochannels. *J. Am. Chem. Soc.* **2012**, *134*, 8360−8363.
(220) Distefano, G.; Suzuki, H.; Tsujimoto, M.; Isoda, S.; Bracco, S.; Comotti, A.; Sozzani, P.; Uemura, T.; Kitagawa, S. Highly Ordered Alignment of a Vinyl Polymer by Host−Guest Cross-Polymerization. *Nat. Chem.* **2013**, *5*, 335.
(221) Ishiwata, T.; Furukawa, Y.; Sugikawa, K.; Kokado, K.; Sada, K. Transformation of Metal−Organic Framework to Polymer Gel by Cross-Linking the Organic Ligands Preorganized in Metal−Organic Framework. *J. Am. Chem. Soc.* **2013**, *135*, 5427−5432.
(222) Tsotsalas, M.; Liu, J.; Tettmann, B.; Grosjean, S.; Shahnas, A.; Wang, Z.; Azucena, C.; Addicoat, M.; Heine, T.; Lahann, J.; et al. Fabrication of Highly Uniform Gel Coatings by the Conversion of

DOI: 10.1021/acs.chemrev.9b00575
Chem. Rev. XXXX, XXX, XXX−XXX

Surface-Anchored Metal−Organic Frameworks. *J. Am. Chem. Soc.* **2014**, *136*, 8−11.
(223) Ishiwata, T.; Kokado, K.; Sada, K. Anisotropically Swelling Gels Attained through Axis-Dependent Crosslinking of MOF Crystals. *Angew. Chem., Int. Ed.* **2017**, *56*, 2608−2612.
(224) Schmitt, S.; Hümmer, J.; Kraus, S.; Welle, A.; Grosjean, S.; Hanke-Roos, M.; Rosenhahn, A.; Bräse, S.; Wöll, C.; Lee-Thedieck, C.; et al. Tuning the Cell Adhesion on Biofunctionalized Nanoporous Organic Frameworks. *Adv. Funct. Mater.* **2016**, *26*, 8455−8462.
(225) Bradshaw, D.; El-Hankari, S.; Lupica-Spagnolo, L. Supramolecular Templating of Hierarchically Porous Metal−Organic Frameworks. *Chem. Soc. Rev.* **2014**, *43*, 5431−5443.
(226) Pham, M.-H.; Vuong, G.-T.; Fontaine, F.-G.; Do, T.-O. A Route to Bimodal Micro-Mesoporous Metal−Organic Frameworks Nanocrystals. *Cryst. Growth Des.* **2012**, *12*, 1008−1013.
(227) Yao, J.; He, M.; Wang, K.; Chen, R.; Zhong, Z.; Wang, H. High-Yield Synthesis of Zeolitic Imidazolate Frameworks from Stoichiometric Metal and Ligand Precursor Aqueous Solutions at Room Temperature. *CrystEngComm* **2013**, *15*, 3601−3606.
(228) Pang, M.; Cairns, A. J.; Liu, Y.; Belmabkhout, Y.; Zeng, H. C.; Eddaoudi, M. Highly Monodisperse MIII-Based soc-MOFs (M = In and Ga) with Cubic and Truncated Cubic Morphologies. *J. Am. Chem. Soc.* **2012**, *134*, 13176−13179.
(229) Pang, M.; Cairns, A. J.; Liu, Y.; Belmabkhout, Y.; Zeng, H. C.; Eddaoudi, M. Synthesis and Integration of Fe-soc-MOF Cubes into Colloidosomes via a Single-Step Emulsion-Based Approach. *J. Am. Chem. Soc.* **2013**, *135*, 10234−10237.
(230) Cai, X.; Deng, X.; Xie, Z.; Bao, S.; Shi, Y.; Lin, J.; Pang, M.; Eddaoudi, M. Synthesis of Highly Monodispersed Ga-soc-MOF Hollow Cubes, Colloidosomes and Nanocomposites. *Chem. Commun.* **2016**, *52*, 9901−9904.
(231) Wang, S.; Lv, Y.; Yao, Y.; Yu, H.; Lu, G. Modulated Synthesis of Monodisperse MOF-5 Crystals with Tunable Sizes and Shapes. *Inorg. Chem. Commun.* **2018**, *93*, 56−60.
(232) Uemura, T.; Hoshino, Y.; Kitagawa, S.; Yoshida, K.; Isoda, S. Effect of Organic Polymer Additive on Crystallization of Porous Coordination Polymer. *Chem. Mater.* **2006**, *18*, 992−995.
(233) Cao, S.; Gody, G.; Zhao, W.; Perrier, S.; Peng, X.; Ducati, C.; Zhao, D.; Cheetham, A. K. Hierarchical Bicontinuous Porosity in Metal−Organic Frameworks Templated from Functional Block co-Oligomer Micelles. *Chem. Sci.* **2013**, *4*, 3573−3577.
(234) Chen, T.-H.; Wang, L.; Trueblood, J. V.; Grassian, V. H.; Cohen, S. M. Poly(isophthalic acid)(ethylene oxide) as a Macromolecular Modulator for Metal−Organic Polyhedra. *J. Am. Chem. Soc.* **2016**, *138*, 9646−9654.
(235) Hwang, J.; Heil, T.; Antonietti, M.; Schmidt, B. V. K. J. Morphogenesis of Metal−Organic Mesocrystals Mediated by Double Hydrophilic Block Copolymers. *J. Am. Chem. Soc.* **2018**, *140*, 2947−2956.
(236) Gu, Y.; Huang, M.; Zhang, W.; Pearson, M. A.; Johnson, J. A. PolyMOF Nanoparticles: Dual Roles of a Multivalent polyMOF Ligand in Size Control and Surface Functionalization. *Angew. Chem., Int. Ed.* **2019**, *58*, 16676−16681.
(237) Zhang, Z.; Nguyen, H. T. H.; Miller, S. A.; Cohen, S. M. polyMOFs: A Class of Interconvertible Polymer-Metal-Organic-Framework Hybrid Materials. *Angew. Chem., Int. Ed.* **2015**, *54*, 6152−6157.
(238) Ayala, S.; Zhang, Z.; Cohen, S. M. Hierarchical Structure and Porosity in UiO-66 polyMOFs. *Chem. Commun.* **2017**, *53*, 3058−3061.
(239) Zhang, Z.; Nguyen, H. T. H.; Miller, S. A.; Ploskonka, A. M.; DeCoste, J. B.; Cohen, S. M. Polymer−Metal−Organic Frameworks (polyMOFs) as Water Tolerant Materials for Selective Carbon Dioxide Separations. *J. Am. Chem. Soc.* **2016**, *138*, 920−925.
(240) Schukraft, G. E. M.; Ayala, S.; Dick, B. L.; Cohen, S. M. Isoreticular Expansion of polyMOFs Achieves High Surface Area Materials. *Chem. Commun.* **2017**, *53*, 10684−10687.
(241) Ayala, S.; Bentz, K. C.; Cohen, S. M. Block co-polyMOFs: Morphology Control of Polymer−MOF Hybrid Materials. *Chem. Sci.* **2019**, *10*, 1746−1753.
(242) MacLeod, M. J.; Johnson, J. A. Block co-polyMOFs: Assembly of Polymer−polyMOF Hybrids via Iterative Exponential Growth and "click" Chemistry. *Polym. Chem.* **2017**, *8*, 4488−4493.
(243) Palomba, J. M.; Ayala, S., Jr.; Cohen, S. M. polyMOF Formation from Kinked Polymer Ligands via ortho-Substitution. *Isr. J. Chem.* **2018**, *58*, 1123−1126.

DOI: 10.1021/acs.chemrev.9b00575
Chem. Rev. XXXX, XXX, XXX−XXX